

SERI/STR-230-2065  
DE84000012

September 1983

# Direct-Contact High-Temperature Thermal Energy Storage Heat Exchanger

## Final Subcontract Report

Joseph Alario  
Richard Brown

Grumman Aerospace Corporation  
Bethpage, New York 11714

Prepared under Subcontract No. XP-0-9383-1



# SERI

## Solar Energy Research Institute

A Division of Midwest Research Institute

1617 Cole Boulevard  
Golden, Colorado 80401

Operated for the

**U.S. Department of Energy**

under Contract No. DE-AC02-83CH10093

Printed in the United States of America  
Available from:  
National Technical Information Service  
U.S. Department of Commerce  
5285 Port Royal Road  
Springfield, VA 22161  
Price:  
Microfiche A01  
Printed Copy A05

#### **NOTICE**

This report was prepared as an account of work sponsored by the United States Government. Neither the United States nor the United States Department of Energy, nor any of their employees, nor any of their contractors, subcontractors, or their employees, makes any warranty, express or implied, or assumes any legal liability or responsibility for the accuracy, completeness or usefulness of any information, apparatus, product or process disclosed, or represents that its use would not infringe privately owned rights.

**SERI/STR-230-2065**  
**UC Category: 62e**  
**DE84000012**

**Direct-Contact  
High-Temperature  
Thermal Energy Storage  
Heat Exchanger  
Final Subcontract Report**

**Joseph Alario  
Richard Brown**

Grumman Aerospace Corporation  
Bethpage, New York 11714

**September 1983**

**Prepared under Subcontract No. XP-0-9383-1**

**SERI Technical Monitor: Werner Luft**

**Solar Energy Research Institute**

A Division of Midwest Research Institute

1617 Cole Boulevard  
Golden, Colorado 80401

Prepared for the  
**U.S. Department of Energy**  
Contract No. EG-77-C-01-4042

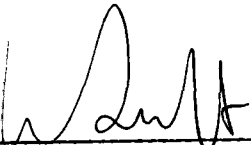
## FOREWORD

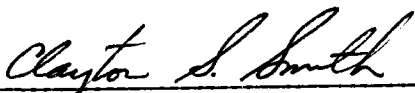
This report describes the results of work done by Grumman Aerospace Corporation under subcontract XP-0-9383-1 for the Solar Energy Research Institute, as a part of task 1298, in WPA 348-82, in the Energy Storage Program. The work was performed over the period 07/15/81 to 02/01/83. The technical review of this work was done by John Wright.

Funds for this work were provided by the Division of Energy Storage Technology of the U.S. Department of Energy.

Approved for the

SOLAR ENERGY RESEARCH INSTITUTE

  
\_\_\_\_\_  
Werner Luft, Manager  
Solar Energy Storage Program

  
\_\_\_\_\_  
Clayton S. Smith, Manager  
Solar Fuels and Chemicals Research  
Division

## ACKNOWLEDGEMENT

The authors wish to acknowledge the following Grumman Aerospace personnel for their important contributions during the design and fabrication of the direct contact thermal energy storage heat exchanger reported herein: Dr. Robert Kosson for his technical counsel; Charles Johnson for the detailed mechanical design drawings; Stanley Baker, Michael Gibbons, and Art Haas for instrumentation support; Rod Lofthouse for mechanical assembly; and Richard Spinos for the materials compatibility study.

We are also grateful to Mr. John Wright of SERI for his guidance and support throughout the program.

## CONTENTS

<u>Section</u>	<u>Page</u>
1	INTRODUCTION . . . . . 1-1
2	SUMMARY . . . . . 2-1
3	EXAMINATION OF THE DAMAGED HARDWARE . . . . . 3-1
4	SYSTEM MODIFICATIONS AND REFURBISHMENT . . . . . 4-1
	4.1 Changed Energy Storage Medium to Lower Melting Point of Inorganic Salt. . . . . 4-1
	4.2 Modified Pumping System . . . . . 4-1
	4.3 New Tanks and Plumbing . . . . . 4-3
	4.4 Elimination of All Internal Heaters . . . . . 4-4
	4.5 100% Trace Heating . . . . . 4-4
	4.6 Automatic Controllers for Heater Circuits . . . . . 4-4
	4.7 Continual Heating of Liquid Metal Lines . . . . . 4-4
5	DETAILED DESIGN SUMMARY OF THE HEAT EXCHANGE COLUMN . . . . . 5-1
	5.1 System Considerations . . . . . 5-1
	5.2 Mass and Flow Rate Requirements . . . . . 5-1
	5.3 Injector Designs . . . . . 5-2
	5.3.1 Molten Salt . . . . . 5-2
	5.3.2 Liquid Metal . . . . . 5-3
	5.4 Liquid Metal Velocity . . . . . 5-3
	5.5 Salt Droplet Velocity . . . . . 5-4
	5.6 Salt Droplet Surface Heat Transfer Coefficient (h) . . . . . 5-5
	5.7 Residence Time for Droplet Solidification . . . . . 5-6

## CONTENTS (contd)

<u>Section</u>	<u>Page</u>
5.8 Required Heat Exchange Column Height . . . . .	5-8
5.9 Required Flow Area . . . . .	5-9
5.10 Heat Exchange Column Geometry . . . . .	5-9
6 MATERIALS COMPATIBILITY STUDY . . . . .	6-1
7 HARDWARE FABRICATION AND SYSTEM ASSEMBLY . . . . .	7-1
8 INSTRUMENTATION . . . . .	8-1
8.1 Heaters/Controllers . . . . .	8-1
8.2 Instrumentation . . . . .	8-1
9 RECOMMENDED TEST PROGRAM . . . . .	9-1
10 REFERENCES . . . . .	10-1

Appendices

A RESIDENCE TIME FOR DROPLET SOLIDIFICATION . . . . .	A-1
B LABORATORY RESULTS OF MATERIALS COMPATIBILITY STUDY . . . . .	B-1
C DESIGN SPECIFICATION SUMMARY FOR DIRECT-CONTACT LATENT THERMAL ENERGY STORAGE HEAT EXCHANGER . . . . .	C-1

## ILLUSTRATIONS

<u>Fig.</u>		<u>Page</u>
1-1	Organic Receiver (Power) Storage System, Direct-Contact HX. . .	1-2
2-1	Original Direct-Contact HX Assembly . . . . .	2-2
2-2	System Schematic (Hybrid Pumping) . . . . .	2-4
2-3	Direct-Contact Heat Exchanger, Refurbished System . . . . .	2-5
3-1	View After Cerablanket Insulation Was Removed. . . . .	3-4
3-2	Rear View of Test Apparatus. . . . .	3-5
3-3	Exterior View from Liquid Metal Module. . . . .	3-6
3-4	Molten Salt Charging Canister . . . . .	3-7
3-5	Liquid Metal Charging Canister. . . . .	3-8
3-6	Heat Exchanger Module Closeup. . . . .	3-9
3-7	Salt Module Exterior Closeup (View 1) . . . . .	3-10
3-8	Salt Module Exterior Closeup (View 2) . . . . .	3-11
3-9	Salt Module Exterior Closeup (View 3) . . . . .	3-12
3-10	Salt Module Interior . . . . .	3-13
3-11	Liquid Metal Module Interior . . . . .	3-14
3-12	Heat Exchange Module Interior . . . . .	3-15
3-13	Heat Exchange Tower Interior . . . . .	3-16
3-14	Heat Exchange Module Cover Interior. . . . .	3-17
4-1	System Schematic (Hybrid Pumping) . . . . .	4-3
5-1	Direct-Contact Heat Exchanger Operating Temperature Limits . . .	5-1
5-2	Orifice Opening . . . . .	5-3
5-3	Liquid Metal Injector Designs . . . . .	5-3



## ILLUSTRATIONS (contd)

<u>Fig.</u>		<u>Page</u>
5-4	Salt Bubble Velocity Vs Time . . . . .	5-6
5-5	Variation of Heat Transfer Coefficient With Time . . . . .	5-7
5-6	Heat Exchanger Column Geometry . . . . .	5-9
7-1	Direct-Contact Heat Exchanger Tower Installed in Tank . . . . .	7-2
7-2	Tanks Mounted and Band Heaters Installed . . . . .	7-3
7-3	Controllers Connected and Plumbing Started . . . . .	7-4
7-4	Liquid Metal Pump Installed and Level Sensors Adjusted . . . . .	7-5
7-5	Air Heat Exchanger Mounted . . . . .	7-6
7-6	Tank Insulation Applied and Line Heaters Installed . . . . .	7-7
7-7	Direct-Contact Heat Exchanger Final Assembly . . . . .	7-8
7-8	Test Data Acquisition Setup . . . . .	7-9
8-1	System Instrumentation Schematic . . . . .	8-2
8-2	Internal Instrumentation . . . . .	8-3

## TABLES

<u>No.</u>		<u>Page</u>
3-1	Post-Test Chemical Analysis . . . . .	3-3
4-1	Nitrate Salt Properties . . . . .	4-2
8-1	Heater Circuit Summary . . . . .	8-1
9-1	Recommended Discharge Cycle Test Conditions . . . . .	9-1

## 1 - INTRODUCTION

Objective

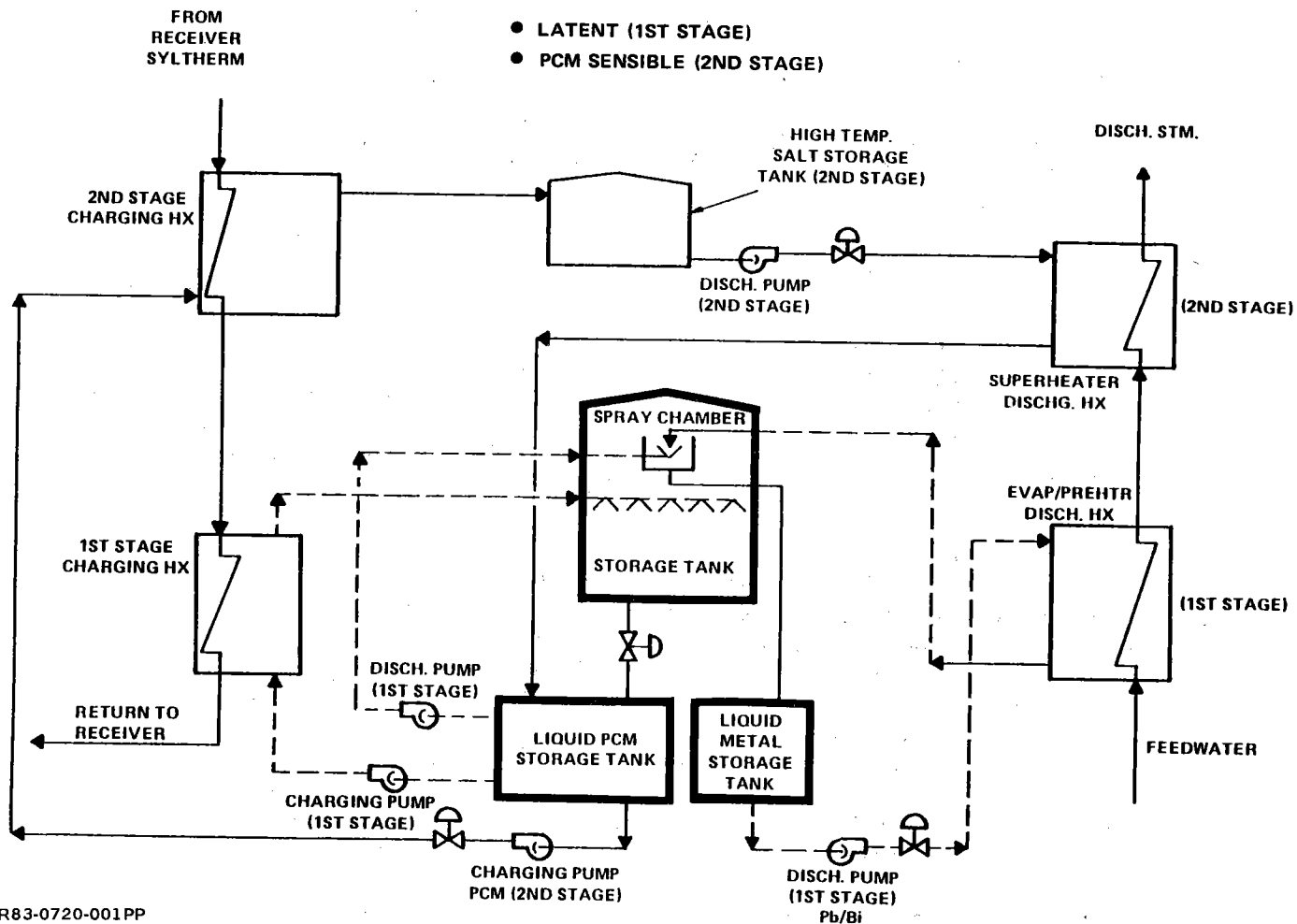
To develop a high-temperature direct-contact latent-heat-exchange thermal energy storage system by demonstration and test evaluation of a 10-kW-h scale model.

Discussion

The development of a viable direct-contact heat exchanger for high-temperature applications (e.g., solar thermal) can yield significant capital equipment cost benefits. In theory, the direct-contact concept requires smaller (and therefore, less costly) heat exchangers because it greatly improves the heat transfer efficiency during extraction of the latent heat of fusion from a thermal energy storage medium.

Conventional tube-shell heat exchangers typically require large heat transfer surface areas to compensate for the continually increasing thermal resistance created by the solidifying thermal energy storage material. The direct-contact process significantly reduces the thermal resistance of the solid phase by promoting the transfer of heat across the phase boundaries of two well-mixed immiscible fluids (the solidifying heat source and the liquid heat sink). In the system under development, molten droplets of salt, which serves as the energy storage medium, are injected at the bottom of a column of liquid metal carrier fluid. As the lighter-weight molten salt droplets rise through the cooler column of liquid metal, they release their heat of fusion and solidify individually.

This research program was structured in three separate phases to permit: Phase I--the inspection and evaluation of the original hardware, which suffered extensive corrosion and damage in a previous experimental program; Phase II--redesign and fabrication of a modified system; and Phase 3--detailed test evaluation. In Phase I, the existing hardware was partially disassembled and examined to determine the state of media contamination, material corrosion, and hardware serviceability. On the basis of these findings, the design was modified to eliminate previous deficiencies. A test plan was also prepared that contained detailed information concerning instrumentation (type and location), measured parameters, and equipment operating procedures. Phase II entailed component procurement and fabrication, system assembly, and instrumentation. At the end of Phase II, the system was in a ready-for-test condition but the program was terminated before the start of the Phase III test evaluation. Since testing was never implemented, this report presents only the results for the design and fabrication phases of the program.



R83-0720-001PP

Fig. 1-1 Organic Receiver (Power) Storage System, Direct-Contact Heat Exchanger

## 2 - SUMMARY

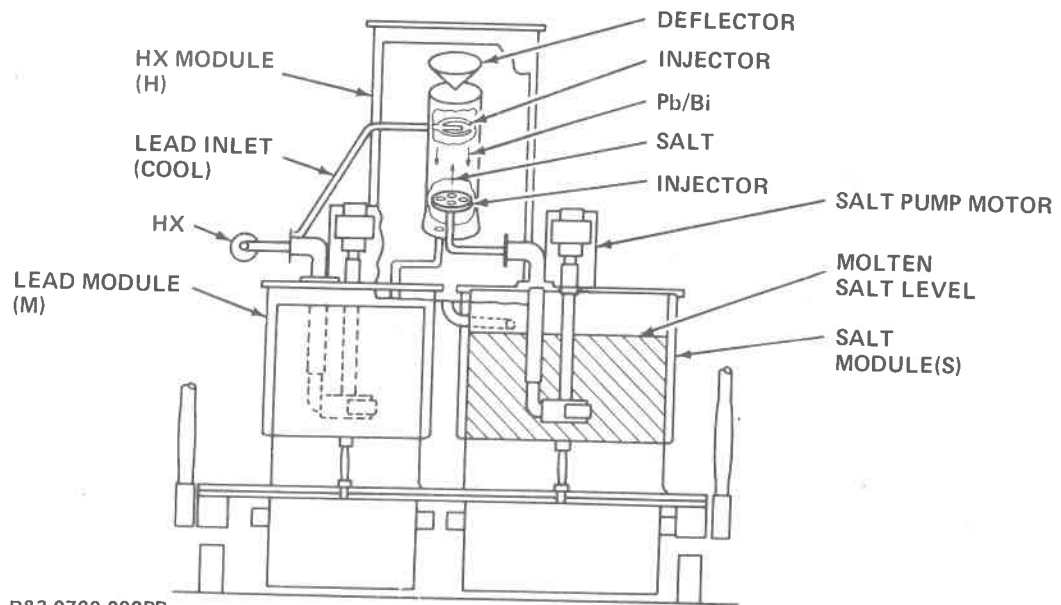
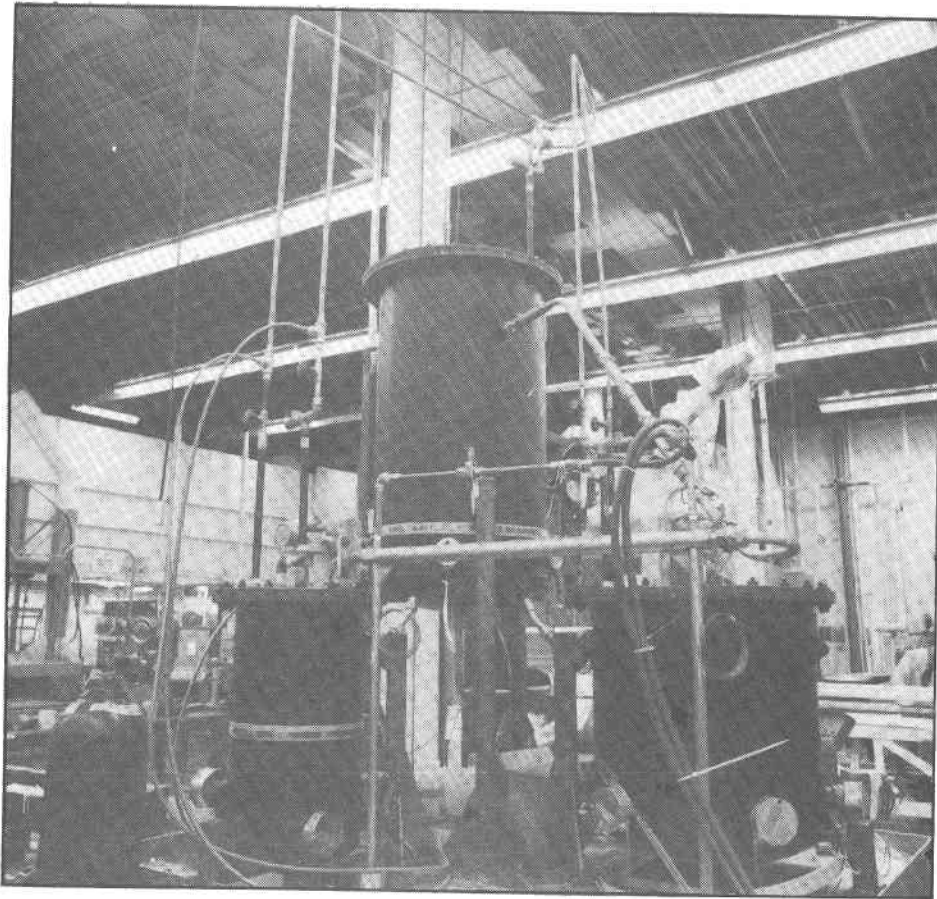
The original system for the direct-contact heat exchanger (see Ref. 2 for details and Fig. 2-1) consisted of two separate supply tanks (liquid metal and molten salt) that were connected to a central heat exchanger module. The salt and lead/bismuth tanks contained air-driven centrifugal pumps to circulate their respective materials. They were also fitted with separate charging canisters (located underneath) and internal immersion-type electrical heaters for temperature regulation. The heat exchange tank module contained the direct-contact heat exchange column and a storage area for the solidified salt (a chloride ternary eutectic). The original test program was eventually terminated because of electrical heater failures and salt leaks.

The significant findings of the physical inspection are summarized below:

- The immersion heaters in the salt module leaked salt vapor through the tapered threads, which eventually corroded the heater terminals and the external surfaces of the tank. There was a large salt leak at the rear of the tank
- The internal surfaces of the salt tank showed no signs of corrosion and the solidified chloride salt was pure white in appearance, showing no evidence of moisture absorption. A nitrogen gas blanket was maintained during system operation but had not been replenished for over three months while the tank was dormant
- There was no evidence of salt in the discharge plumbing, indicating that there was a local "cold spot" (possibly at the impeller) that prevented pumping
- Liquid metal had been pumped into the heat exchange tower and was encrusted around the salt injector plate. Some liquid metal had overflowed the tower and was solidified at the bottom of the heat exchange tank, within the volume set aside for storing solidified salt
- The appearance of the liquid metal and heat exchange modules was acceptable, but each would require significant refurbishment to remove the immersion heaters
- Tanks and lines showed charring due to over-temperature of the external band and line heaters
- Melting point measurements of the media showed no change in the lead-bismuth metal eutectic ( $124^{\circ}\text{C}$ ), but the chloride salt melt range ( $328\text{--}429^{\circ}\text{C}$ ) exceeded the specified value ( $385\text{--}393^{\circ}\text{C}$ )
- Most of the thermocouple instrumentation was unusable, but the two flowmeters (metal and salt) and the liquid level indicators in the heat exchange tower were salvageable.

Modifications made to improve the system design and refurbish the hardware are summarized below:

- New tanks (mild steel) were fabricated for all three modules (salt, metal, and heat exchange). This eliminated all immersion heaters and any instrumentation penetration beneath the liquid levels



R83-0720-002PP

Fig. 2-1 Original Direct-Contact Heat Exchanger Assembly

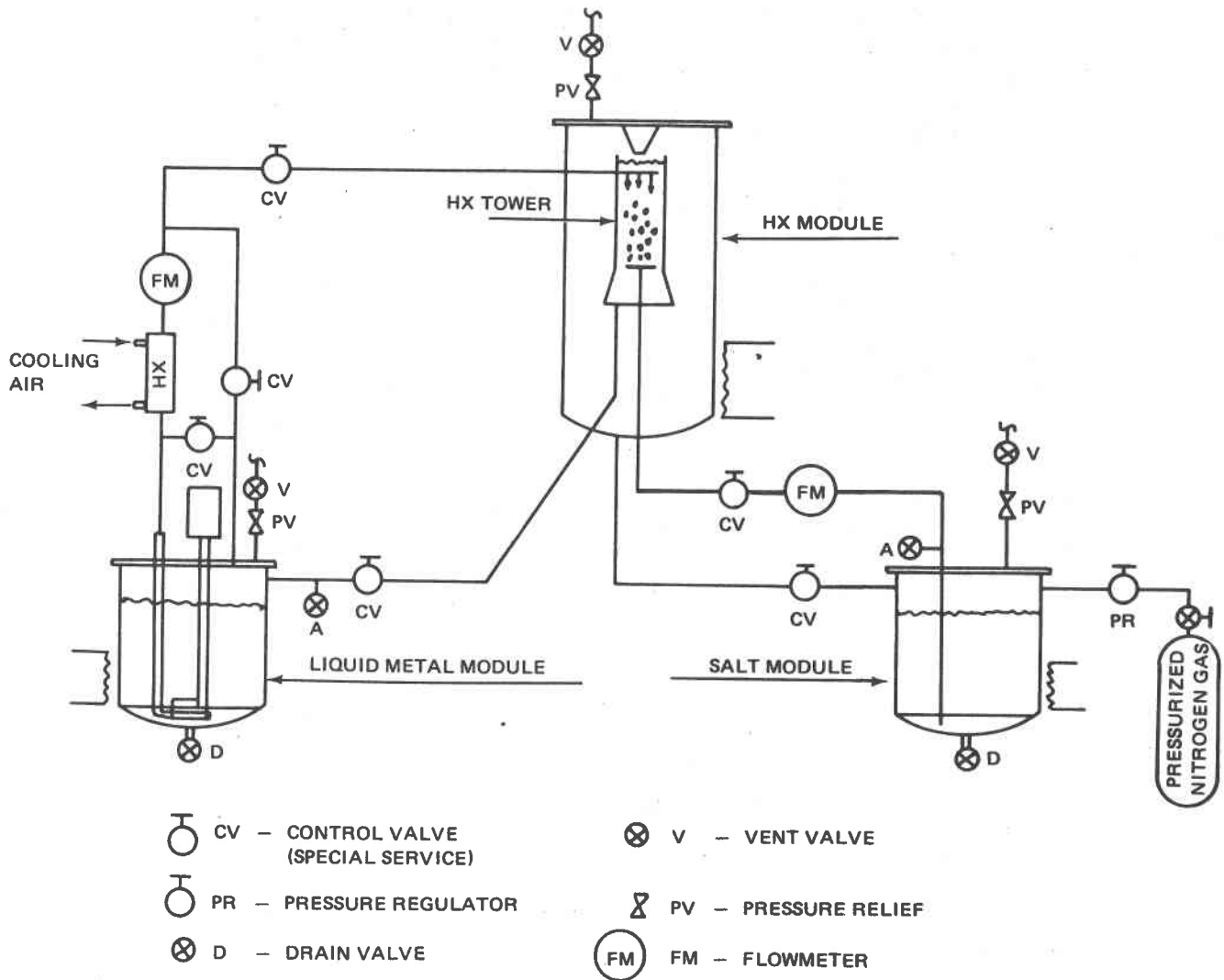
- The liquid metal pump was upgraded to increase lift capability and improve seal design. The new centrifugal pump can provide a 12-ft lift and comes attached to the cover of the liquid metal tank as a complete assembly. It is powered by a 2-hp electric motor instead of the 1-hp air-driven motor previously used
- In view of the batch-type discharge cycle, the salt pump was replaced by a pressurized nitrogen gas pumping system
- The salt medium was changed from the chloride eutectic (20.5% KCl, 24.5% NaCl, 55.0% MgCl<sub>2</sub>) to draw salt (46% NaNO<sub>3</sub>, 54% KNO<sub>3</sub>) because of the latter's widespread use in sensible heat storage systems. Thus, latent storage test data would be of more immediate use in augmenting these existing sensible systems. Also, the lower melting point of the draw salt (222°C) would simplify operation of this demonstration system since it would be easier to preheat tanks and lines and to control temperature
- All heater circuits were equipped with proportional controllers to achieve accurate temperature regulation. The tanks used external band heaters, while the plumbing, valves, and fittings were traced with adhesive-backed heater tape (serviceable up to 316°C)
- The filling system for both the molten salt and liquid metal tanks was changed from one that used a canister beneath the tank, containing liquefied material that was then pressurized, to a system using an access port in the lid through which solid material is introduced. The new method is simpler for a one-time evaluation and also permits mixing and processing of materials in place. Material removal is effected by melting and draining from the bottom of the tank
- The length of the heat exchange tower was increased by 0.38 m (to 0.76 m) to accommodate uncertainties in the reported value for thermal conductivity of the solidified salt. The modified design is suited for values of salt conductivity as low as 0.60 W/mK
- An access port was included in the top cover of the heat exchange module to permit sampling of the solidified salt droplets for subsequent measurement and analysis.

Figure 2-2 is a schematic diagram of the revised system. A photograph of the hardware in a ready-to-test condition is shown in Fig. 2-3.

Theoretical chemical reaction equilibria analyses had shown that oxidation of the liquid metal is possible when mixed with certain molten salts, especially nitrates (our prime candidate). However, information on the rate of reaction and the catalyzation requirement was lacking and in-house laboratory tests were run.

A brief statement of the important test results follows. Contrary to the actual application, the materials were in constant contact with each other during the test.

- The "as received" commercial-grade salts all contain sufficient impurities that cause them to quickly react with the liquid metal



R83-0720-003PP

Fig. 2-2 System Schematic (Hybrid Pumping)

- Laboratory-grade salts did not react with the liquid metal after 6-8 hours of contact and only moderately after 48 hours, reaching a steady state condition (no change was noticed after 120 hours)
- Commercial-grade nitrates salts that have been dissolved in water, filtered, and dried behave like the laboratory grade salts and react moderately with the liquid metal.



Fig. 2-3 Direct-Contact Heat Exchanger, Refurbished System



**SERIO** 

### 3 - EXAMINATION OF THE DAMAGED HARDWARE

The test equipment was wrapped completely with Cerablanket thermal insulation, which was removed to permit easy access and inspection of all components. None of the insulation was reusable due to the excessive handling it received during the initial test evaluation and troubleshooting. Figure 3-1 shows an overall view of the exterior, from the salt module side. A closeup of the rear of the apparatus is shown in Fig. 3-2. Note the congealed mass of insulation and salt near the bottom of the tank, which is from an obvious salt leak at an immersion heater junction box. A view from the lead module side is shown in Fig. 3-3; it appears relatively unscathed. No leaks were evident at any of the threaded connections.

Pictures of the charging canisters are provided by Fig. 3-4 (salt) and Fig. 3-5 (liquid metal). Leaks were apparent at the immersion heater junction boxes in both cases. Note the mass of salt-impregnated insulation hanging above the salt canister near the inlet line.

A closeup view of the heat exchanger module (Fig. 3-6) shows no real structural damage. Only the heaters were destroyed due to the over-temperature conditions achieved during testing. Closeup views of the salt module are given in Fig. 3-7, 3-8, and 3-9. The extent of the external corrosion is obvious. Severe scaling and flaking is rampant near every immersion heater penetration. This was caused by the corrosive effects of the salt vapor leaks. The tank was unusable and all heaters were destroyed.

To effect removal of the salt lid, the pump discharge line and shaft had to be cut. An interior view is given in Fig. 3-10. The inside wall of the salt module showed evidence of a "bathtub ring" which corresponded to the liquid level of the molten salt. It was located 152 mm above the solid salt surface. Separate salt weight calculations using the liquid and solid volumes and densities gave answers of 225 kg and 215 kg, respectively. This agrees with the 180-228 kg initial charge. Corrosion of the inside wall of the salt module was minimal and confined to the top

few centimeters near the lid. The top surface of the solidified salt mass appeared pure white upon removal of the lid. However, it gradually took on a yellow color after a few days of exposure to the atmosphere.

The interior lid of the salt module was not corroded. Inspection of the gasket seal showed no signs of distress and confirmed the use of the Grafoil material. Although operated for a short time, there was no evidence of any salt within the discharge line from the pump. Indeed, inspection of the salt pump outlet plumbing revealed only the presence of solidified liquid metal which probably flowed down through the salt injector during the checkout runs for the liquid metal pump. For some reason, the salt pump could not displace this material when it was finally activated. Both the salt and liquid metal pumps were of the same design and rating and this should not have occurred. The only explanation is a local "cold spot" that went undetected.

As a general observation, operation at temperatures above the salt melting point ( $385^{\circ}\text{C}$ ) caused equipment problems that were unrelated to the heat exchange mechanism being investigated. Too much time was wasted heating up, controlling temperatures (manually), and cooling down (to permit system modification and heater replacement). The heaters that were not corroded due to salt leaks were irreparably damaged due to overheating resulting from poor manual on/off control. The extra initial cost of automatic controllers ( $\sim\$300$  per circuit) would have been more than justified by saving the much larger labor and material costs associated with heater replacement after the system had been assembled and energized.

The interior of the liquid metal module is shown in Fig. 3-11. The inside wall revealed a "bathtub ring" about 102 mm above the solidified surface. This corresponds to a material loss of 98 kg since there is only a small density change between solid and liquid in this case. The particular 55% Bi/45% Pb alloy that was used actually expands slightly upon solidification. The calculated initial weight is 368 kg assuming that the bathtub ring indicates the original fill level. A charge of 408 kg was specified and the difference is attributed to the residue at the bottom of the charging canister.

The lead/bismuth inside the pump module appeared contaminated; it had a murky brown color instead of silver gray. Samples taken to the Grumman Chemical

Lab for analysis revealed traces of iron. There was no noticeable corrosion of the lead-bismuth tank module itself.

The exterior of the heat exchange module showed no evidence of corrosion and only slight scaling due to overheating. The interior of the tank and the heat exchange tower located inside also showed only slight scaling due to overheating (see Fig. 3-12). There was evidence (solidified drops, particles, and slugs) of lead/bismuth inside the heat exchange tower. The salt injector plate was also encrusted with the solidified metal (see Fig. 3-13). The inside cover of the heat exchange module, with one of the level sensors in place, is shown in Fig. 3-14.

Examination of the plumbing after disassembly showed that liquid metal had entered the salt injector line and accumulated in the horizontal section of line that included the salt flowmeter. There was no evidence of salt flow anywhere in the system, including the salt discharge line. Our conclusion is that there was a plug somewhere in the salt discharge line within the salt module tank which prevented molten salt from being pumped through the injector line. Changing to a lower melting point salt for the purposes of this technology demonstration should alleviate the problem.

Table 3-1 summarizes the post-test chemical analyses for the chloride salt and lead-bismuth metal. A differential scanning calorimeter (DSC) was used to determine melting point; a scanning electron microscope (SEM) identified element composition and atomic absorption determined metal alloy composition. Of note is the wide range for the salt melting point (382-429°C) which far exceeds the expected nominal 385 to 393°C value. Inadvertent localized solidification within the salt module could have been possible with this particular salt.

TABLE 3-1 POST-TEST CHEMICAL ANALYSIS

SAMPLE	MP, °C	SEM X-RAY			% Pb	% Bi
		MAJOR	MINOR	TRACE		
METAL	125.7-128.2	Pb, Bi		Cr, Fe	45.7	54.3
"RED" RESIDUE IN METAL	--	Pb, Bi		Fe		
SALT MATRIX	382-429	Cl	Mg, K, Na	Fe		
"GRAY" RESIDUE IN SALT	--	Cl	Mg, K, Na	Fe		
R83-0720-019PP						

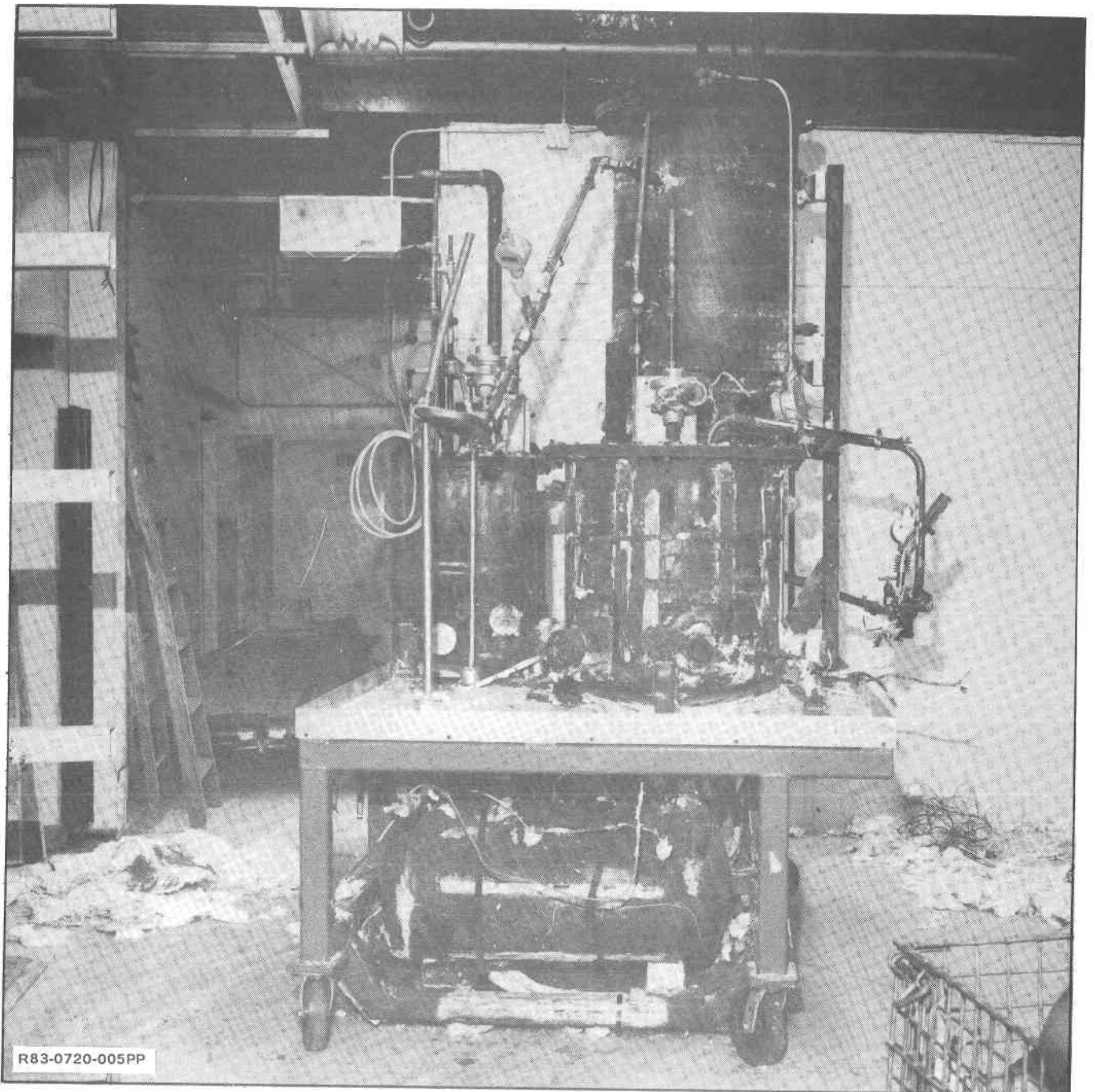


Fig. 3-1 View After Cerablanket Insulation Was Removed

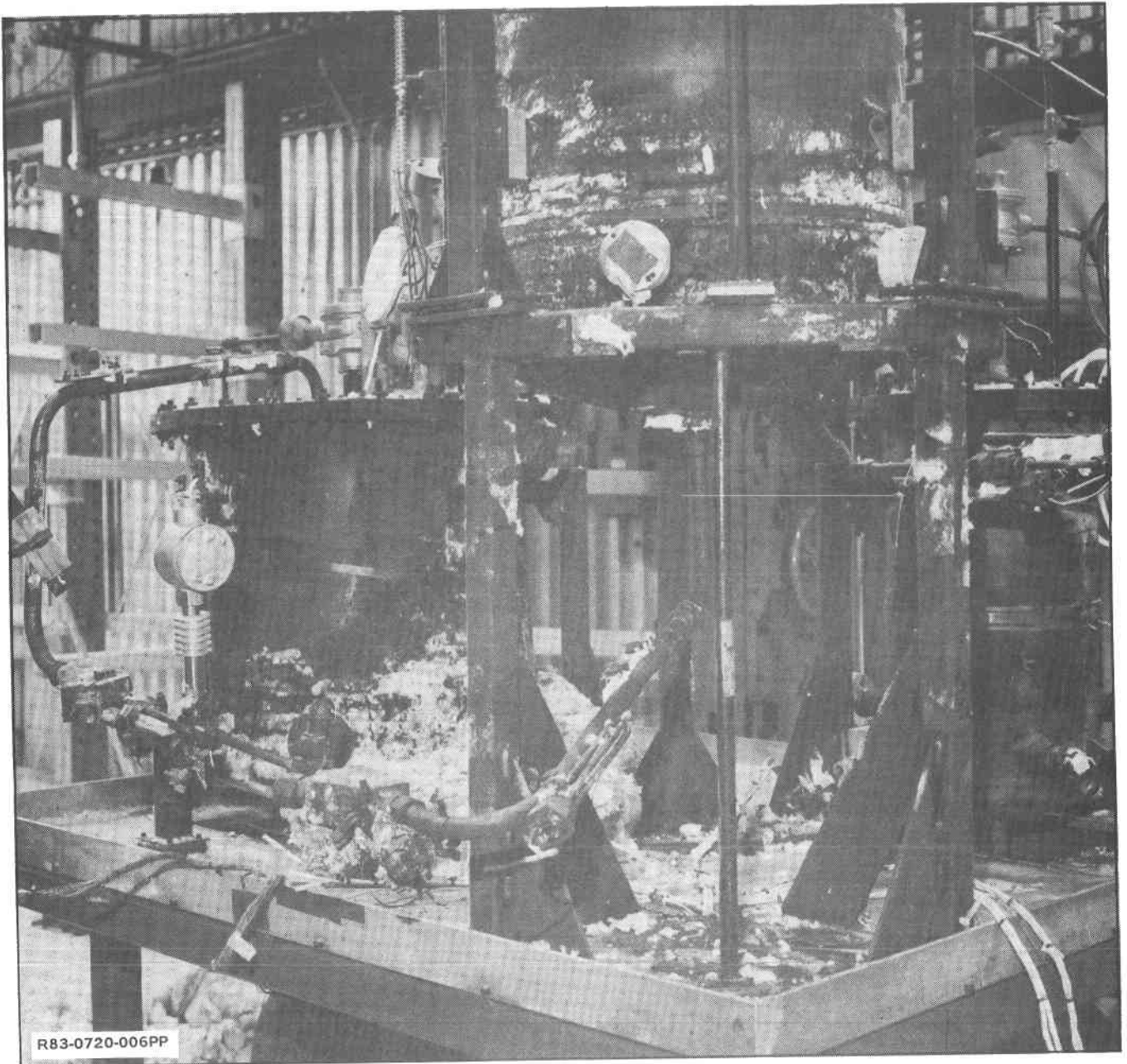


Fig. 3-2 Rear View of Test Apparatus



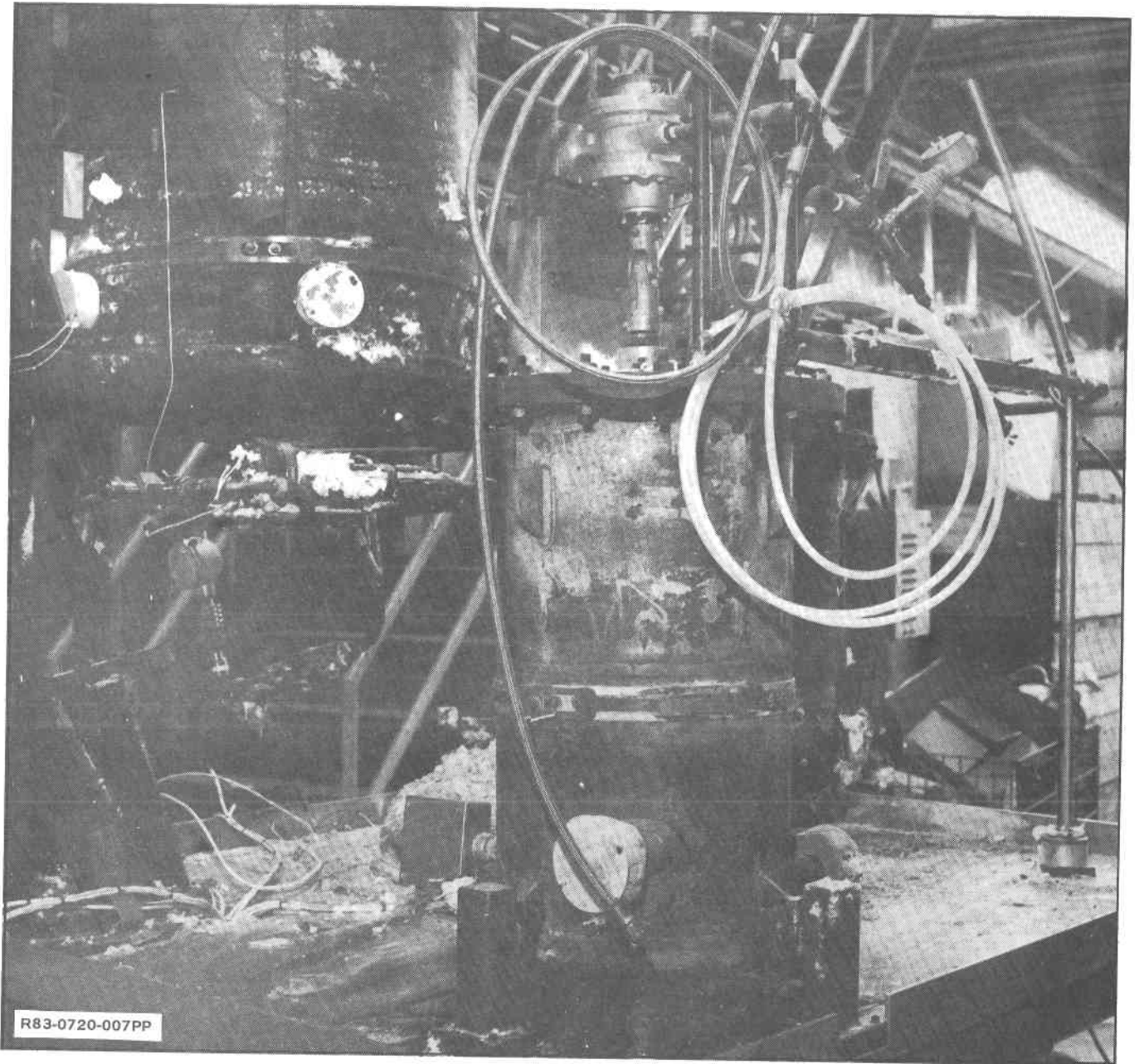


Fig.3-3 Exterior View from Liquid Metal Module

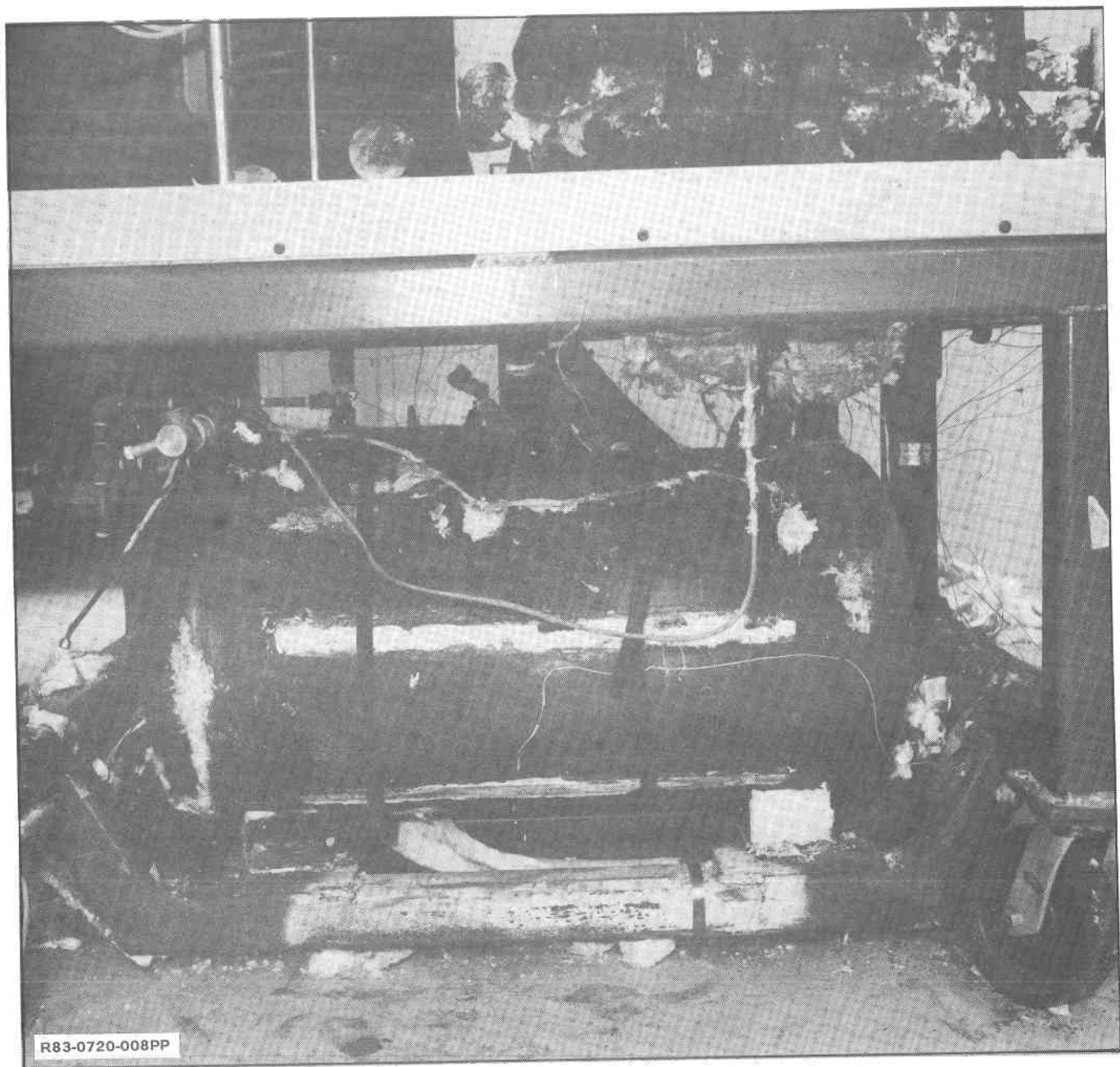


Fig. 3-4 Molten Salt Charging Canister



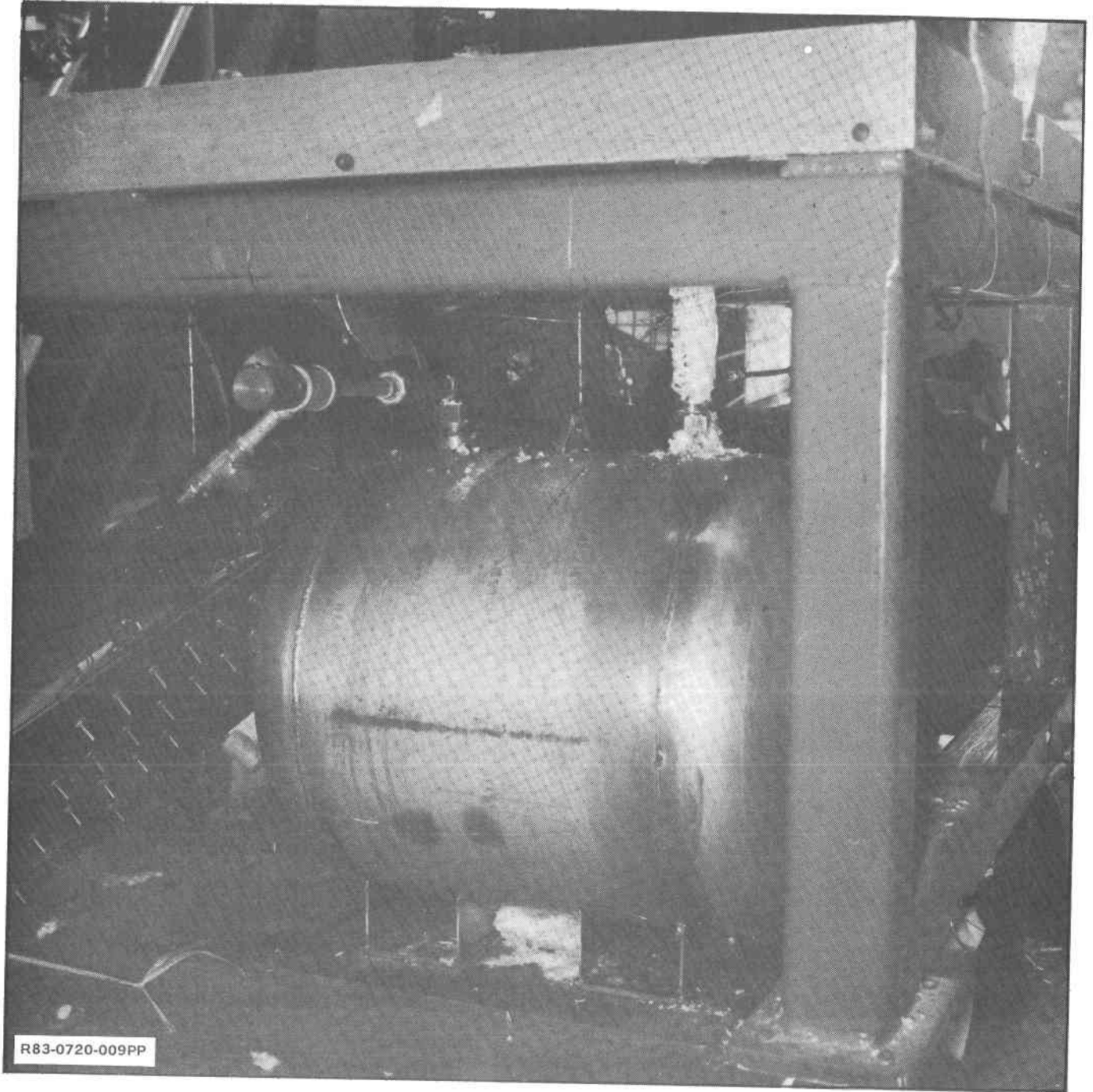


Fig. 3-5 Liquid Metal Charging Canister

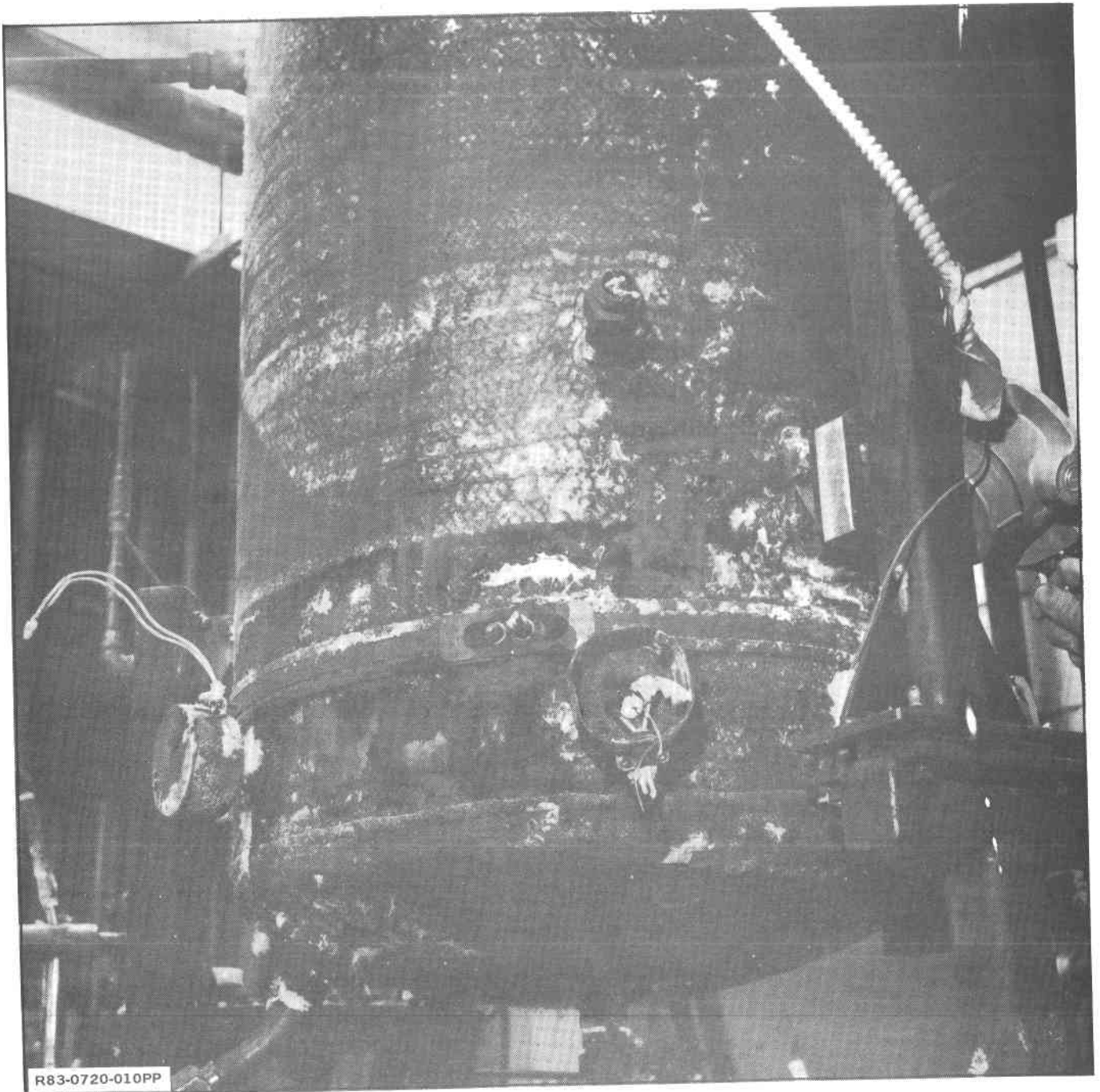


Fig. 3-6 Heat Exchanger Module Closeup

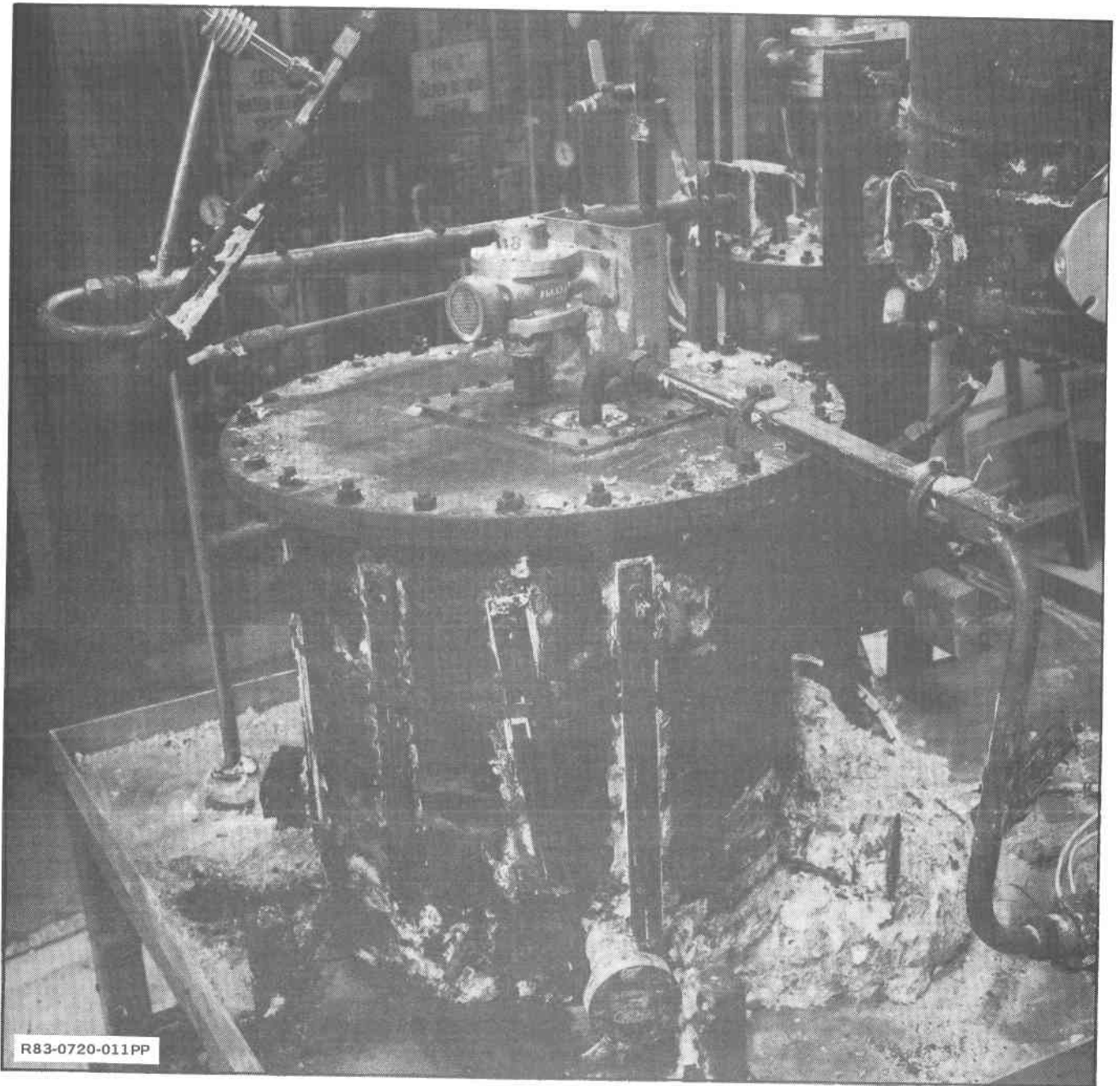


Fig. 3-7 Salt Module Exterior Closeup (View 1)





Fig. 3-8 Salt Module Exterior Closeup (View 2)



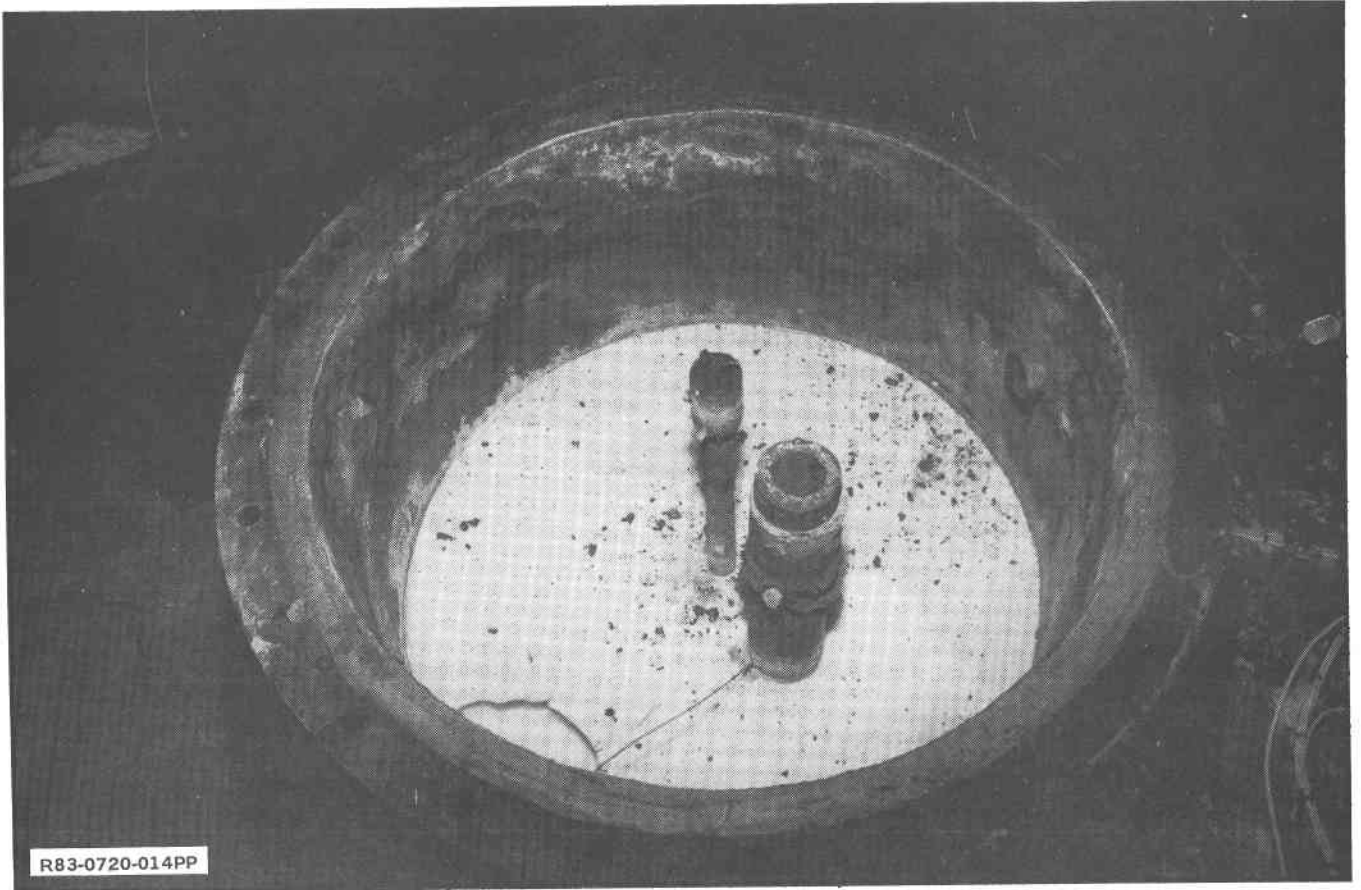


Fig. 3-10 Salt Module Interior

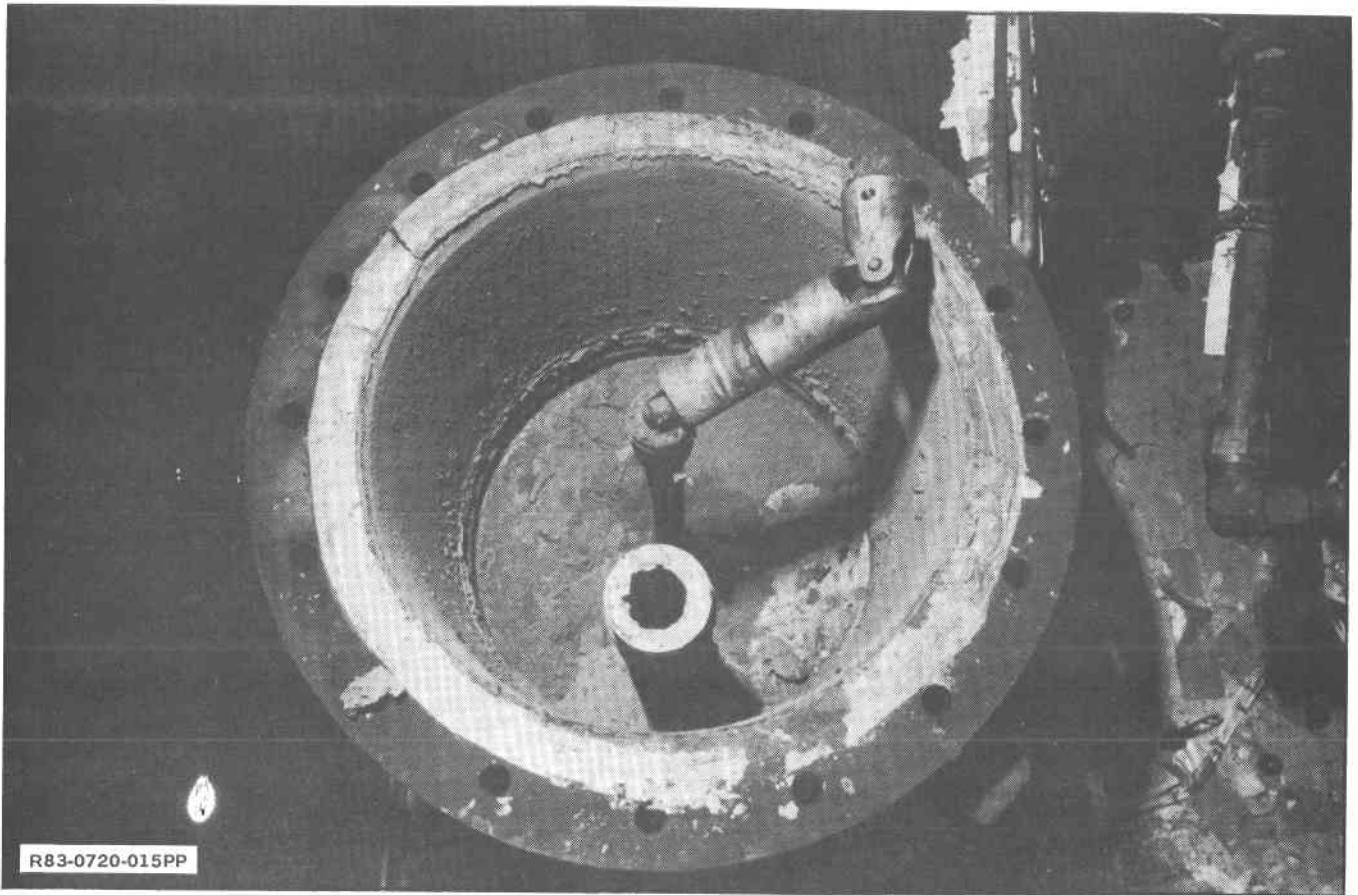


Fig. 3-11 Liquid Metal Module Interior

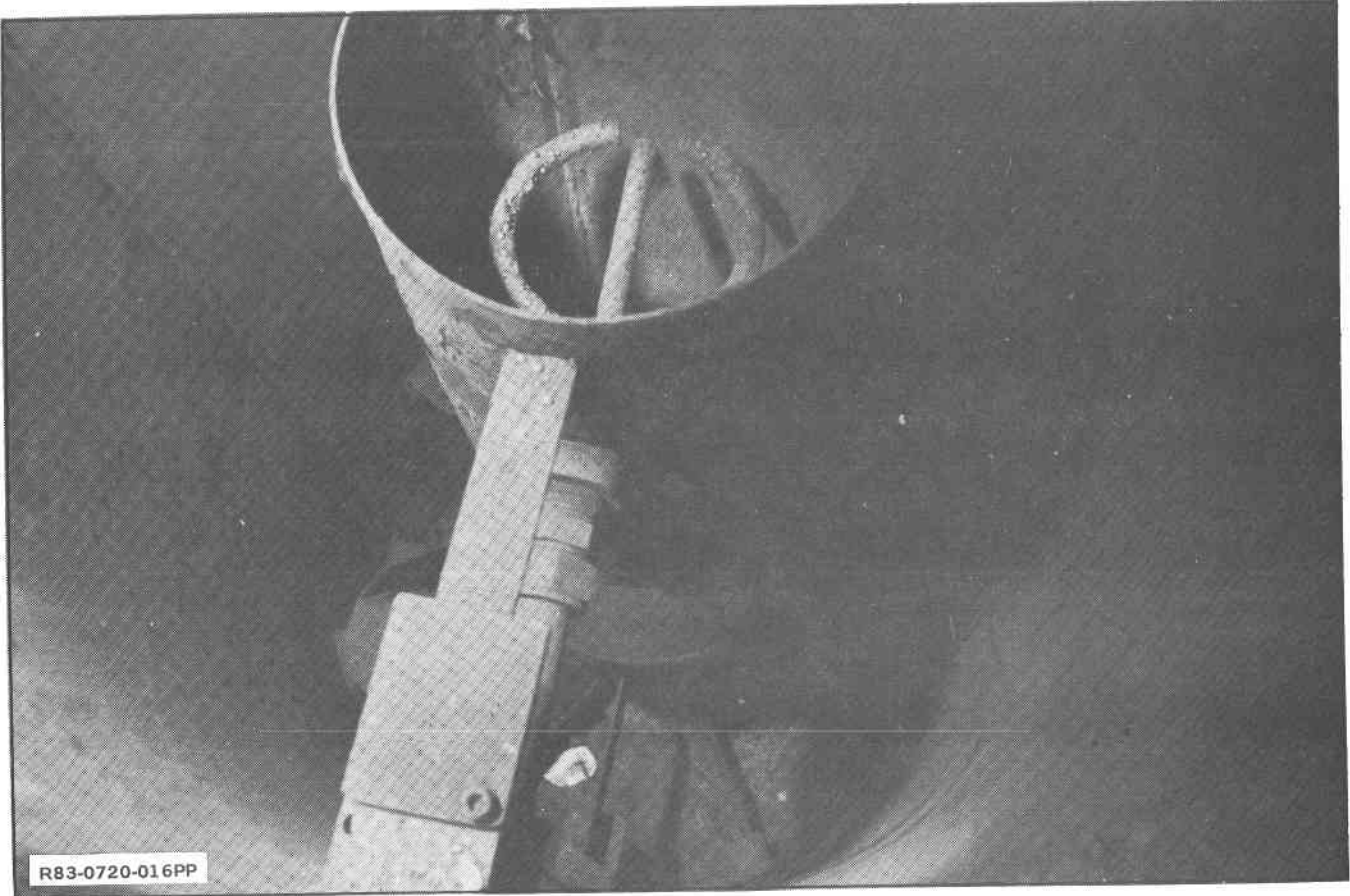


Fig. 3-12 Heat Exchange Module Interior



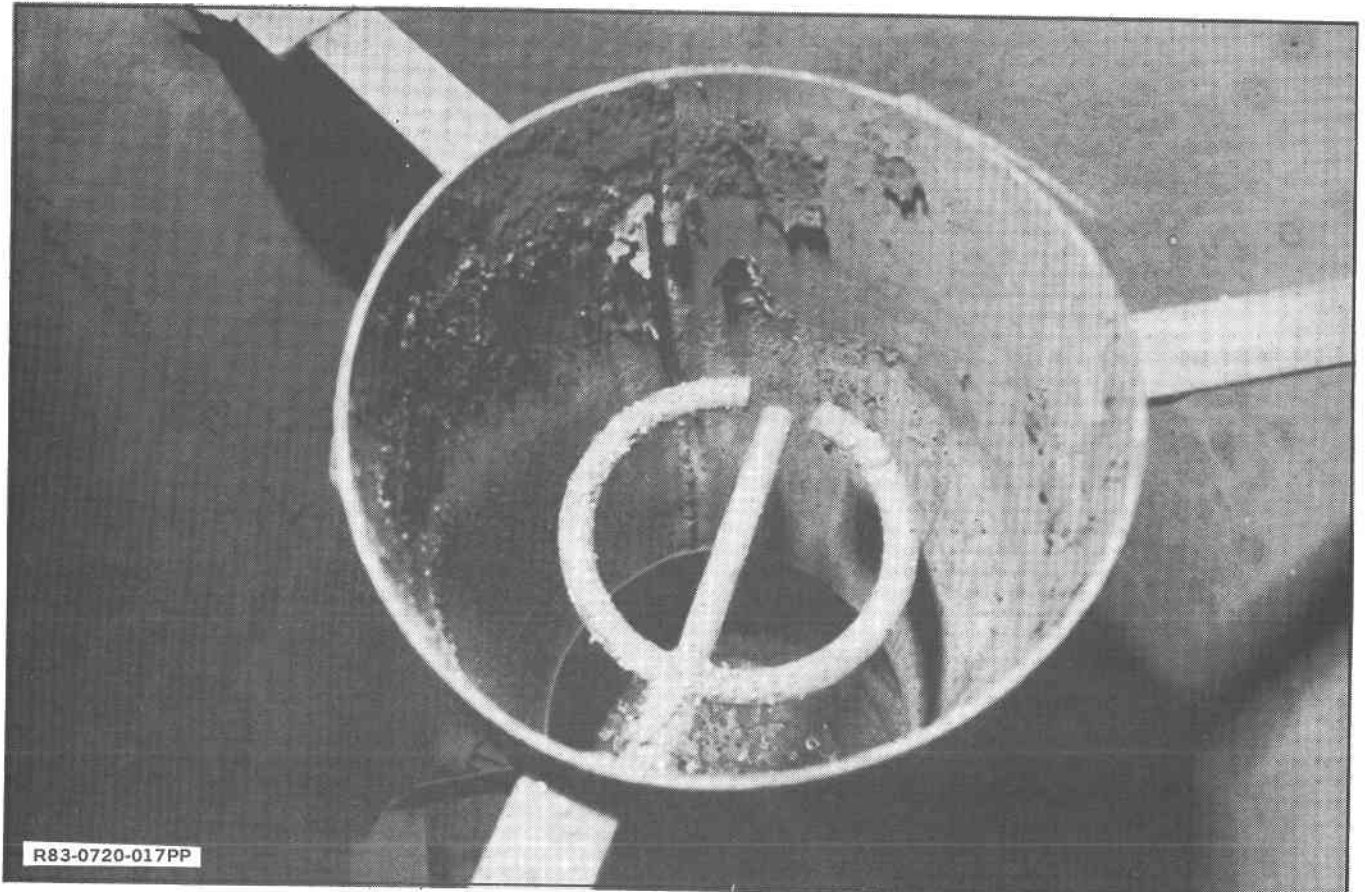


Fig. 3-13 Heat Exchange Tower Interior

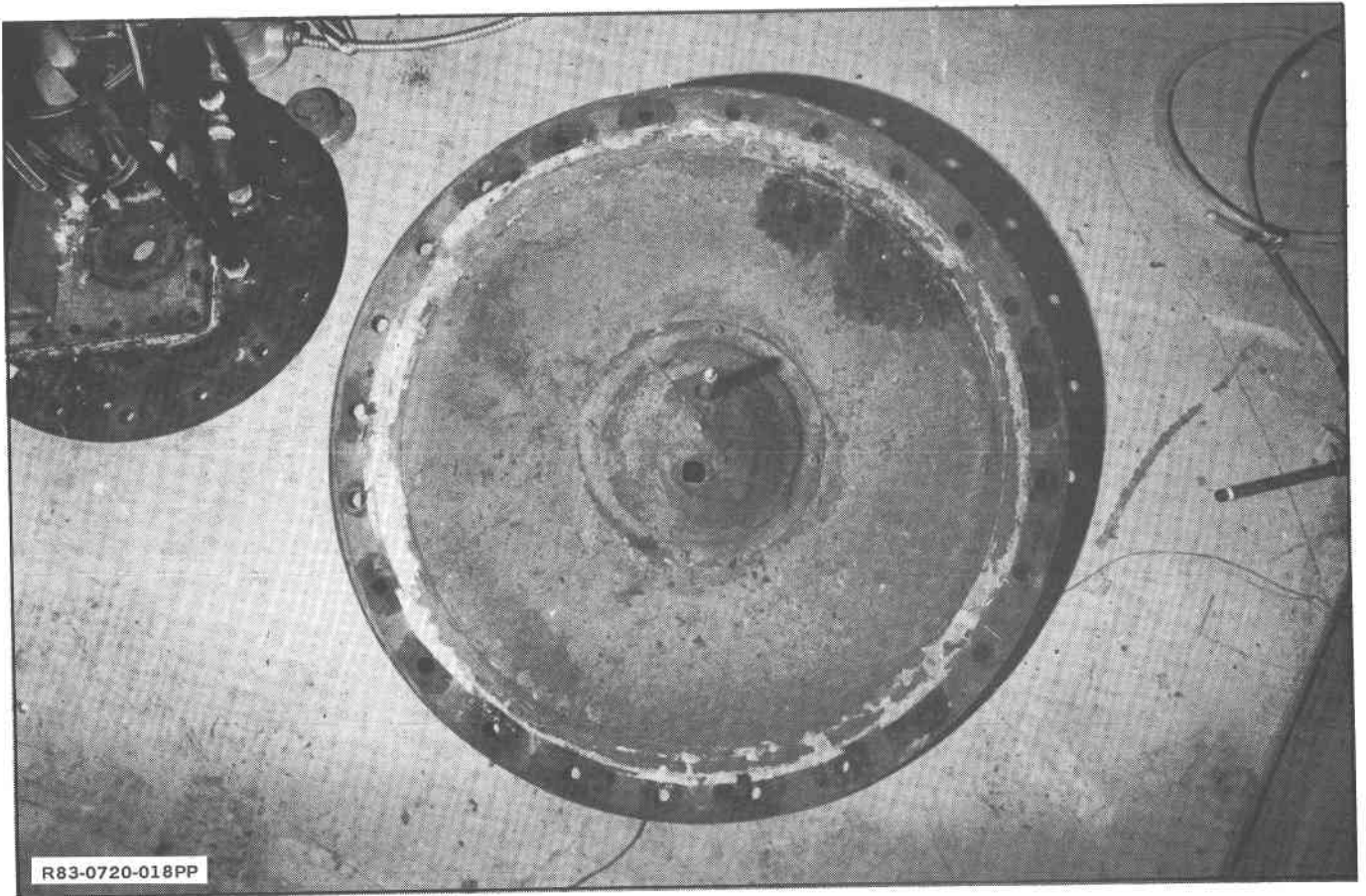


Fig. 3-14 Heat Exchange Module Cover Interior

**SERI** 

## 4 - SYSTEM MODIFICATIONS AND REFURBISHMENT

The following major system modifications were made to simplify the design and improve performance:

- Changed energy storage medium
- Modified pumping system
- Added new tanks and plumbing
- Eliminated all internal heaters
- Provided 100% trace heating
- Included automatic controllers for heater circuits
- Provided continual heating of liquid metal lines.

### 4.1 CHANGED ENERGY STORAGE MEDIUM TO LOWER MELTING POINT OF INORGANIC SALT

The high melting point (385°C) chloride eutectic originally involved complicated system operation by requiring excessively long times to preheat. Experience showed that heating to a 260°C level could be readily accomplished; thus, using a salt with a lower melting point would be easier. Two candidate salts were recommended from a survey of the literature: draw salt (46%  $\text{NaNO}_3$ /54%  $\text{KNO}_3$ ) and pure sodium nitrate ( $\text{NaNO}_3$ ). A summary of their properties is presented in Table 4-1.

Draw salt (46%  $\text{NaNO}_3$ /54%  $\text{KNO}_3$ ) was ultimately selected because of its widespread use in sensible heat storage systems. Augmenting these sensible heat systems with a latent heat storage capability has been shown to be economically feasible in preliminary studies of large solar power systems. Therefore, these test data could be of immediate use.

### 4.2 MODIFIED PUMPING SYSTEM

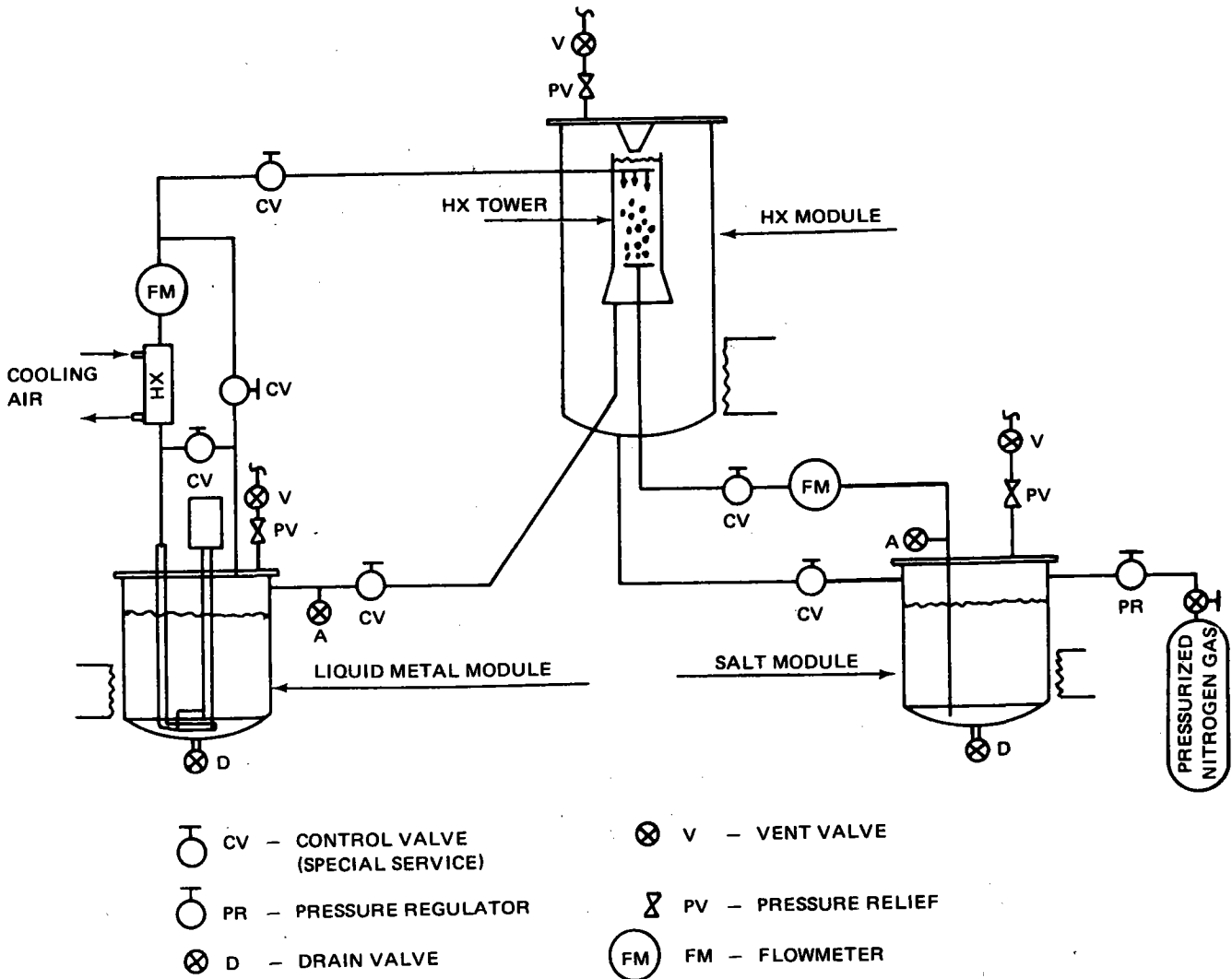
The original pumping system resulted in many of the operational problems previously encountered. Pumping lift margins were inadequate and the "leak-tight" seals malfunctioned at operating temperature. Thermal distortion caused binding of the impeller which could only be relieved by compromising the seals.

TABLE 4-1 NITRATE SALT PROPERTIES

PROPERTY	NaNO <sub>3</sub> · KNO <sub>3</sub>	NaNO <sub>3</sub>
MOLECULAR WEIGHT	93.06	84.99
MELTING POINT, K	500	580
HEAT OF FUSION, kJ/kg	137.3	182.1
SPECIFIC HEAT, kJ/kgK		
• SOLID	1.46	1.88
• LIQUID	1.8	1.84
THERMAL CONDUCTIVITY, W/mK		
• SOLID	--	0.57
• LIQUID	0.57	0.61
DENSITY, kg/m <sup>3</sup>		
• SOLID	2178	2258
• LIQUID	1885	1906
DECOMPOSITION TEMP, K	773	653
SURFACE TENSION @ T <sub>MELT</sub> , N/m	0.122	0.119
VISCOSITY, Pa · S	0.0047 AT 247°C	0.0029 AT 317°C
R83-0720-020PP		

The modified system was designed to provide leak-tight operation and sufficient pumping capacity (see Fig. 4-1). The centrifugal pump in the salt module was replaced by a pressurized nitrogen gas pumping system. This was possible because of the noncontinuous nature of the discharge (heat recovery) cycle which involves a single pass of the entire molten salt charge through the heat exchanger column. Solidified droplets and slurry are held at the bottom of the heat exchange tower where they are melted during a separate charging cycle.

Liquid metal pumping was provided using a special-purpose centrifugal pump which is driven by a 2-hp electric motor. The selected pump is manufactured by Lawrence Pumps for special-purpose high-temperature applications. It is designed with mechanical seals and slip joints located outside the tank module to provide very low gas leak rates at high operating temperatures. To simplify installation, the manufacturer supplied the pump already attached to the proper tank lid cover. All that need be done was to place the pump and cover assembly on the tank and secure the bolts.



R83-0720-021PP

Fig. 4-1 System Schematic (Hybrid Pumping)

### 4.3 NEW TANKS AND PLUMBING

All three tanks were replaced since this was both less expensive and more reliable than reclaiming the old tanks. In addition, access ports were provided in the cover lids of each tank. The ports in the salt and liquid metal lids were used for loading materials. The access port in the heat exchanger can be used to extract samples of the solidified salt after a test run.

All plumbing was replaced with new 1-in. (inside diameter) stainless steel tubing. Swagelok threaded-type connections were tightened while being heated (torch) to preclude leaks during actual operation.

#### 4.4 ELIMINATION OF ALL INTERNAL HEATERS

All the internal "firerod" heaters became inoperable during the first test series, either due to shorts, open circuits, or corrosion. Therefore, all internal-type heaters were eliminated. Tank heating was supplied by external band heaters prefitted to the proper diameter; these are relatively inexpensive and worked well during the first tests. Redundancy of the band heaters was provided in case of single heater failure.

#### 4.5 100% TRACE HEATING

All plumbing lines and valves were completely trace-heated using adhesive-backed electrical ribbon. The heating tape was helically wound using 0.61 m of tape for every 0.30 m of line. Supporting laboratory tests verified service temperatures up to 425°C.

#### 4.6 AUTOMATIC CONTROLLERS FOR HEATER CIRCUITS

All six major heater circuits were equipped with proportional controllers to regulate temperature. This will avoid the overheating problems and numerous heater failures that occurred during the first test series when manual control was used. Also, the liquid metal requires that the liquid metal lines be heated at all times to prevent inadvertent solidification and subsequent rupture due to expansion.

#### 4.7 CONTINUAL HEATING OF LIQUID METAL LINES

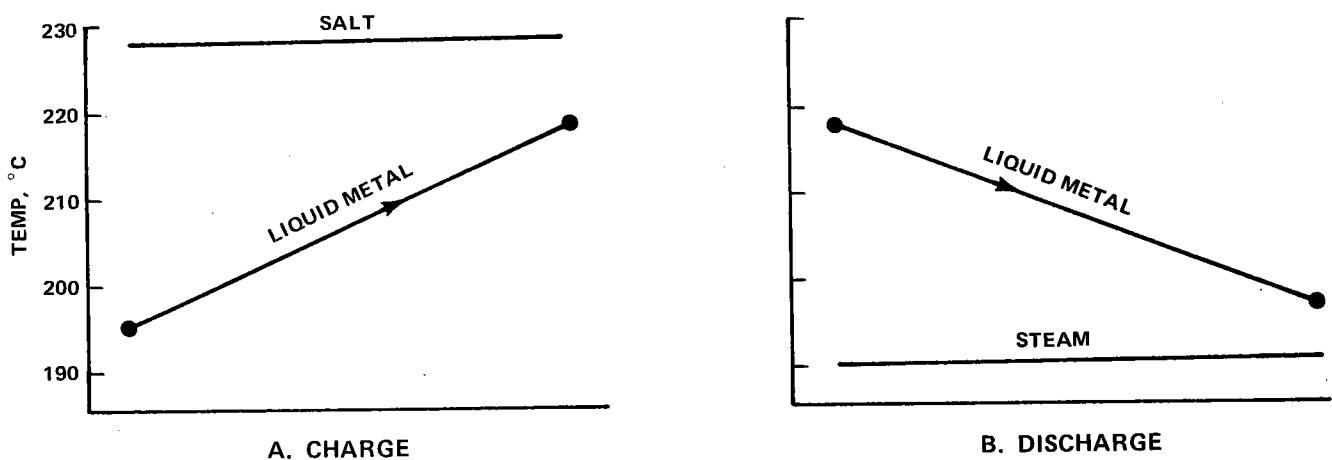
The liquid metal carrier fluid is Indalloy 225, a fusible eutectic of lead and bismuth (44.5% Pb/55.5% Bi) that melts at 124°C. It exhibits a cumulative growth upon solidification of up to 0.0022, which could cause pipe rupture if the liquefied material cannot be adequately drained after system operation. To prevent this, the liquid metal lines will always be trace-heated. Thermal property data for Indalloy 255 are given below:

- Melt Point..... 331K
- Density, Kg/m<sup>3</sup>..... 9995
- Specific Heat..... 146
- Thermal Conductivity, W/mK.... 10.69
- Viscosity, Pa.S..... 0.0017

## 5 - DETAILED DESIGN SUMMARY OF THE HEAT EXCHANGE COLUMN

### 5.1 SYSTEM CONSIDERATIONS

The direct-contact heat exchanger must operate between the temperature limits imposed by the melting point of the energy storage medium and the temperature requirement of the ultimate heat sink. This is illustrated in Fig. 5-1 for typical liquid metal charge and discharge cycles using drawsalt (melting point = 227°C) as the energy storage heat source for generating steam at 27 kPa (190°C). A temperature-drop allowance must also be provided at the points of heat transfer to the intermediate liquid metal carrier fluid loop. Typical allowances (called pinch points) are about 8°C. Smaller temperature differences are uneconomical since they require larger, more expensive heat exchangers and larger pinch points waste the available energy.



R83-0720-022PP

Fig. 5-1 Direct-Contact Heat Exchanger Operating Temperature Limits

### 5.2 MASS AND FLOW RATE REQUIREMENTS

The following amounts of material and flow rates are needed to provide a 10 kWh storage and 10 kW heat transfer rate:

- Draw Salt

$$\text{Mass} = \frac{Q}{\lambda} = 263 \text{ kg}$$

$$\text{Flow Rate} = \frac{q}{\lambda} = 0.073 \text{ kg/s}$$



- Liquid Metal

Mass = 499 kg (based on system volume considerations: liquid metal module, heat exchange column, plumbing)

$$\begin{aligned} \text{Flow Rate} &= \frac{q}{C_p \Delta T} \\ &= 3.07 \text{ kg/s (using } \Delta T = 22^\circ\text{C)} \end{aligned}$$

### 5.3 INJECTOR DESIGNS

#### 5.3.1 Molten Salt

Treybal (Ref. 3) contains design rules for countercurrent liquid extraction towers that apply to this heat exchanger concept. To ensure the formation of a bubble or drop of salt from the injector orifice, the maximum orifice exit velocity should be 0.09 m/s. Higher exit velocities will result in jetting or streaming of the salt with breakup some distance away into highly nonuniform particle sizes. The recommended orifice diameters should not be smaller than 2.5 mm to prevent clogging or larger than 6.4 mm to avoid excessively large drops.

Treybal also gives an empirical equation (engineering units) which permits the calculation of drop volume (and diameter) for the dispersed liquid for nozzle velocities up to 0.09 m/s. For our system, the approximate general equation becomes:

$$\frac{\pi}{6} d^3 = 0.0203 \frac{\sigma d_o}{\Delta \rho} + \frac{5.942 d_o^{1.12} \bar{v}_o^{0.547} \mu_f^{0.279}}{\Delta \rho^{1.5}} \quad (5.1)$$

where  $d$  = drop diameter, in.

$d_o$  = orifice diameter, in.

$\Delta \rho$  =  $(\rho_f - \rho_L)$ , lb/ft<sup>3</sup>

$\bar{v}_o$  = exit velocity, ft/sec (0.3 ft/s, max)

$\mu_f$  = viscosity, centipoise

$\sigma$  = surface tension, dyne/cm

Using a value for the surface tension of 0.12 N/m (120 dyne/cm) and a 3.2 mm (0.125 in.) orifice diameter yields a droplet diameter of about 2.7 mm over an inlet velocity range of 0.03 - 0.09 m/s. This value is smaller than the orifice diameter, which is not physically possible. Therefore, the expected droplet diameter will be assumed equal to the orifice diameter of 3.2 mm.

The salt injector has 128 orifice openings for a total orifice area equal to  $1.02 \text{ m}^2$ . The average injection velocity at the nominal  $0.073 \text{ kg/s}$  flow rate will be  $0.038 \text{ m/s}$ . The 128 holes can be equally distributed on a 152-mm diameter circular spray head. To promote proper droplet formation, each orifice should protrude a small distance, up to one half the orifice diameter ( $1.6 \text{ mm max}$ ), as shown in Fig. 5-2.

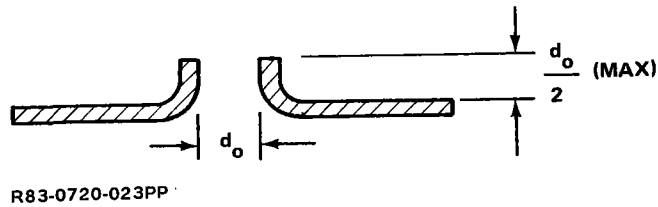


Fig. 5-2 Orifice Opening

### 5.3.2 Liquid Metal

For the liquid metal injector, there should be a minimum of 50 entry points per square meter of column area. Several designs are possible (see Fig. 5-3).

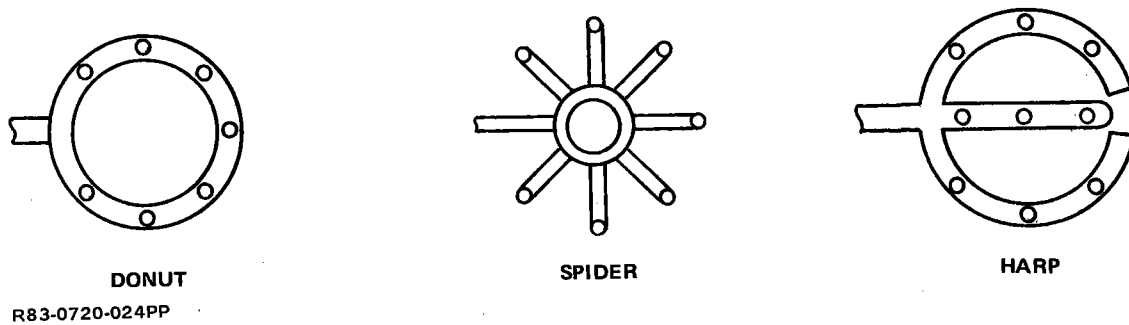


Fig. 5-3 Liquid Metal Injector Designs

The harp concept offers the best combination of uniform carrier fluid distribution and least interference with the rising agglomeration of solid salt particles. Nominal pipe diameters of  $0.20$  to  $0.30 \text{ cm}$  can be used with holes of the same diameter cut out to the centerline of the tube.

### 5.4 LIQUID METAL VELOCITY

The heat exchange reservoir is the most critical component of the system since all of the latent heat transfer occurs here. It is the mixing chamber for the liquid

metal carrier fluid, which enters from the top, and the molten salt droplets, which are injected from below. The required cross-sectional area is governed by the fluid flow rates and the limiting velocities. The column height (i.e., flow path length) is a function of the residence time required for solidification and the relative flow velocity of the salt droplet.

Successful operation of a counterflow spray tower requires that the downward linear velocity of the heavy liquid (carrier fluid) be kept well below the rising velocity of the lighter dispersed fluid droplets; otherwise the lighter fluid will be swept toward the bottom of the reservoir and possibly into the exit of the carrier fluid. When this happens, the tower is "flooded" and satisfactory operation is impossible. The flooded condition can actually be caused by increasing the flow rate of either phase and, for each flow rate of light liquid, there is a flow rate for the heavy liquid that results in flooding. Treybal gives the following empirical expression (engineering units) for flooding velocity ( $\bar{V}_{ff}$ ):

$$\bar{V}_{ff} = \frac{(10^4) \Delta\rho^{0.28}}{\left[ 0.483 \mu_f^{0.075} \rho_f^{0.5} + d^{0.056} \rho_L^{0.5} \left( \frac{\dot{V}_s}{V_f} \right)^{0.5} \right]^2} \quad (5.2)$$

where  $\bar{V}_{ff}$  = flooding velocity, ft/h

$\Delta\rho$  =  $(\rho_f - \rho_L)$ , lb<sub>m</sub>/ft<sup>3</sup>

$d$  = drop diameter, ft

$V_s, V_f$  = ft<sup>3</sup>/hr of salt(s) and carrier fluid(f)

$\rho_f, \rho_L$  = density of carrier fluid (f) and molten salt (L), lb/ft<sup>3</sup>

$\mu_f$  = carrier fluid viscosity, centipoise

Using the nominal design conditions, Eq 5.2 gives 0.02 m/s for the flooding velocity limit. A conservative value of 0.01 m/s has been used in the design for the carrier fluid velocity.

## 5.5 SALT DROPLET VELOCITY

The velocity of a rising salt droplet can be obtained from a dynamic force balance, which yields:

$$\frac{dV}{dt} = \frac{F_B - F_D}{m}$$

where

$$F_B = (\rho_f - \rho_L) \frac{\pi}{6} d^3$$

$$F_D = \frac{\pi d^2}{4} \frac{C_D \rho_f}{2g} (V_S + V_f)^2$$

$$m = \rho_L \frac{\pi}{6} d^3$$

Upon substitution (using  $C_D = 0.4$ ) and defining  $V = (V_S + V_f)$ ,

$$\frac{dV}{dt} = 4.34 - 4.80 V^2 \quad (5.3)$$

Using numerical techniques, an expression for  $V$  as a function of time can be obtained. With  $V_f = 0.01$  m/s, the bubble reaches a maximum velocity of 0.28 m/s after 0.7 sec. have elapsed, or after it has risen 0.17 m. A graph of bubble velocity versus time is given in Fig. 5-4. The area under the curve is equal to the height at which the terminal velocity is reached.

## 5.6 SALT DROPLET SURFACE HEAT TRANSFER COEFFICIENT (h)

The Nusselt number correlation for liquid metal flow over a sphere is:

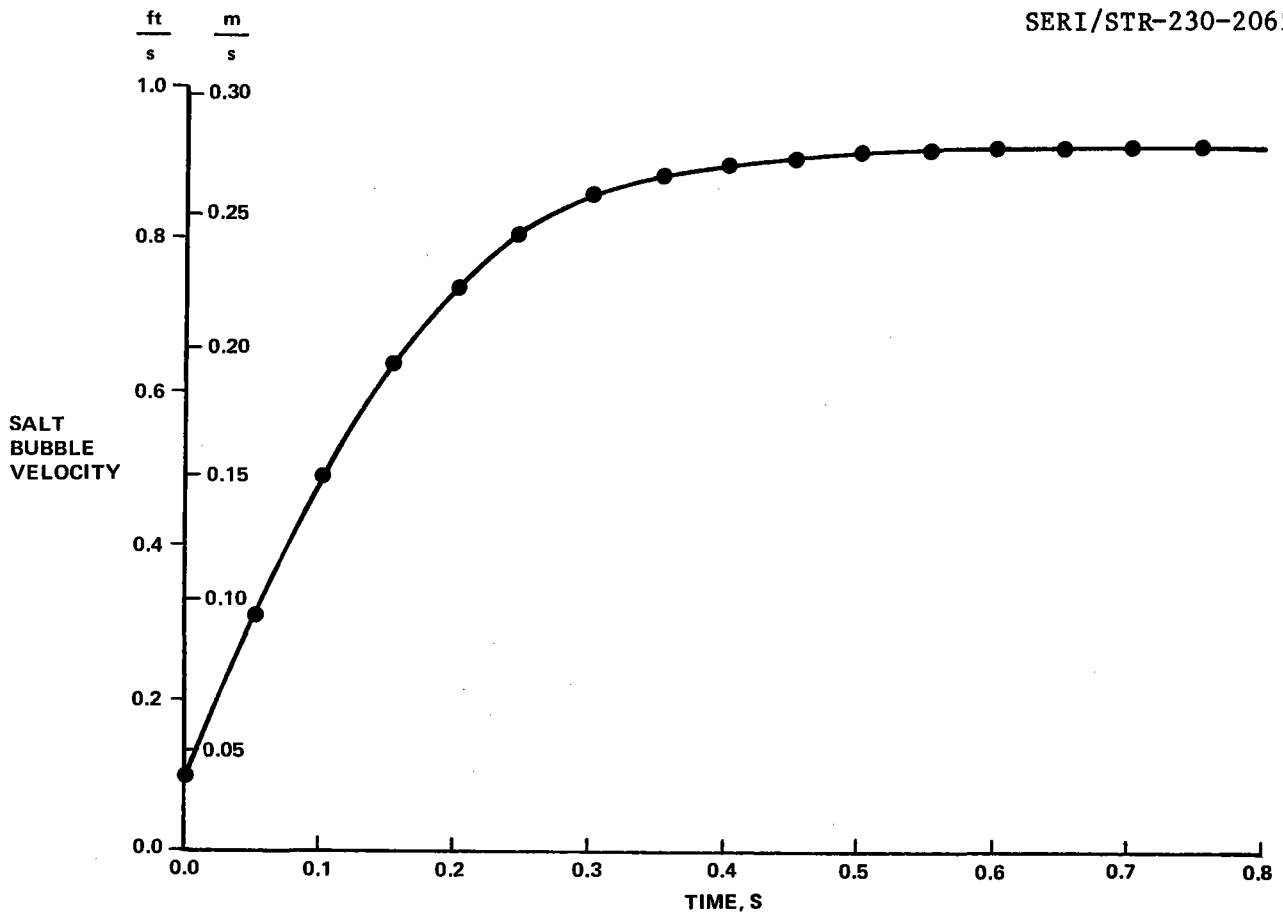
$$\frac{hd}{k_f} = 2 + 0.386 (\text{RePr})^{1/2}$$

The Reynolds number is given by:

$$\text{Re} = \frac{\rho_f d (V_S + V_f)}{\mu_f}$$

For  $\text{Pr} = 0.024$  and  $k_f = 10.7$  W/mK

$$h = 6688 + 27426 (V_S + 0.01)^{1/2}$$



R83-0720-025PP

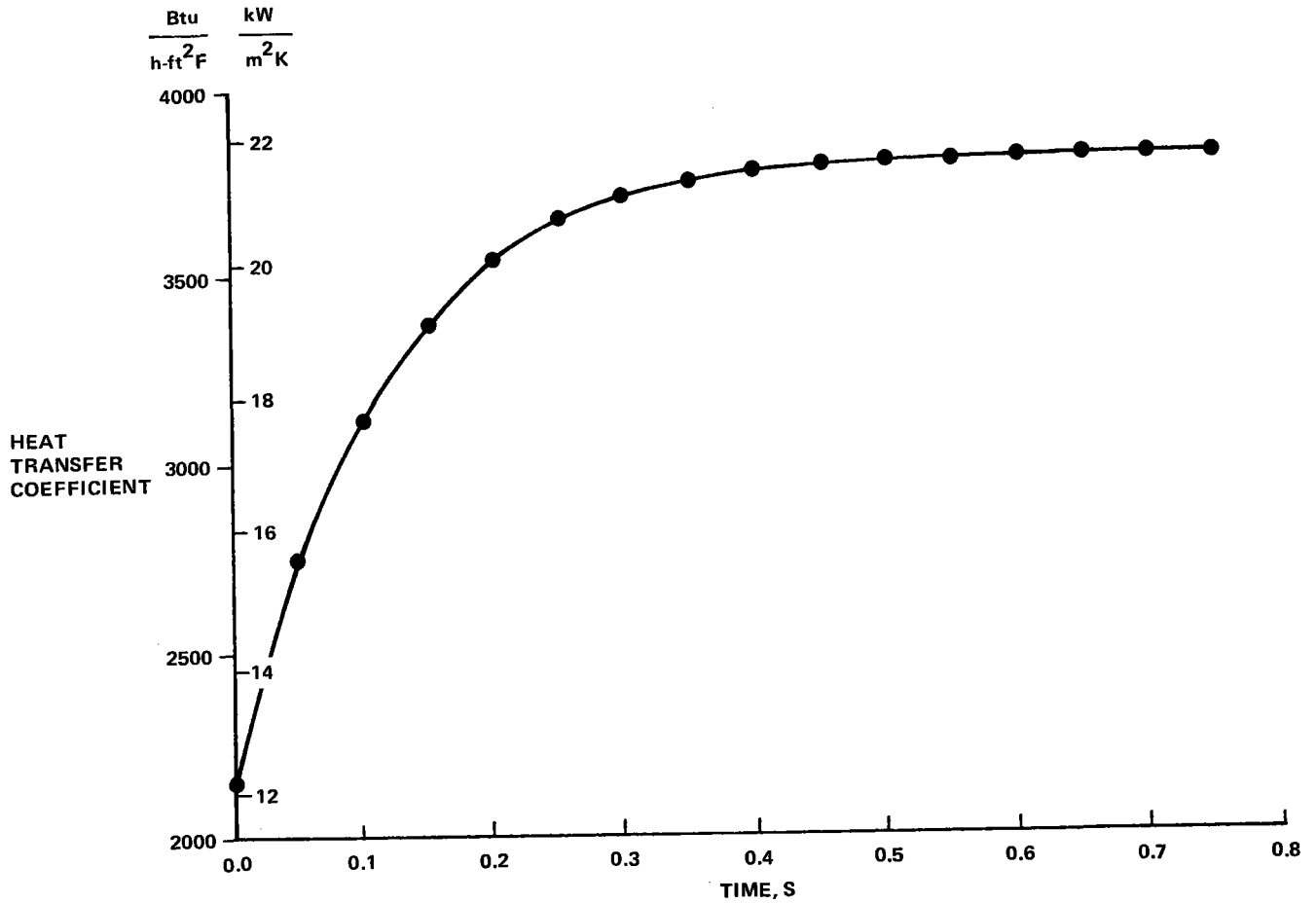
Fig. 5-4 Salt Bubble Velocity Vs Time

Now, since  $V_s$  is a function of time,  $h$  will also vary with time. However, as shown in Fig. 5-5,  $h$  approaches a limiting value rapidly; to simplify the calculations, the limiting value of  $h = 22000 \text{ W/m}^2\text{K}$  will be used.

### 5.7 RESIDENCE TIME FOR DROPLET SOLIDIFICATION

The residence time required to solidify a molten salt droplet which is rising through a counterflowing stream of liquid metal can be calculated by quantifying the heat transfer at each bubble in terms of the given physical parameters. Such an analysis is presented in Appendix A. The results are summarized below:

$$t_{\text{res}} = \frac{a\rho_s C_{p_f}}{3B} \left\{ \frac{a}{k_s \zeta} \left[ \frac{1}{2} \ln \frac{\left( \frac{\zeta^2 - \zeta + 1}{(\zeta + 1)^2} \right)}{\left( \frac{\zeta^2 - \alpha\zeta + \alpha^2}{(\zeta + \alpha)^2} \right)} + \sqrt{3} \left[ \tan^{-1} \left( \frac{2 - \zeta}{\sqrt{3}\zeta} \right) - \tan^{-1} \left( \frac{2\alpha - \zeta}{\sqrt{3}\zeta} \right) \right] \right] \right. \\ \left. + \left( \frac{1}{h} - \frac{a}{k_s} \right) \ln \left[ \frac{(A+B)}{(A+B\alpha^3)} \right] \right\}$$



R83-0720-026PP

Fig. 5-5 Variation of Heat Transfer Coefficient With Time

where

$$A = \frac{C_{p_f} (T_m - T_{f_o})}{\lambda} + \left( \frac{\dot{m}_s}{\dot{m}_f} \right) \left( \frac{\rho_s}{\rho_L} \right) \qquad B = - \left( \frac{\dot{m}_s}{\dot{m}_f} \right) \left( \frac{\rho_s}{\rho_L} \right)$$

$$\zeta = \left( \frac{A}{B} \right)^{1/3} = (-1) \left[ \left( \frac{\rho_L}{\rho_s} \right) \frac{\dot{m}_f C_{p_f} (T_m - T_{f_o})}{\dot{m}_s \lambda} + 1 \right]^{1/3}$$

$$\alpha = \left( 1 - \frac{\rho_L}{\rho_s} \right)^{1/3}$$

and

- a = bubble outside radius
- $C_{p_f}$  = specific heat of carrier fluid
- h = outside film heat transfer coefficient
- $k_s$  = thermal conductivity of solid salt
- $m_f$  = mass flow rate of carrier fluid
- $m_s$  = mass flow rate of salt
- $T_m$  = salt melt temperature
- $T_{f_o}$  = carrier fluid outlet temperature (Hot)
- $\rho$  = salt density (s = solid, L = liquid)
- $\lambda$  = salt latent heat of fusion

Since there is some uncertainty as to the thermal conductivity of the solid salt, the above equation was solved for different values of  $k_s$  ranging from 0.48 to 1.22 W/mK. The calculated residence times ranged from 3.57 to 1.53 sec, respectively.

## 5.8 REQUIRED HEAT EXCHANGE COLUMN HEIGHT

The required column height is determined by the following equation:

$$L_{req} = (t_{res}) (V_s - V_f)$$

$(V_s - V_f)$  is the net droplet velocity in the column. For values of  $t_{res}$  greater than 0.7 sec,  $V_s$  is a constant equal to 0.28 m/s. The velocity varies for values of  $t_{res}$  less than 0.7 sec, but it has been already determined that the droplet will rise 0.16 m during this initial transient period.

Using  $V_f = 0.01$  m/s, the total required column height is given below for three different assumed values of  $k_s$ :

$k_s, W/mK$	$t_{res}, s$	$L_{req}, m$
0.48	3.57	0.95
0.73	2.45	0.64
1.22	1.53	0.39

For this design, a column height (i.e., distance between salt and liquid metal injectors) of 0.76 m was used.

## 5.9 REQUIRED FLOW AREA

The required flow area for the heat exchange column can be determined from the flow stream continuity equations. For the liquid metal carrier fluid:

$$A_f = \frac{\dot{m}_f}{\rho_f V_f}$$

$$A_f = 0.0335 \text{ m}^2$$

For the salt stream:

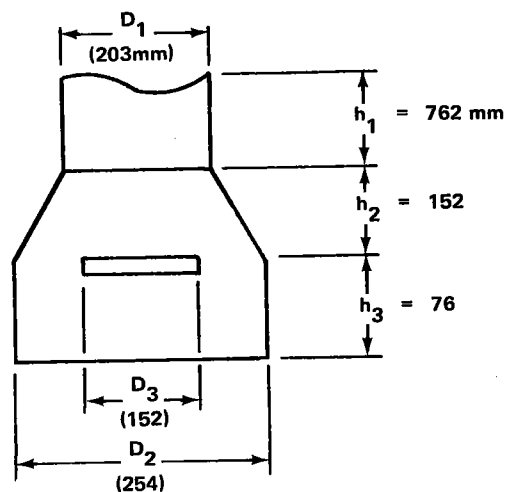
$$A_s = \frac{\dot{m}_s}{\rho_s (V_s - V_f)}$$

$$A_s = 1.4 (10^{-4}) \text{ m}^2$$

The total area required is the sum of  $A_s$  and  $A_f$ , or  $0.0336 \text{ m}^2$ . This can be obtained using a circular cylinder with a nominal 203-mm diameter.

## 5.10 HEAT EXCHANGE COLUMN GEOMETRY

To alleviate any difficulty arising from restricted flow area at the point of salt injection, the HX reservoir should be flared as shown in Fig. 5-6. The injector spray head is 0.15 m in diameter ( $D_3$ ). If the net flow area of the surrounding



R83-0720-027PP

Fig. 5-6 Heat Exchanger Column Geometry



annulus is set equal to the total area of the cylindrical section ( $D_1$ ), a base inside diameter ( $D_2$ ) of about 0.26 m will be needed. The calculated total net volume of this heat exchange column is  $0.0349 \text{ m}^3$ .

An additional feature of the design includes two liquid level sensors positioned 50 mm above and below the desired liquid metal carrier fluid level. This will permit necessary flow rate adjustments to be made, maintaining the fluid level at a nominal 76 mm above the liquid metal injector.

## 6 - MATERIALS COMPATIBILITY STUDY

It was known from the preceding program (Ref. 2) that certain combinations of molten salt and liquid metal could cause excessive oxidation of the metal. Subsequent operational problems might range from a slight change in the eutectic compositions of the materials to clogging of lines, valves, and fittings due to insoluble precipitates.

The original material combination was a chloride eutectic molten salt and lead-bismuth liquid metal which was shown to be a compatible mixture. However, the desire to change to a more generally used salt with a lower melting point created the need for another screening procedure.

Theoretical chemical reaction equilibria analyses were first run to determine the possibility of an oxidation reaction occurring. The results indicated that many of the candidate salts, including the prime nitrate salt, would react with the lead-bismuth carrier fluid. This in itself was not enough to eliminate these salts since nothing was known about the time needed to complete the reaction. Consequently, in-house laboratory tests were run to qualitatively determine the rate of reaction and catalyzation requirements so that an evaluation could be made. The specific objective was to determine if a nitrate salt could be used in the limited time needed for this technology demonstration.

The laboratory tests for each candidate salt consisted of a melting point determination followed by an insitu observation of reaction products when each salt was mixed with the liquefied lead-bismuth carrier fluid. Melting point measurements were made using a Perkin-Elmer DSC-2 Differential Scanning Calorimeter. The compatibility experiment apparatus consisted of a double-armed glass reaction vessel which was temperature-controlled. A continuous nitrogen gas purge was maintained over the melted samples. Contrary to the actual application, the materials were in constant contact with each other, which represents a very conservative situation.

The materials evaluated consisted of the following: both commercial-grade and reagent-grade mixtures of potassium nitrate and sodium nitrate salts from several manufacturers; reagent-grade potassium chloride and zinc chloride; and reagent-grade sodium hydroxide. Several samples were also run using the commercial-grade nitrate salts that were subsequently purified by filtering the insoluble impurities.

The important test results, which are detailed in Appendix B, are summarized below:

- The "as received" commercial-grade salts all contain sufficient impurities which cause them to quickly react with the liquid metal
- Laboratory-grade salts did not react with the liquid metal after 6-8 hours of contact and only moderately after 48 hours, reaching a steady state condition
- Commercial-grade nitrate salts which have been dissolved in water, filtered, and dried behave like the laboratory-grade salts and react moderately with the liquid metal
- The nitrate salts were judged suitable for conducting an evaluation of the direct-contact heat exchange concept.

These results have important implications when considering larger-scale applications of this direct-contact heat exchange system. The much less expensive commercial-grade materials, while economically attractive, cannot be used directly due to the attendant oxidation problems. However, the cost of reagent-grade materials (~\$5 per kg) makes them prohibitively expensive. The only realistic solution would be to purify the commercial-grade materials by simply filtering the insoluble impurities. This is best handled in bulk quantities at the point of manufacture. Olin Corp., the manufacturer of Solar Salt, has indicated a willingness to include a final filtration step in their production plant if a large enough market could be identified. This would create a suitable supply of nitrate salt (draw salt) at about \$1 per kg which could be used directly from the shipping containers. Otherwise, a specialized filtering step must be included on-site before the salt is loaded into its supply tank. These extra costs must be considered in the overall economic evaluation.

## 7 - HARDWARE FABRICATION AND SYSTEM ASSEMBLY

This section presents a photographic record of the modified direct-contact heat exchange system. Figure 7-1 shows the heat exchange tower after final installation. This is the same part that was used on the first test article, but it has been mechanically cleaned and a 0.38 m-long cylindrical extension inserted between the molten salt and liquid metal injectors. The three tank modules and their external band heaters are shown in Fig. 7-2. The automatic heater controllers for six circuits are shown mounted in Fig. 7-3. A view of the liquid metal pump installation is given in Fig. 7-4. Figure 7-5 shows the air heat exchanger and the liquid metal flowmeter. An opposite perspective, shown in Fig. 7-6, gives a better view of the line trace heaters and thermal insulation. The insulation is a low-binder fiberglass roll (Owens-Corning SR-26) which was applied in a minimum 0.23-m thickness to each tank and 76 mm around all lines and valves. Heat losses at operating temperature were estimated at less than 5% of the 10-kW design heat transfer rate.

Photographs of the final installation in a ready-to-test condition are shown in Fig. 7-7 and 7-8. Appendix C contains the design specification summary. Detailed operating instructions have been prepared and documented in Ref. 5.

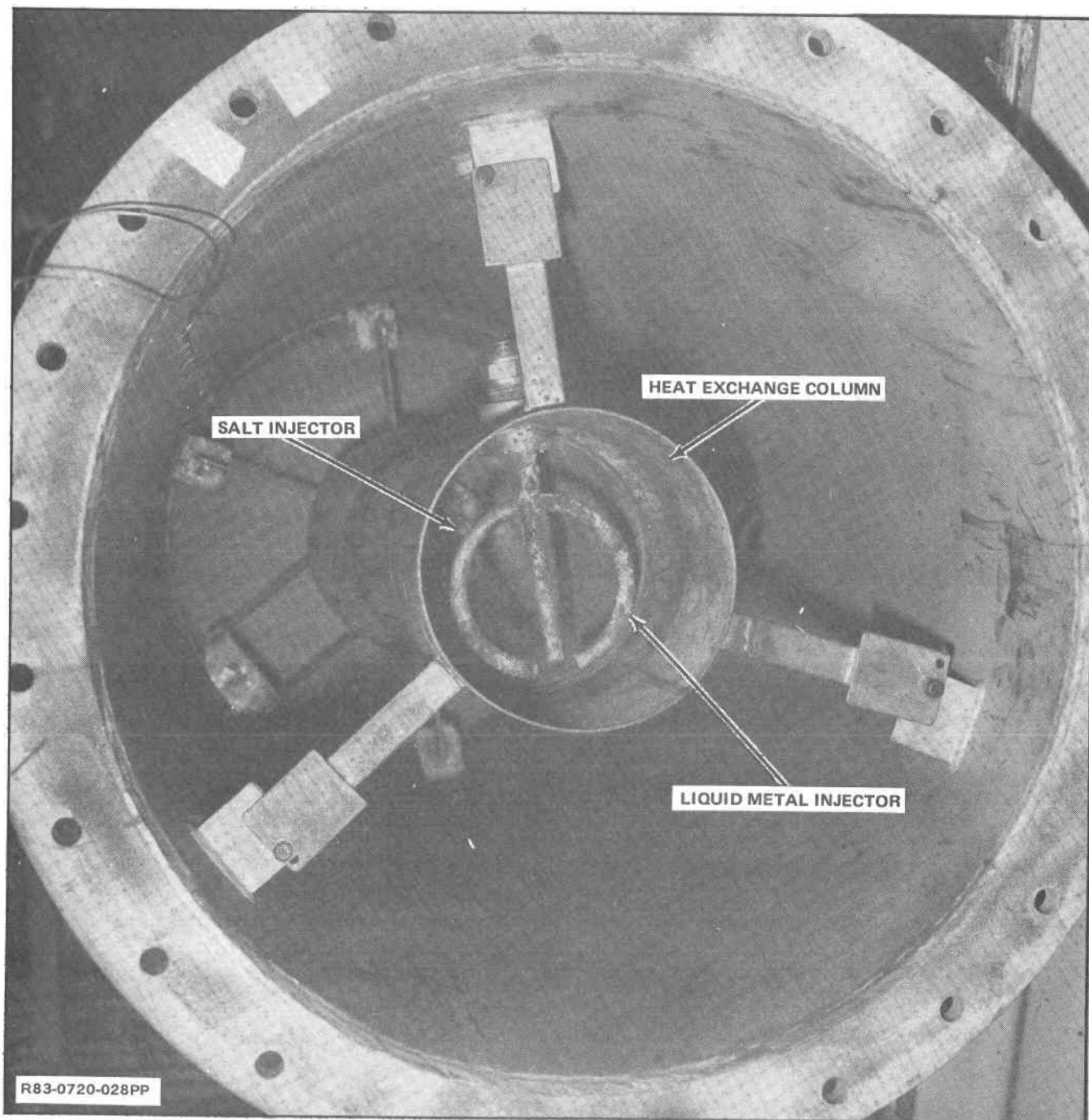


Fig. 7-1 Direct-Contact Heat Exchanger Tower Installed in Tank

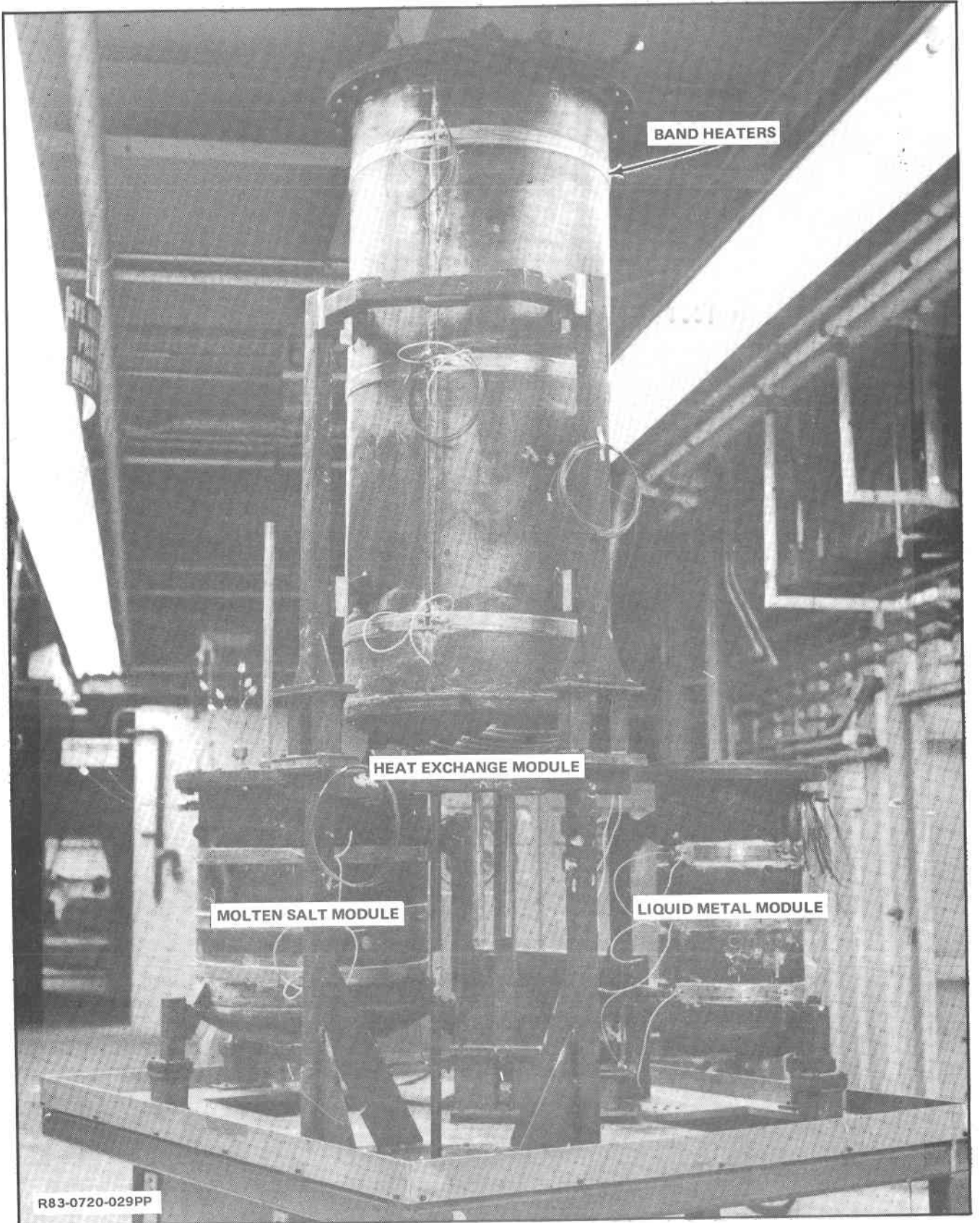
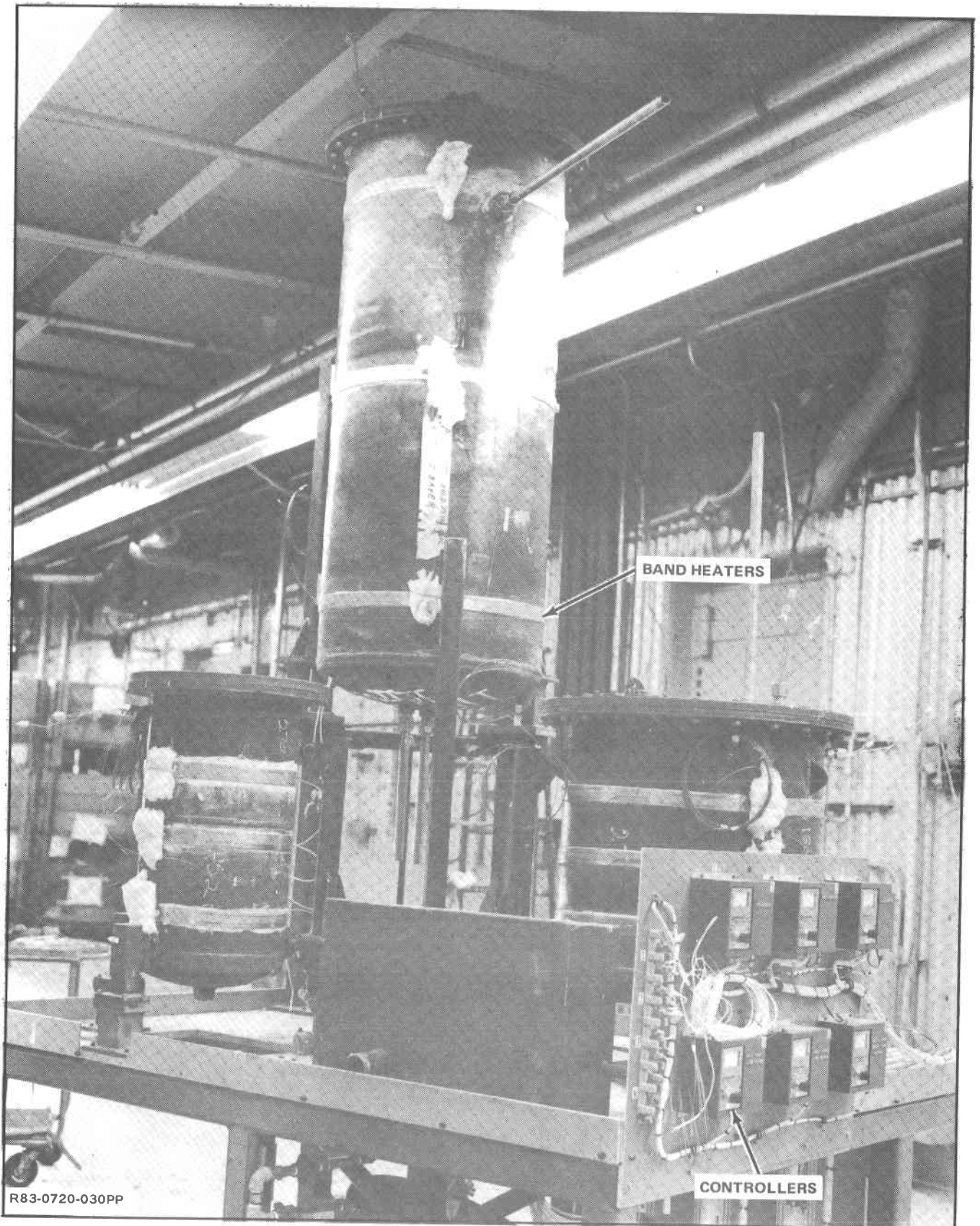


Fig. 7-2 Tanks Mounted and Band Heaters Installed





R83-0720-030PP

Fig. 7-3 Controllers Connected and Plumbing Started

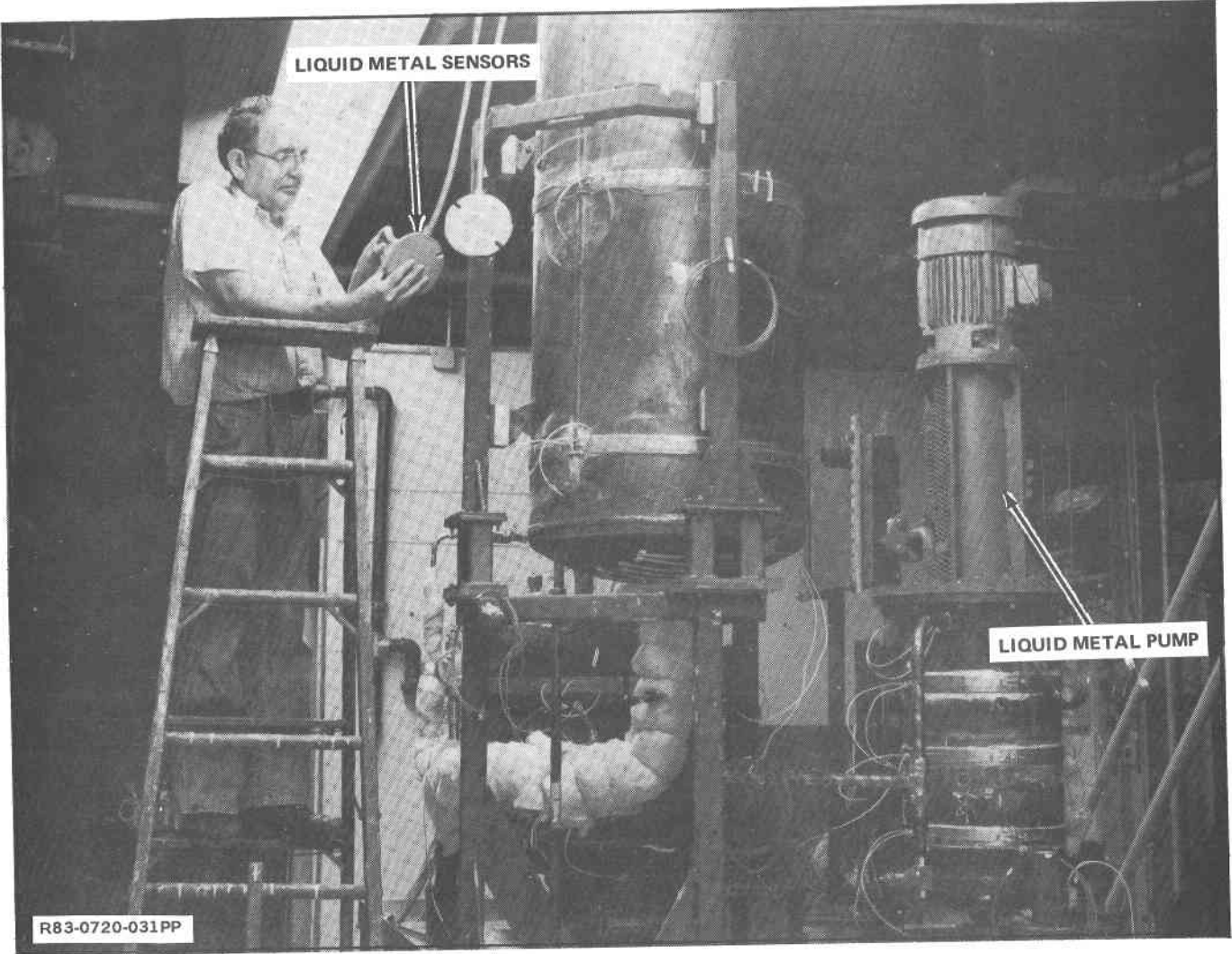
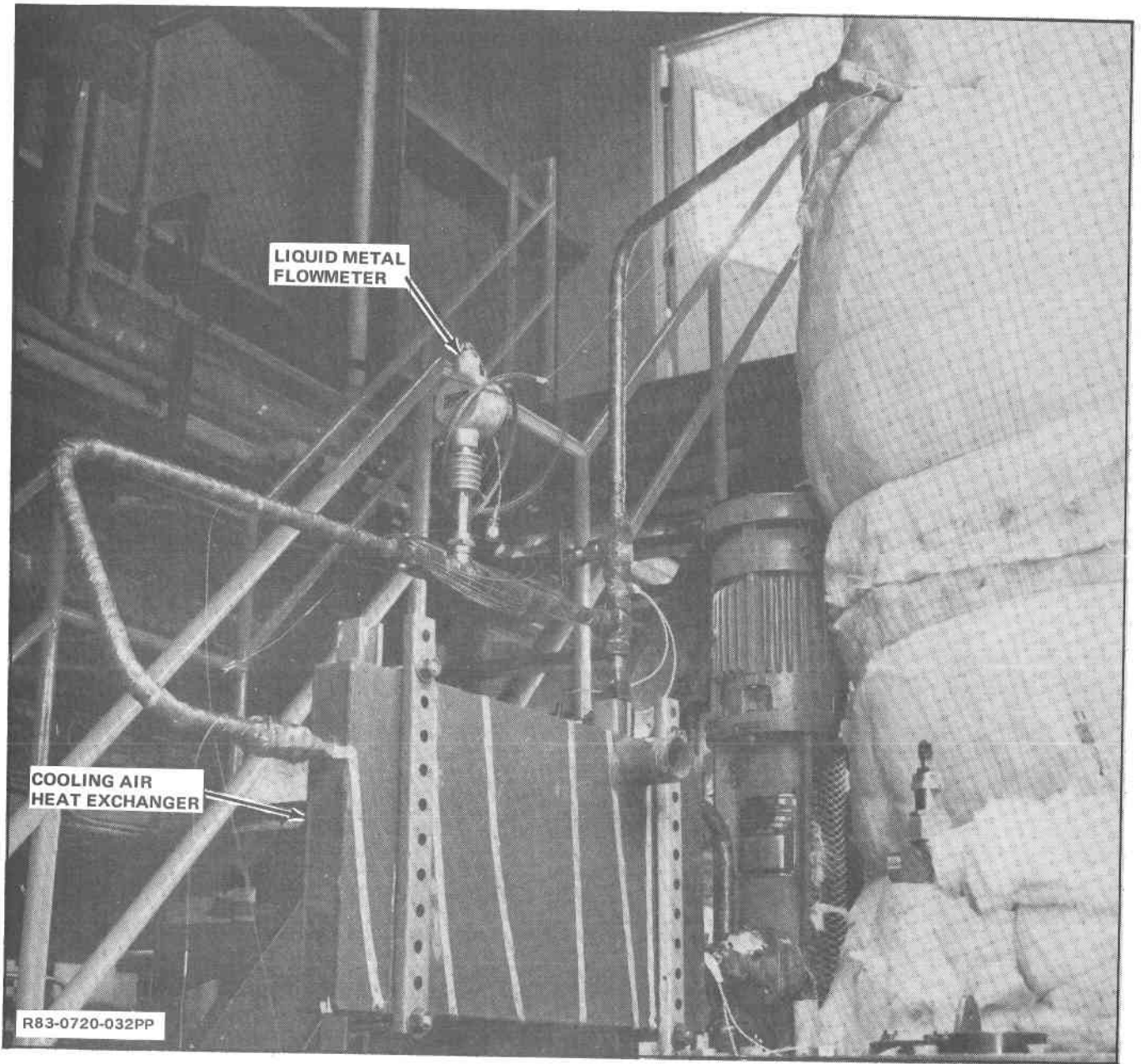


Fig. 7-4 Liquid Metal Pump Installed and Level Sensors Adjusted





LIQUID METAL  
FLOWMETER

COOLING AIR  
HEAT EXCHANGER

R83-0720-032PP

Fig. 7-5 Air Heat Exchanger Mounted

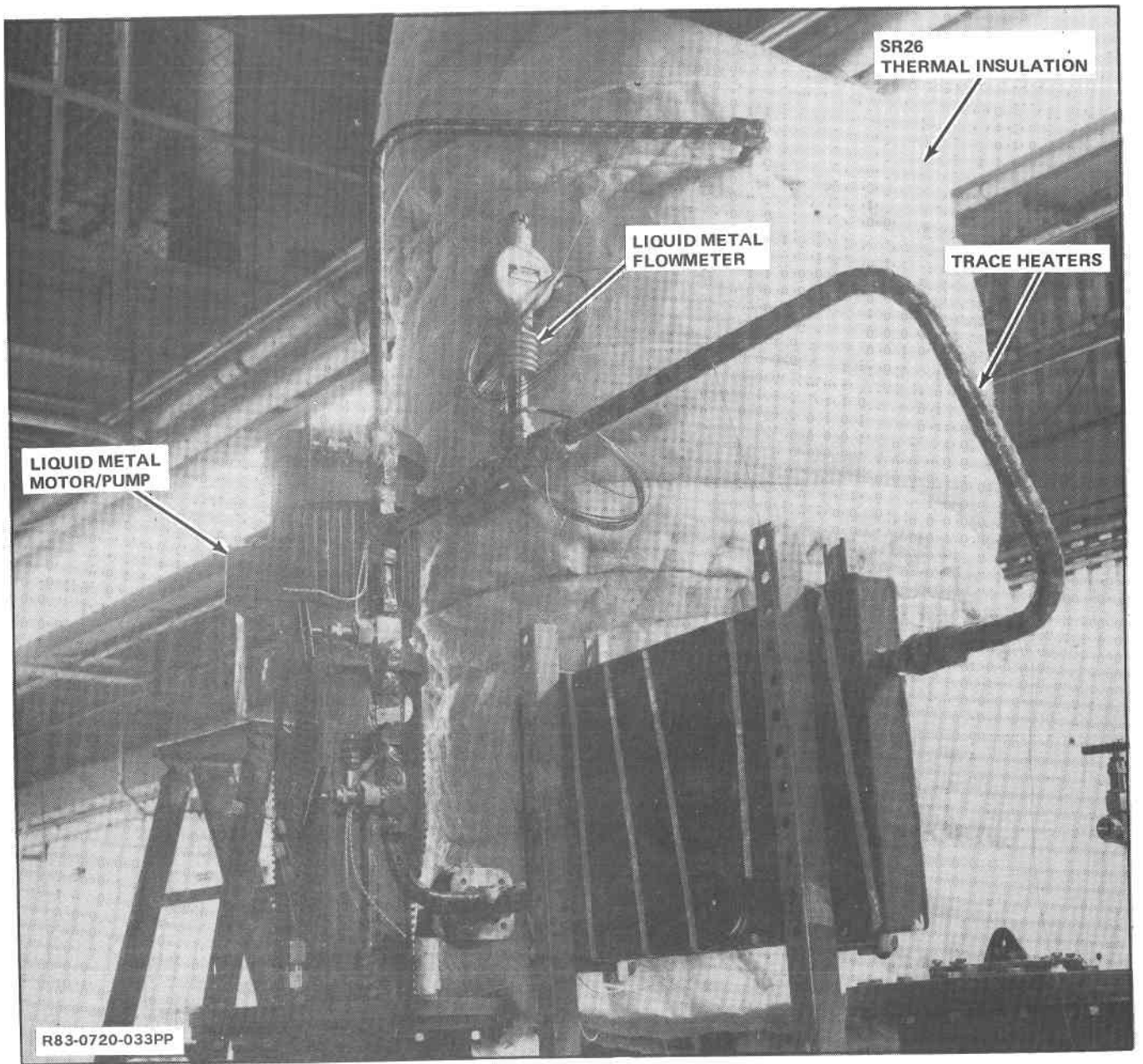
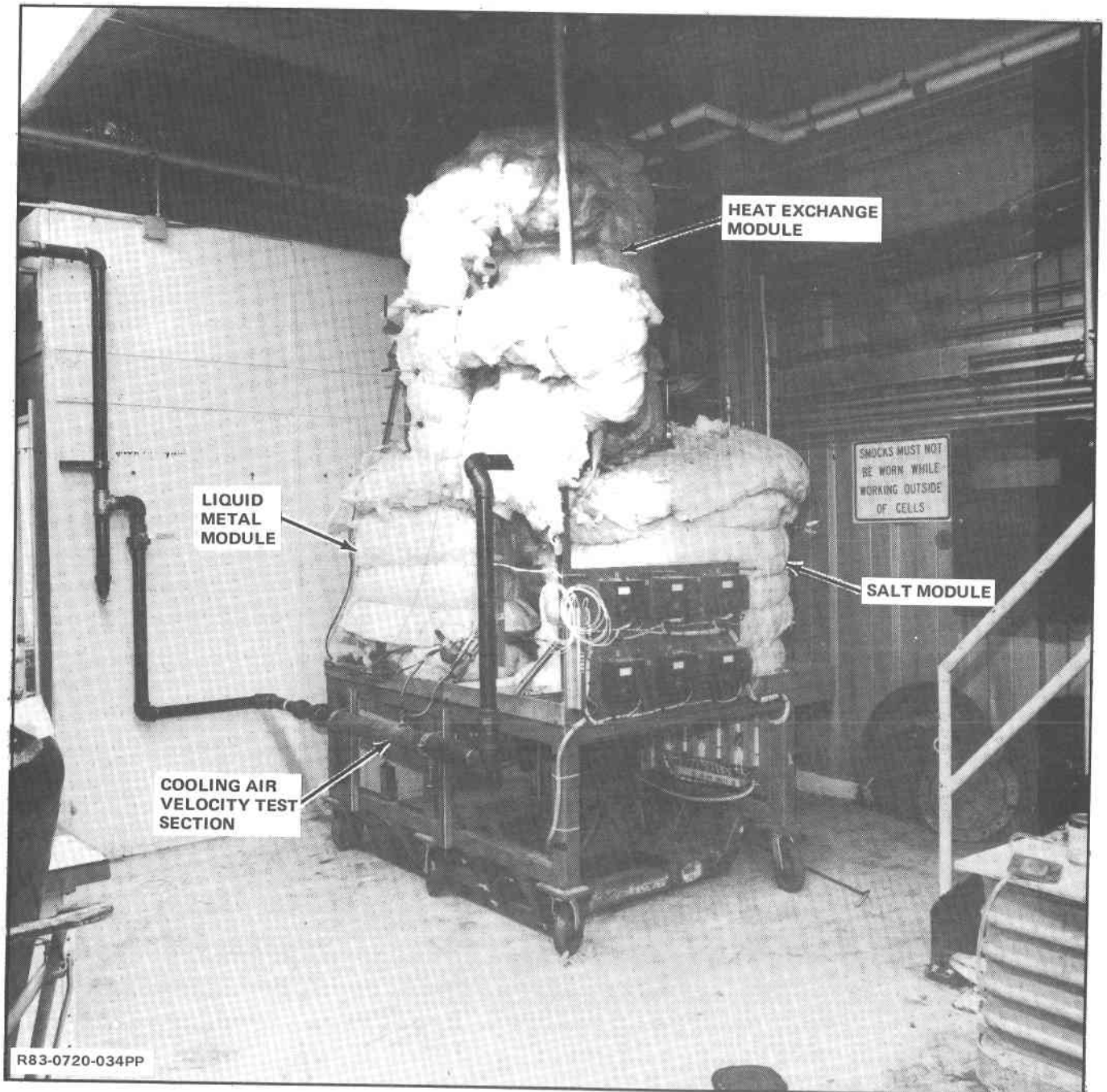


Fig. 7-6 Tank Insulation Applied and Line Heaters Installed



R83-0720-034PP

Fig. 7-7 Direct-Contact Heat Exchanger Final Assembly



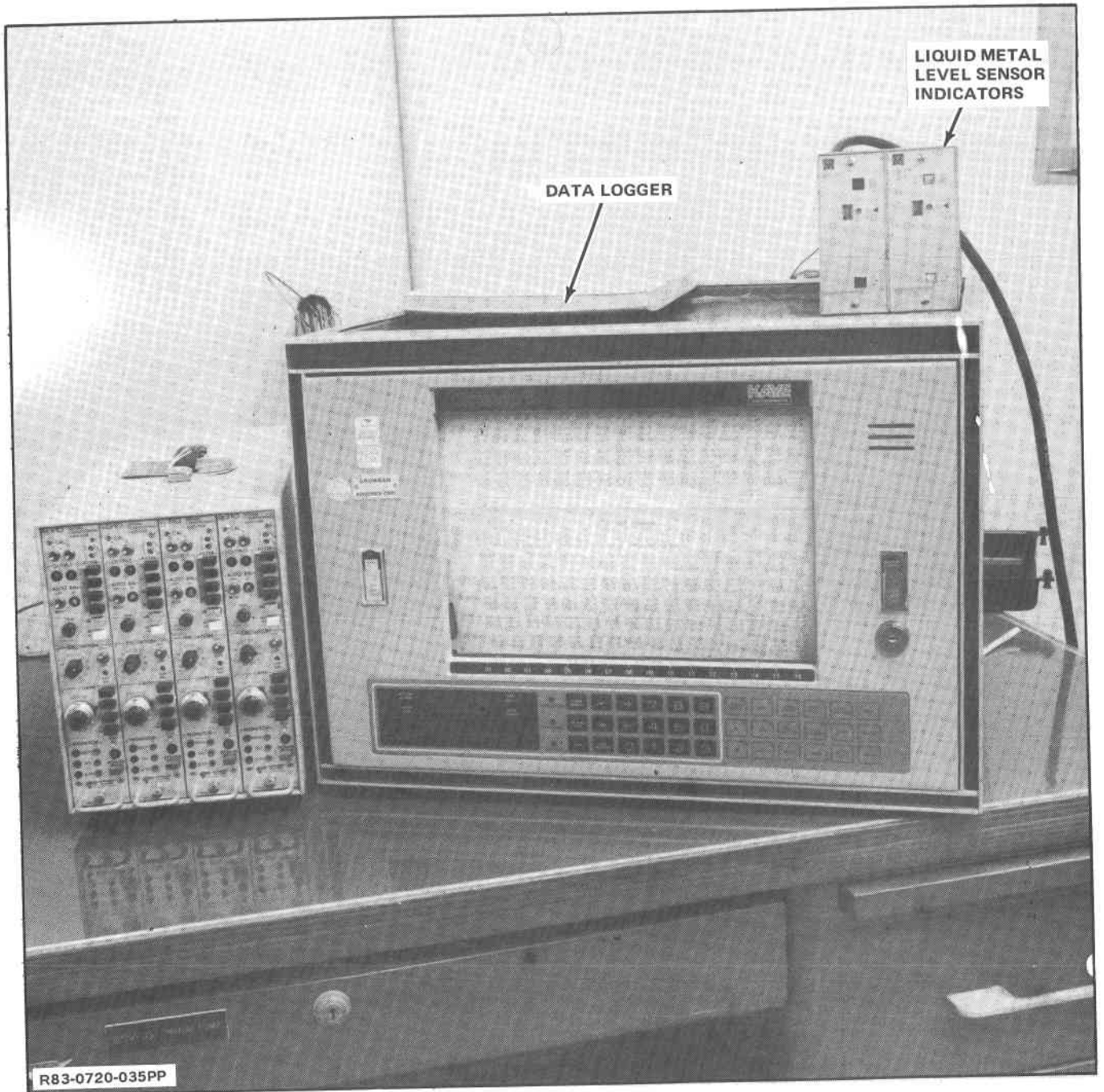


Fig. 7-8 Test Data Acquisition Setup



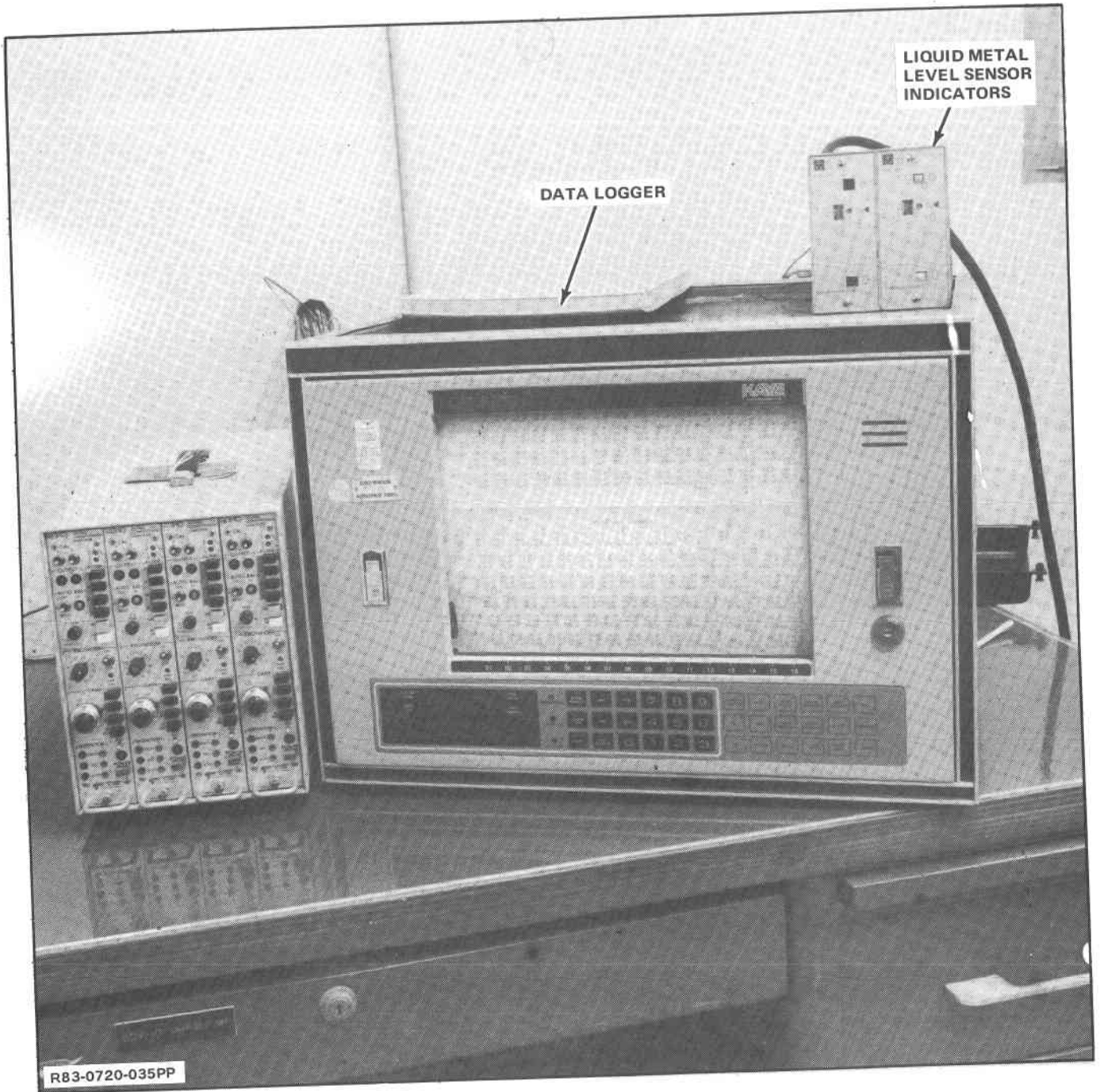


Fig. 7-8 Test Data Acquisition Setup

**SERIO** 

## 8 - INSTRUMENTATION

## 8.1 HEATERS/CONTROLLERS

Two types of electrical heaters are used: steel sheathed band heaters (three per tank module) which control tank temperatures, and adhesive-backed electrical ribbon heaters for line and valve traceheating. The automatically controlled heater circuits are summarized in Table 8-1.

TABLE 8-1 HEATER CIRCUIT SUMMARY

CIRCUIT IDENTIFICATION	DESCRIPTION	TEMPERATURE LIMIT, °C
CTR #1	HEAT EXCHANGE MODULE BAND HEATERS	650
CTR #2	SALT MODULE BAND HEATERS	650
CTR #3	LEAD MODULE BAND HEATERS	650
CTR #4	LIQUID METAL INLET LINE HEATERS	425
CTR #5	SALT INLET LINE HEATERS	425
CTR #6	LIQUID METAL & MOLTEN SALT RETURN LINE HEATERS	425

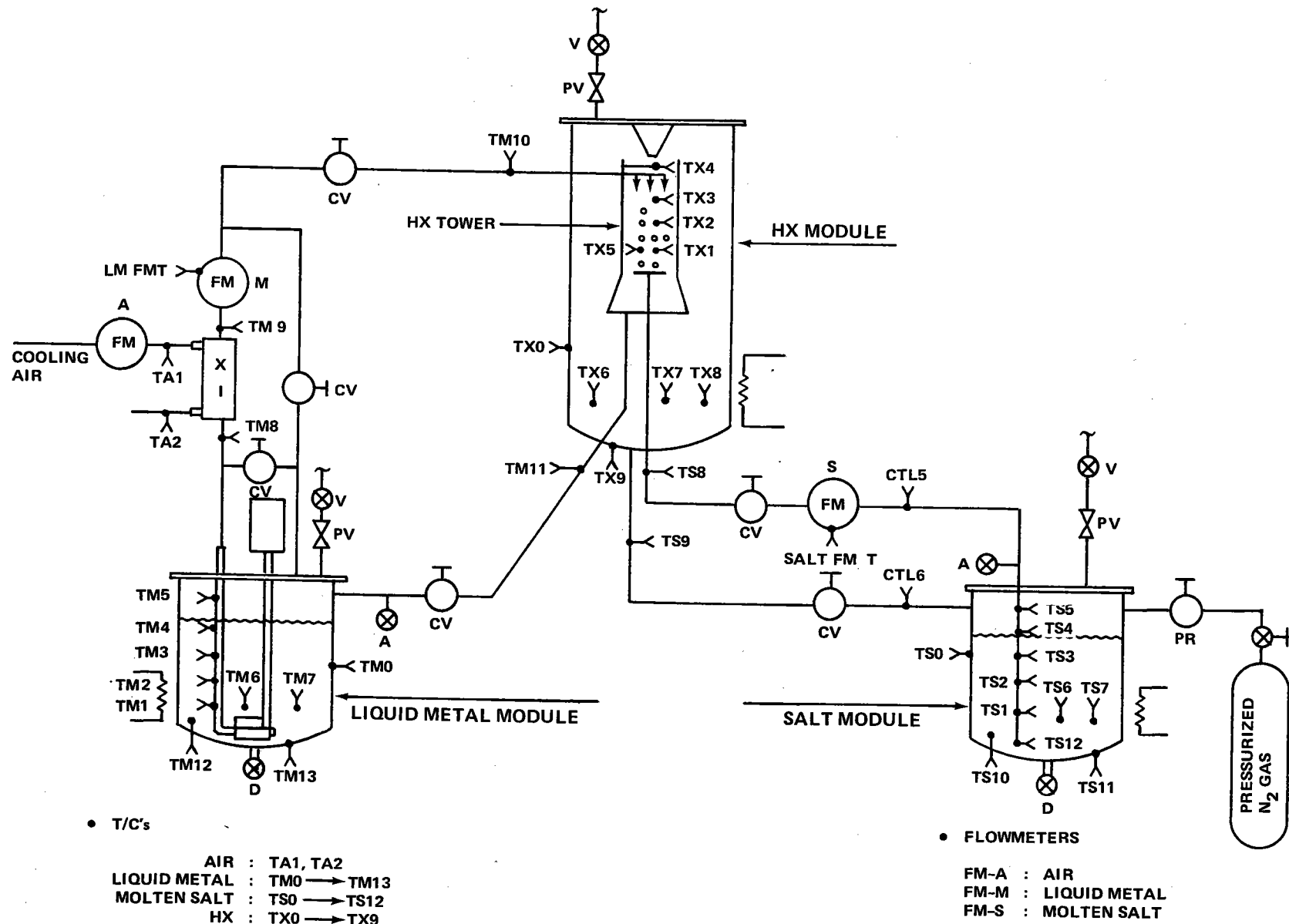
R83-0720-036PP

## 8.2 INSTRUMENTATION

The test instrumentation consists of type K thermocouples, flowmeters (liquid metal, molten salt, and cooling air), and special liquid metal level sensors. The thermocouple measurements are used to monitor heat transfer rates and control surface temperatures. The liquid metal and molten salt flowmeters are special service devices manufactured by Ramapo Instruments (Mark V series, target-type). Their design principle is based on a strain gage bridge. The cooling-air flow measurement is made using a pitot-static pressure sensor which has been calibrated to measure the average air stream velocity in a one-meter-long, 76-mm-diameter test section. The liquid metal level sensors are capacitive-type detectors located  $\pm 50$  mm about the desired liquid metal surface (i.e., 76 mm above metal injector) and used to position the salt-liquid metal interface within the heat exchange column.

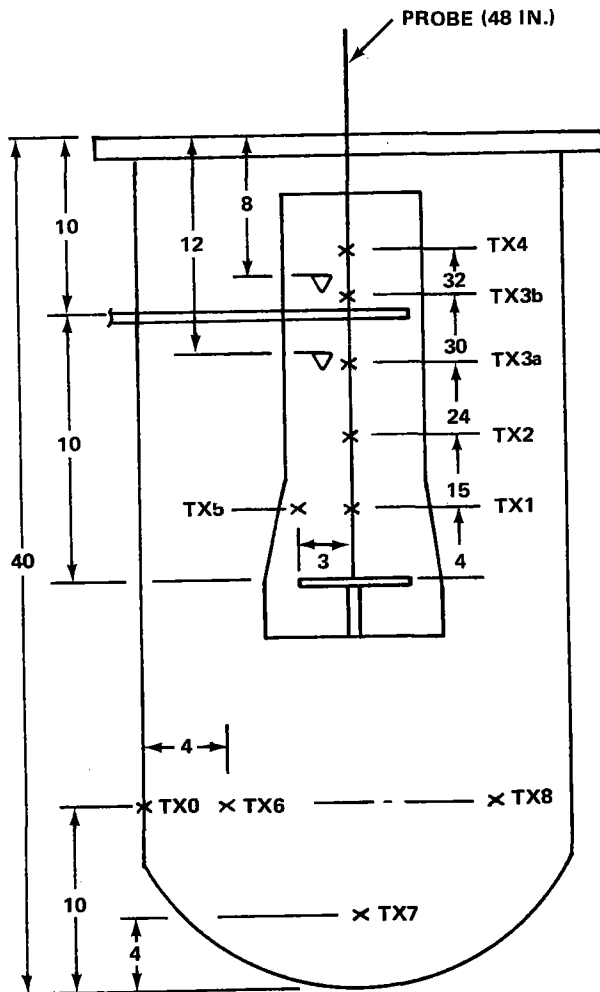
An instrumentation schematic which shows the number and location of the instrumentation is given in Fig. 8-1. A more complete description of the internal thermocouples is given in Fig. 8-2.





R83-0720-037PP

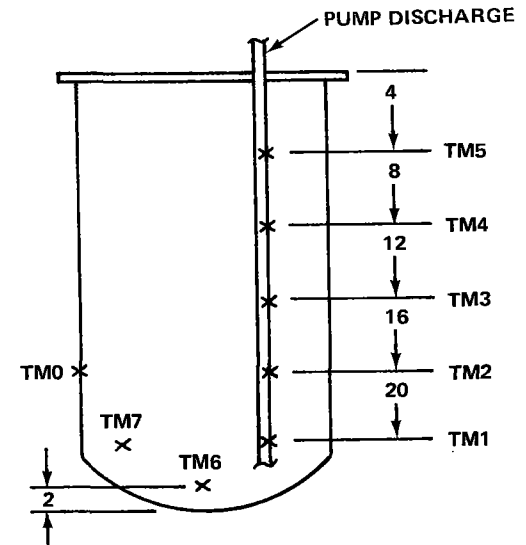
Fig. 8-1 System Instrumentation Schematic



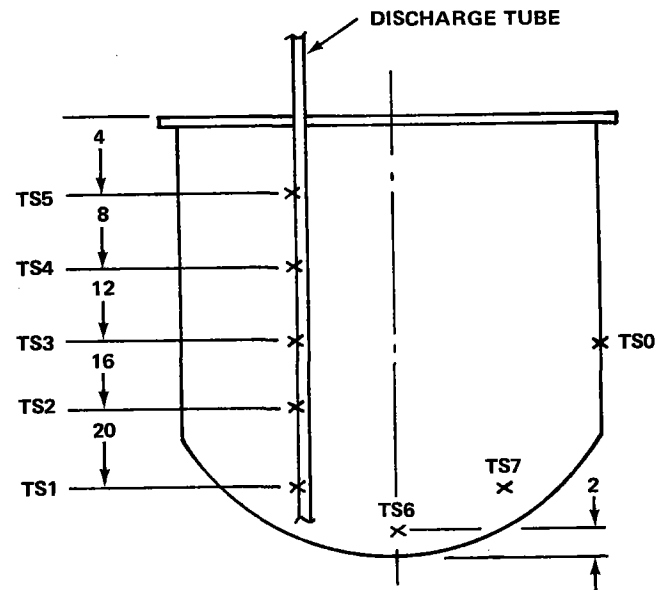
HX MODULE

R83-0720-038PP

X - THERMOCOUPLE  
 ▽ - LEVEL SENSOR



LIQUID METAL MODULE



SALT MODULE

Fig. 8-2 Internal Instrumentation

**SERIO** 

## 9 - RECOMMENDED TEST PROGRAM

The recommended test program for Phase III is intended to accomplish the following basic goals: (1) evaluate the overall effectiveness of the direct-contact heat exchange system in extracting the latent heat of fusion from the salt storage media; and (2) validate the model for the heat transfer mechanism between the dispersed (salt) and continuous (metal) fluid streams within the heat exchange column.

To accomplish the above, multiple charge/discharge cycles should be run while continually measuring temperatures and flow rates throughout the system. Suggested test points to evaluate both nominal and off-design conditions are summarized in Table 9-1. For each run, the following should be evaluated:

- Energy consumption during the charging cycle
- Heat transfer across each fluid stream during discharge
- Percent energy recovery from molten salt by measuring heat transfer versus time
- Operating power requirement by calculations from flow rate data and pressure drop estimates
- Size distribution of the solidified salt droplets by extracting samples and measuring diameters
- Internal structure of solidified droplets by bisecting and examining for voids and surface cracks.

**TABLE 9-1 RECOMMENDED DISCHARGE CYCLE TEST CONDITIONS**

TEST POINT	LIQUID METAL		MOLTEN SALT	
	FLOW RATE, Kg/s	INLET TEMP, °C	FLOW RATE, Kg/s	INLET TEMP, °C
NOMINAL (3 TIMES)	3.07	204	0.07	232
HIGH MOLTEN SALT FLOW	3.07	204	0.139	232
LOW MOLTEN SALT FLOW	3.07	204	0.035	232
HIGH LIQUID METAL FLOW	6.14	204	0.07	232
LOW LIQUID METAL FLOW	1.53	204	0.07	232
HIGH SALT INLET TEMPERATURE	3.07	204	0.07	260

R83-0720-039PP

**SERIO** 

## 10 - REFERENCES

1. Dubberly, L.J., et al, "Cost and Performance of Thermal Storage Concepts in Solar Thermal Systems. Phase I; Water/Steam, Organic Fluid and Closed Air-Brayton Receivers," Final Report Prepared by Sterns-Rodger Services Inc. under subcontract to the Solar Energy Research Institute, dated Nov. 1981.
2. Alario, J., Kosson, R., and Haslett, R., "Topical Report, Active Heat Exchange System Development for Latent Heat Thermal Energy Storage," NASA CR 159726, Jan. 1980.
3. Treybal, R., *Mass Transfer Operations*, McGraw-Hill Book Co. Inc., 1955.
4. Eckert, E. and Drake, R., *Heat and Mass Transfer*, McGraw-Hill Book Co. Inc., 1959.
5. Alario, J., "Operation Manual: Direct Contact High Temperature Thermal Energy Storage Heat Exchanger," TR-2766-04, Feb. 1983.

**SERIO** 

## APPENDIX A

### RESIDENCE TIME FOR DROPLET SOLIDIFICATION

#### A.1 NOMENCLATURE

- a = salt droplet outside radius
- $C_p$  = specific heat
- h = heat transfer coefficient at droplet surface
- $k_s$  = solid salt thermal conductivity
- m = mass flow rate
- n = number of salt droplets per unit time
- $q_d$  = heat transfer rate per droplet
- r = radius at liquid interface
- T = temperature
- t = time
- V = droplet volume
- $\bar{V}_f$  = velocity of carrier fluid
- $\bar{V}_t$  = salt droplet terminal velocity
- $\lambda$  = salt latent heat of fusion
- $\rho$  = density

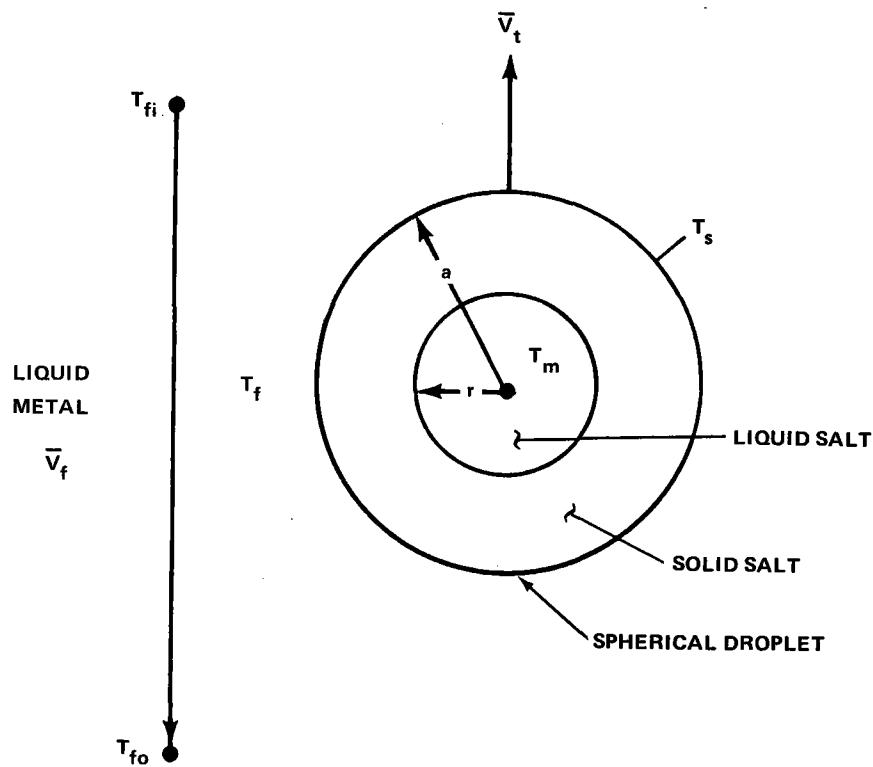
#### A.2 SUBSCRIPTS

- f = carrier fluid
- i = inlet
- L = liquid salt
- m = melt
- o = outlet
- res = residence
- s = solid salt

#### A.3 BOUNDARY CONDITIONS

The idealized physical situation for a single droplet of salt undergoing solidification is shown in Fig. A-1. Assuming that the outside diameter remains the





R83-0720-040PP

Fig. A-1 Model for Solidified Salt Droplet

same for either a liquid or solid salt droplet and using conservation of mass, the following relationships can be used for the problem boundary conditions:

1. At  $t = 0$ ,  $T_f = T_{fo}$ ,  $r/a = 1$
2. At  $t = t_{res}$ ,  $T_f = T_{fi}$ ,  $\frac{r}{a} = \left(1 - \frac{\rho_L}{\rho_S}\right)^{1/3}$

The following heat transfer relationships can also be written:

1. Heat transfer per spherical droplet ( $q_d$ )

$$q_d = -4\pi r^2 k_s \frac{dT}{dr} = 4\pi k_s \frac{(ra)}{a-r} (T_m - T_s) \quad (A.1)$$

where the first term represents the heat transfer at the surface of the droplet and the second term defines the heat transfer through the solid spherical annulus.

2. Heat transfer between droplet surface and carrier fluid.

$$q_d = 4\pi a^2 h (T_s - T_f) \quad (\text{A.2})$$

3. Heat transfer for droplet latent heat of fusion

$$q_d = \rho_s \lambda \frac{dV}{dt} = -\rho_s \lambda 4\pi r^2 \frac{dr}{dt} \quad (\text{A.3})$$

Combining Eq A.1 and A.2 to eliminate  $T_s$  and equating the results for  $q_d$  to Eq A.3 yields the following expression:

$$-\rho_s \lambda r^2 \frac{dr}{dt} = \frac{(T_m - T_f)}{\frac{a-r}{ark_s} + \frac{1}{ha^2}} \quad (\text{A.4})$$

4. Heat transfer to carrier fluid from each droplet

$$\dot{m}_f c_{p_f} \int_{T_{f_0}}^{T_f} \frac{dT_f}{dt} = \dot{n} 4\pi \rho_s \lambda \int_a^r r^2 \frac{dr}{dt}$$

$$\frac{\dot{m}_f}{\dot{n}} c_{p_f} (T_f - T_{f_0}) = \frac{4}{3} \pi \rho_s \lambda (r^3 - a^3) \quad (\text{A.5})$$

Also,  $\dot{n}$  can be expressed in terms of the molten salt flow rate as follows:

$$\dot{m}_s = \dot{n} \left( \frac{4}{3} \pi a^3 \right) \rho_L$$

or

$$\dot{n} = \frac{\dot{m}_s}{\left( \frac{4}{3} \pi a^3 \right) \rho_s (\rho_L / \rho_s)} \quad (\text{A.6})$$

Substituting Eq A.6 into A.5 and then solving for the quantity  $(T_m - T_f)$  gives:

$$(T_m - T_f) = (T_m - T_o) + \frac{\dot{m}_s \lambda (\rho_s / \rho_L)}{\dot{m}_f C_{p_f}} \left[ 1 - \left( \frac{r}{a} \right)^3 \right] \quad (A.7)$$

Substituting Eq A.7 into A.4 and rearranging terms yields the following expressions for dt:

$$-dt = \frac{\left\{ \frac{a}{k_s} \left[ \left( \frac{r}{a} \right) - \left( \frac{r}{a} \right)^2 \right] + \frac{1}{h} \left( \frac{r}{a} \right)^2 \right\} \rho_s C_{p_f} a}{\frac{C_{p_f} (T_m - T_o)}{\lambda} + \left( \frac{\dot{m}_s}{\dot{m}_f} \right) \left( \frac{\rho_s}{\rho_L} \right) \left[ 1 - \left( \frac{r}{a} \right)^3 \right]} d \left( \frac{r}{a} \right) \quad (A.8)$$

Now define the following terms and substitute into Eq A.8:

Let  $\beta = r/a$

$$\alpha = (1 - \rho_L / \rho_s)^{1/3}$$

then,

$$-\int_0^{t_{res}} dt = \int_1^\alpha \frac{\left[ \frac{a}{k_s} (\beta - \beta^2) + \frac{1}{h} \beta^2 \right] \rho_s C_{p_f} a}{C_{p_f} \frac{(T_m - T_o)}{\lambda} + \left( \frac{\dot{m}_s}{\dot{m}_f} \right) \left( \frac{\rho_s}{\rho_L} \right) [1 - \beta^3]} d\beta \quad (A.9)$$

Equation A.9 can now be integrated to give the following expression for the residence time ( $t_{res}$ ) required for droplet solidification:

$$t_{res} = \frac{a \rho_s C_{p_f}}{3B} \left\{ \frac{a}{k_s \zeta} \left[ \frac{1}{2} \ln \frac{\left( \frac{\zeta^2 - \zeta + 1}{(\zeta+1)^2} \right)}{\left( \frac{\zeta^2 - \alpha\zeta + \alpha^2}{(\zeta+\alpha)^2} \right)} + \sqrt{3} \left[ \tan^{-1} \left( \frac{2-\zeta}{\sqrt{3}\zeta} \right) - \tan^{-1} \left( \frac{2\alpha-\zeta}{\sqrt{3}\zeta} \right) \right] \right] \right. \\ \left. + \left( \frac{1}{h} - \frac{a}{k_s} \right) \ln \frac{(A+B)}{(A+B\alpha^3)} \right\} \quad (A.10)$$

where

$$A = \frac{C_{p_f} (T_m - T_{f_o})}{\lambda} + \frac{\dot{m}_s \rho_s}{\dot{m}_f \rho_f}$$

$$B = - \left( \frac{\dot{m}_s}{\dot{m}_f} \right) \left( \frac{\rho_s}{\rho_f} \right)$$

$$\zeta = \left( \frac{A}{B} \right)^{1/3} = - \left[ \left( \frac{\rho_L}{\rho_s} \right) \frac{\dot{m}_f C_{p_f} (T_m - T_{f_o})}{\dot{m}_s \lambda} + 1 \right]^{1/3}$$

**SERIO** 

APPENDIX B  
LABORATORY RESULTS OF MATERIALS  
COMPATIBILITY STUDY

**SERIO** 

CONTRACT REQUIREMENTS	CONTRACT ITEM	MODEL	CONTRACT NO.
			XP-0-9383-1
<p>REPORT</p> <p>NO. <u>M&amp;ME-TS443-82R-030</u>      DATE: <u>10 December 1982</u></p> <p><u>SELECTION OF MOLTEN SALT COMPATIBLE WITH</u> <u>HEAT EXCHANGER CARRIER FLUID</u></p> <p>CODE 26512</p> <p>Requested By: Joe Alario</p> <p>PREPARED BY: <u>R. Spinos <i>RS</i></u>      TECHNICAL APPROVAL: <u>R. Holden <i>RH</i></u></p> <p>CHECKED BY: <u>H. Noonan <i>HN</i></u>      APPROVED BY: <u>C. J. Weizenecker <i>CJW</i></u></p> <p>DEPARTMENT: <u>Manufacturing &amp; Materials Eng't.</u>      APPROVED BY:</p> <p>SECTION: <u>Chemical Engineering Laboratory</u>      APPROVED BY:</p>			
REVISIONS			
DATE	REV. BY	REVISIONS & ADDED PAGES	REMARKS

GAC 324A REV. 3  
10-70



INTRODUCTION:

Advanced Thermal Systems is currently involved with the construction of a high temperature direct contact heat exchanger. The Chemical Engineering Laboratory was asked to assist in the selection of a molten salt compatible with the lead/bismuth liquid metal carrier fluid used in the exchanger. Candidate salts under consideration were a eutectic mixture of potassium and sodium nitrate, sodium hydroxide and a eutectic mixture of potassium and zinc chloride. Initial theoretical reaction analyses had shown that oxidation of the metals was possible when in contact with the nitrate salts. Testing was performed to determine the effect that entrapped moisture and salt impurities would have on the theoretical melting temperatures and the rate of the oxidation reaction.

RESULTS:Materials Evaluated:

1. Partherm 430 - Potassium nitrate-sodium nitrate mixture manufactured by **Park Chemical Company**
2. Potassium nitrate-sodium nitrate mixture manufactured by the **Rosborough Chemical Company**
3. Olin Solar Nitrate Salt - Potassium nitrate-sodium nitrate mixture manufactured by the **Olin Chemical Corporation**
4. F.C.C., Food Grade potassium nitrate-sodium nitrate - salts shipped separately, manufactured by the **J. T. Baker Chemical Company**
5. Reagent Grade potassium nitrate-sodium nitrate - salts shipped separately, manufactured by the **J. T. Baker Chemical Company**
6. Reagent Grade potassium chloride and zinc chloride - in-house salts, manufactured by the **J. T. Baker Chemical Company**
7. Reagent Grade sodium hydroxide - in-house sample, manufactured by the **J. T. Baker Chemical Company**

Melting Point Determinations of Nitrate Salts:

The composition of all nitrate salts was 54 mol percent potassium nitrate. The theoretical melting point was 222°C. Melting point determinations were made using a Perkin-Elmer DSC-2 Differential Scanning Calorimeter. Small samples were prepared as indicated, encapsulated and heated at 20°C/minute. Results were as follows:

RESULTS: (Continued)

<u>SALTS</u>	<u>DSC SCAN</u>
<u>Partherm 430</u>	
Ground and mixed	Small peak at 129°C Peak at 220°C Broad peak between 240-305°C (Figure 1)
Melted, mixed and cooled	Small peak at 110°C Small peak at 220°C Broad peak between 247-302°C (Figure 2)
Dissolved in water, mixed and dried	Small peak at 112°C Small peak at 218°C Broad peak between 243-291°C (Figure 3)
<u>Rossborough Salts</u>	
As received	Small peak at 130°C Strong peak at 219°C Peak at 239°C Broad peak between 249-296°C (Figure 4)
Ground and mixed	Small peak at 128°C Peak at 220°C Broad peak between 242-293°C (Figure 5)
Dissolved in water, mixed, filtered (Whatman #5 qualitative filter) and dried	Small peak at 127°C Strong, slightly broadened peak at 218°C (Figure 6)
<u>Olin Solar Salts</u>	
As received	Small peak at 130°C Strong peak at 222°C Small, broad peak between 247-290°C (Figure 7)
Dissolved in water, mixed, filtered and dried	Small peak at 120°C Strong peak at 221°C (Figure 8)
<u>J. T. Baker Salts</u>	
F.C.C. Food Grade, as received	Small peak at 130°C Strong, slightly broadened peak at 222°C (Figure 9)
Reagent Grade, as received	Small peak at 129°C Strong peak at 222°C

RESULTS: (Continued)

The small peaks present between 110-130°C are attributed to entrapped moisture. Sharp peaks with an onset temperature of 222°C are indicative of the eutectic melting point. The broad peaks evident in some of the thermograms indicate a melting range. The results obtained for the reagent grade and filtered commercial salts suggests that the erratic melting behavior of the "as received" commercial grade salts is due to the water insoluble impurities (~ 1% by weight in the Partherm 430).

A DSC scan of sodium hydroxide sampled directly from the jar produced a non-descript spectrum, most likely an effect of large amounts of moisture present (sodium hydroxide - extremely hygroscopic). A scan of the potassium chloride and zinc chloride mixture (also extremely hygroscopic) produced similar results.

Unacceptable results obtained for initial reaction experiments performed with sodium hydroxide and the potassium chloride and zinc chloride mixture made further attempts at determining melting points unnecessary.

Lead/Bismuth (Pb/Bi) - Nitrate Salt Compatibility Experiment

Pb/Bi : Salt (5.61 : 1 by weight)

The commercial grade salts were ground and mixed prior to heat-up. Samples were also dissolved in water, filtered (Whatman #5 qualitative filter) and re-dried to determine the effect water insoluble impurities would have on the corrosion process. The J. T. Baker food and reagent grade salts were run "as is." All salts were dried for 24 hours at 150°C. Small samples of steel and weldment material, of the type used to construct the heat exchanger containment tank, were added to some of the reaction vessels.

The Pb/Bi salt mixtures were melted in a double-armed glass reaction vessel. Heat was applied using a heating mantle and Variac voltage regulator. The arms of the vessel served as inlet and outlet ports for a continuous nitrogen purge. The liquid metal-salt mixture was maintained at approximately 550°F. Results were as follows:

<u>SALT</u>	<u>OBSERVATIONS</u>
<u>Partherm 430</u>	
Ground and mixed	Salts melted slowly between 250-300°C. Light brown corrosion product visible after 1 hour. Corrosion excessive within 2-3 hours.

RESULTS: (Continued)

<u>SALT</u>	<u>OBSERVATIONS</u>
<u>Rosborough Salts</u>	
Ground and mixed	Salts melted slowly between 250-300°C. Corrosion visible after $\frac{1}{2}$ hour. Corrosion excessive within 1-2 hours.
Filtered Sample	Salts melted fairly quickly between 220-250°C. Salt remained clear. No discoloration of metals. Slight corrosion after 6 hours.
<u>Olin Solar Salts</u>	
Ground and mixed	Salts melted slowly between 250-300°C. Corrosion was excessive within 1 hour.
Filtered Sample	Salts melted fairly quickly between 220-250°C. Slight corrosion after 6-8 hours. Salts remained clear. No discoloration of metals. Moderate ( $\frac{1}{2}$ -1% by wt.) corrosion after 48 hours. No change after additional 80 hours.
Filtered Sample and Steel and Weldment Material	Salts melted between 220-250°C. No corrosion after 6 hours. Moderate corrosion after 24 hours. No change after additional 48 hours. Steel and weldment material appeared to be unaffected. Corrosion comparable to vessel without steel.
<u>J. T. Baker Salts</u>	
F.C.C., Food Grade "As is"	Salts melted slowly between 250-300°C. Corrosion was excessive within 1-2 hours.
Reagent Grade "As is"	Salts melted quickly just above 222°C. Very slight corrosion visible after 8 hours. Salts clear, no discoloration of metals. Slight corrosion after 24 hours.
Reagent Grade and Steel and Weldment Material	Same as without steel. Corrosion slight after 48 hours. Steel and weldment material appeared to be unaffected.

RESULTS: (Continued)

It is assumed that water was effectively eliminated from the salts and reaction chamber. Results suggest that the amount of corrosion is related to the amount of water insoluble impurities present.

Analysis of the light brown Pb/Bi-nitrate salt corrosion product was performed on a Perkin-Elmer 283B Infrared Spectrophotometer at normal settings. The spectrum obtained for the corrosion material matched well with a file spectrum of lead oxide.

Lead/Bismuth (Pb/Bi) - Potassium Chloride (KCl) and Zinc Chloride (ZnCl<sub>2</sub>) Compatibility Experiment

Composition: 54% by weight ZnCl<sub>2</sub>  
Theoretical Melt: 228°C

In-house samples of reagent grade KCl and ZnCl<sub>2</sub>, manufactured by J. T. Baker Chemical Company, were weighed, mixed and dried under vacuum for 24 hours at 400°F.

The Pb/Bi-salt mixture was melted in a nitrogen environment and held at approximately 750°F. Within 2-3 hours, the salts took on a dull gray color, suggesting some measure of metal-salt solubility. No corrosion products were observable - vessel was shut down.

Pb/Bi - Sodium Hydroxide (NaOH)

In-house sample of reagent grade NaOH was dried for 48 hours at 400°F. The salt-Pb/Bi mixture was melted and maintained between 650-700°F under a nitrogen environment. After 2 hours at temperature the salt was clear, there was no discoloration of the metals and no indication of corrosion. Extensive condensation was present in both arms of the reaction vessel - vessel was shut down. Either during cool-down or heat-up the following morning, the reaction vessel cracked. The liberated NaOH corroded the heating mantle and thermocouple - test was aborted.

Summary:

1. The concentration of water insoluble impurities in the commercial grade nitrate salts is sufficient to cause erratic melting behavior and excessive corrosion when in contact with the liquid lead/bismuth mixture.
2. The high purity reagent grade nitrate salts melt at the 222°C theoretical eutectic melting point and react only slightly with the metals.
3. The liquid lead/bismuth appeared to be somewhat soluble in the liquid potassium chloride-zinc chloride salt mixture.

Summary: (Continued)

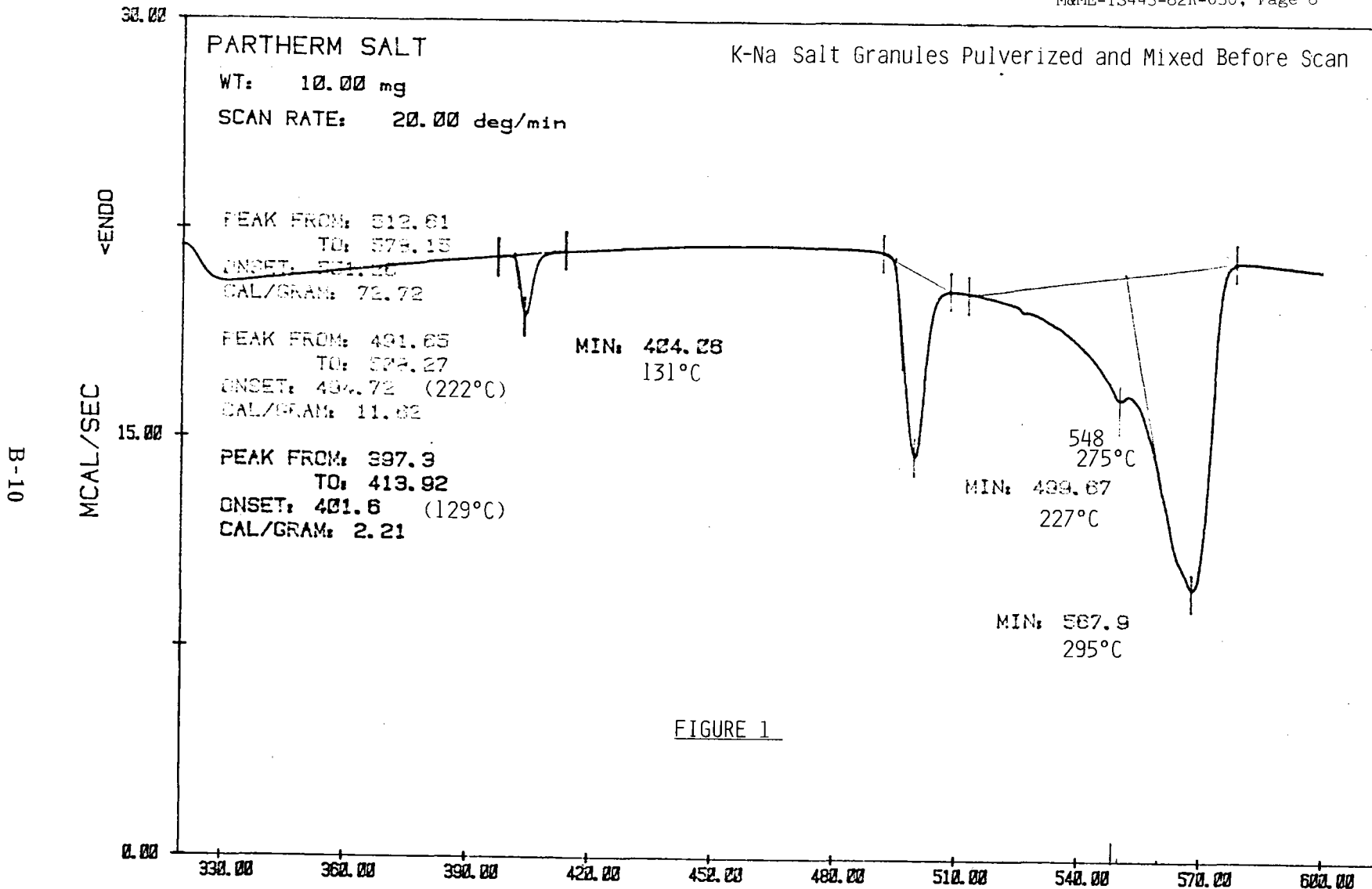
4. The sodium hydroxide did not react with the Pb/Bi when tested for a short period. The material, however, is extremely difficult to dry and potentially hazardous.

GAC 328A REV. 3  
9-81 20M

REPORT M&ME-TS443-82R-030  
DATE 12/10/82

**Grumman Aerospace Corporation**

CODE 26512

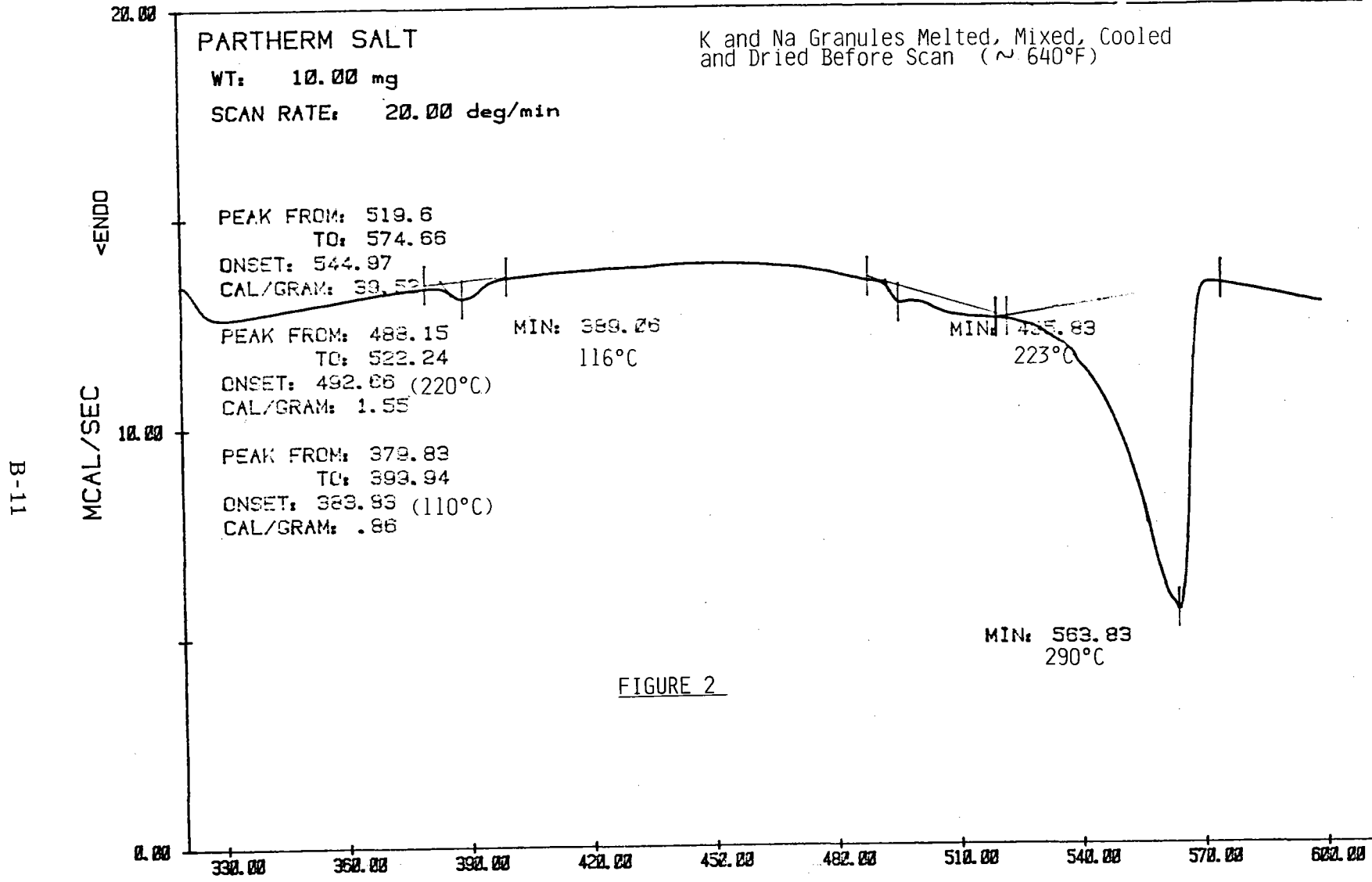


R SPINDS FILE: QSAVE.DA  
 DATE: 06/11/82 TIME: 08:51

TEMPERATURE (K)

DSC

PERKIN-ELMER Thermal Analysis



PARTHARM SALT

K and Na Granules Melted, Mixed, Cooled and Dried Before Scan (~ 640°F)

WT: 10.00 mg  
SCAN RATE: 20.00 deg/min

PEAK FROM: 519.6  
TO: 574.66  
ONSET: 544.97  
CAL/GRAM: 33.52

PEAK FROM: 488.15  
TO: 522.24  
ONSET: 492.66 (220°C)  
CAL/GRAM: 1.55

PEAK FROM: 379.83  
TO: 393.94  
ONSET: 389.93 (110°C)  
CAL/GRAM: .86

MIN: 389.93  
116°C

MIN: 488.15  
223°C

MIN: 519.6  
290°C

FIGURE 2

R SPINDS FILE: QSAVE.DA  
DATE: 06/11/82 TIME: 07:51

TEMPERATURE (K)

DSC

PERKIN-ELMER Thermal Analysis



PARTHERM SALT

WT: 10.00 mg

SCAN RATE: 20.00 deg/min

K and Na Salts Dissolved in Water, Mixed and Dried Before Scan

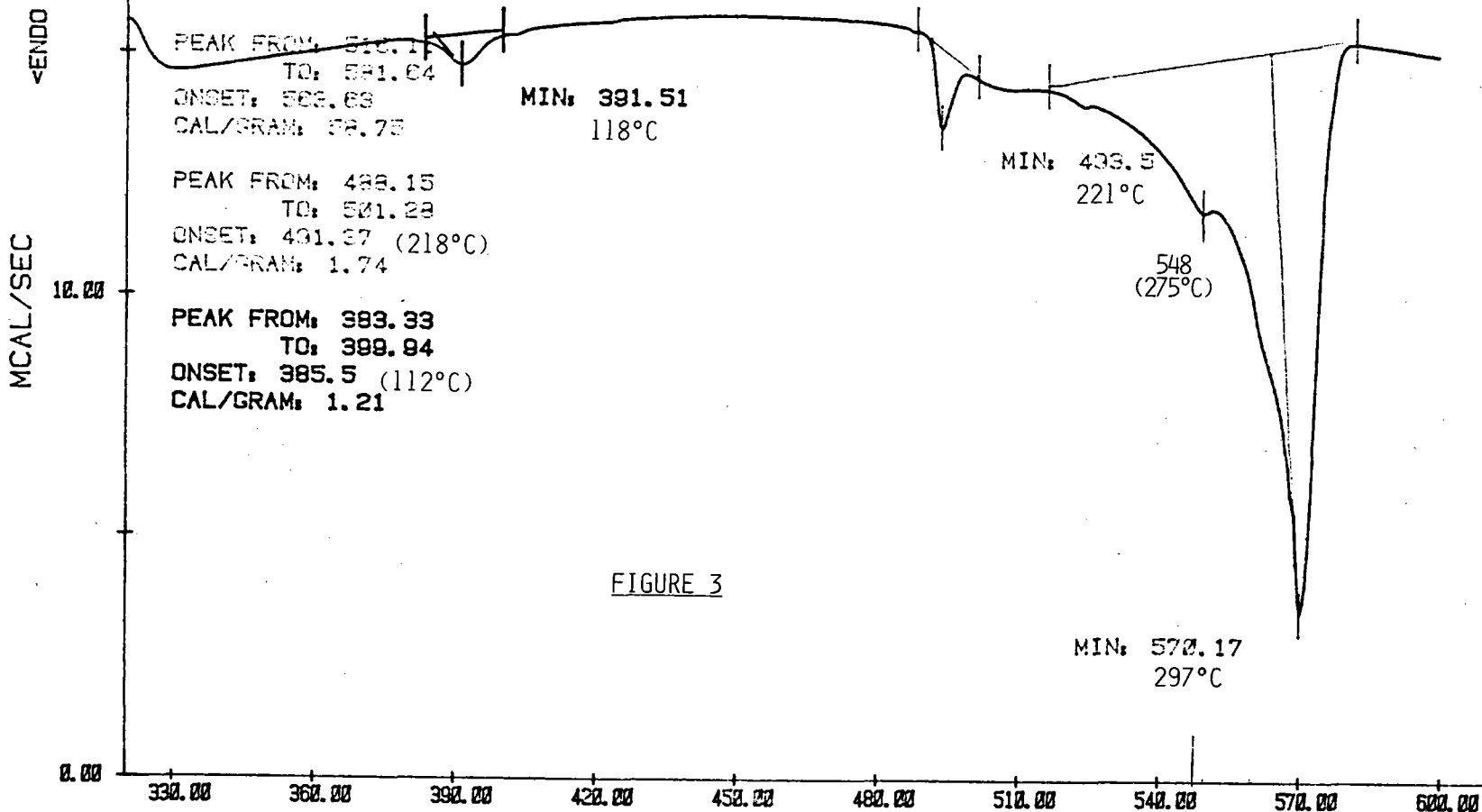


FIGURE 3

R SPINDS FILE: QSAVE.DA

DATE: 06/11/82 TIME: 09:28

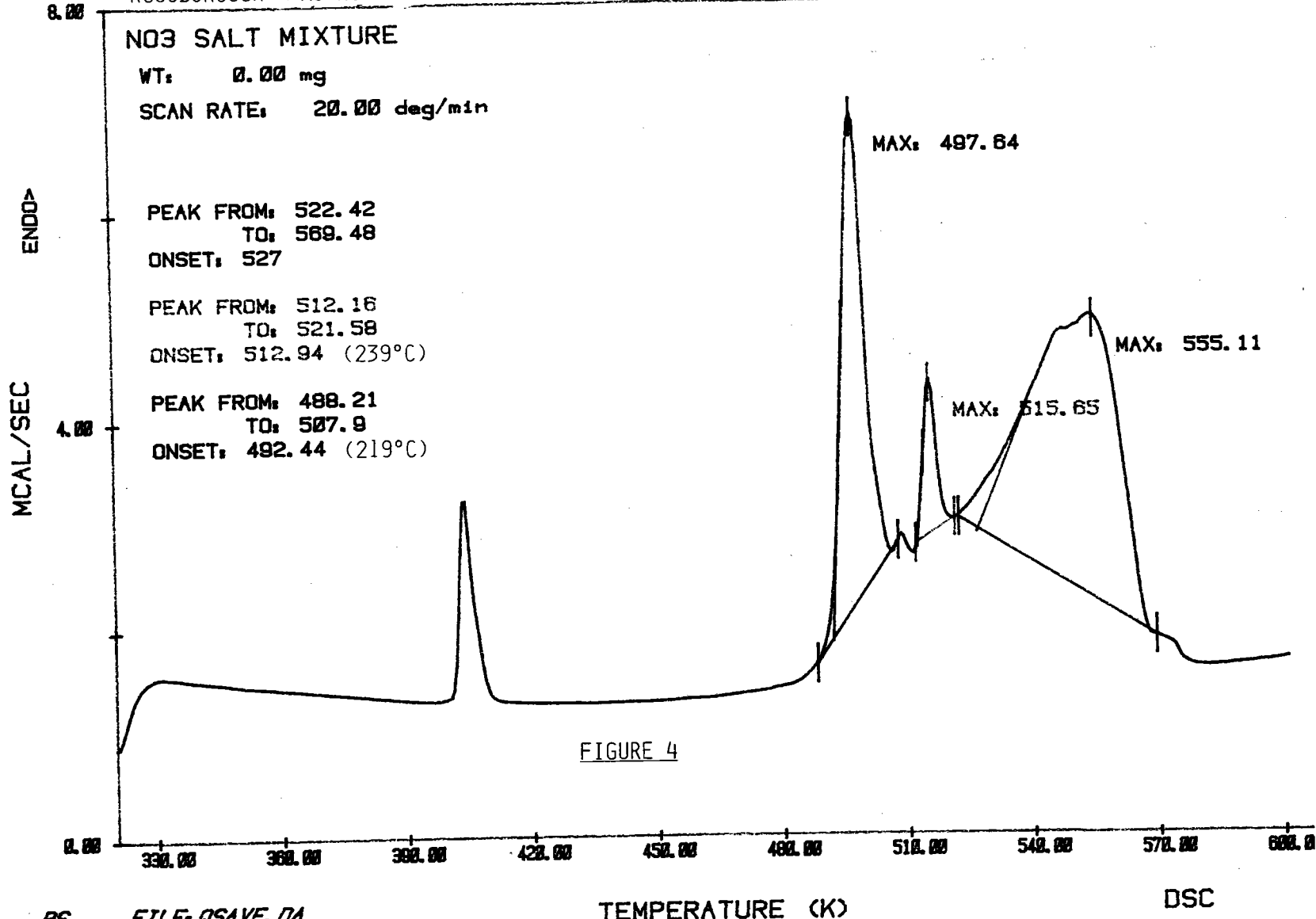
TEMPERATURE (K)

DSC

PERKIN-ELMER Thermal Analysis

B-12

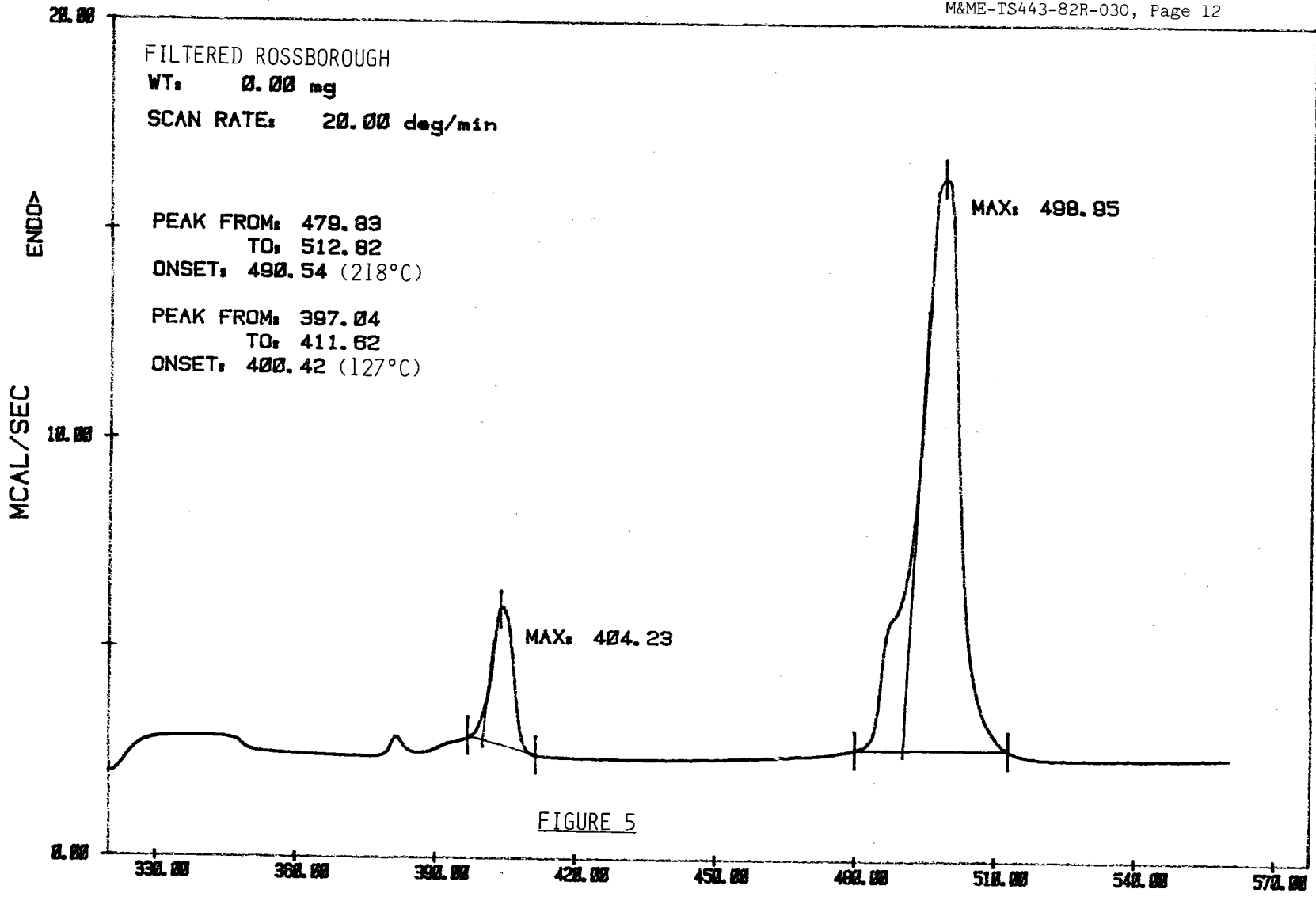
SERI/STR-230-2065



B-13

RS FILE: QSAVE.DA  
DATE: 08/03/82 TIME: 14:08

SERI/STR-230-2065



B-14

RS FILE: QSAVE.DA  
DATE: 08/05/82 TIME: 11:36

SERI/STR-230-2065

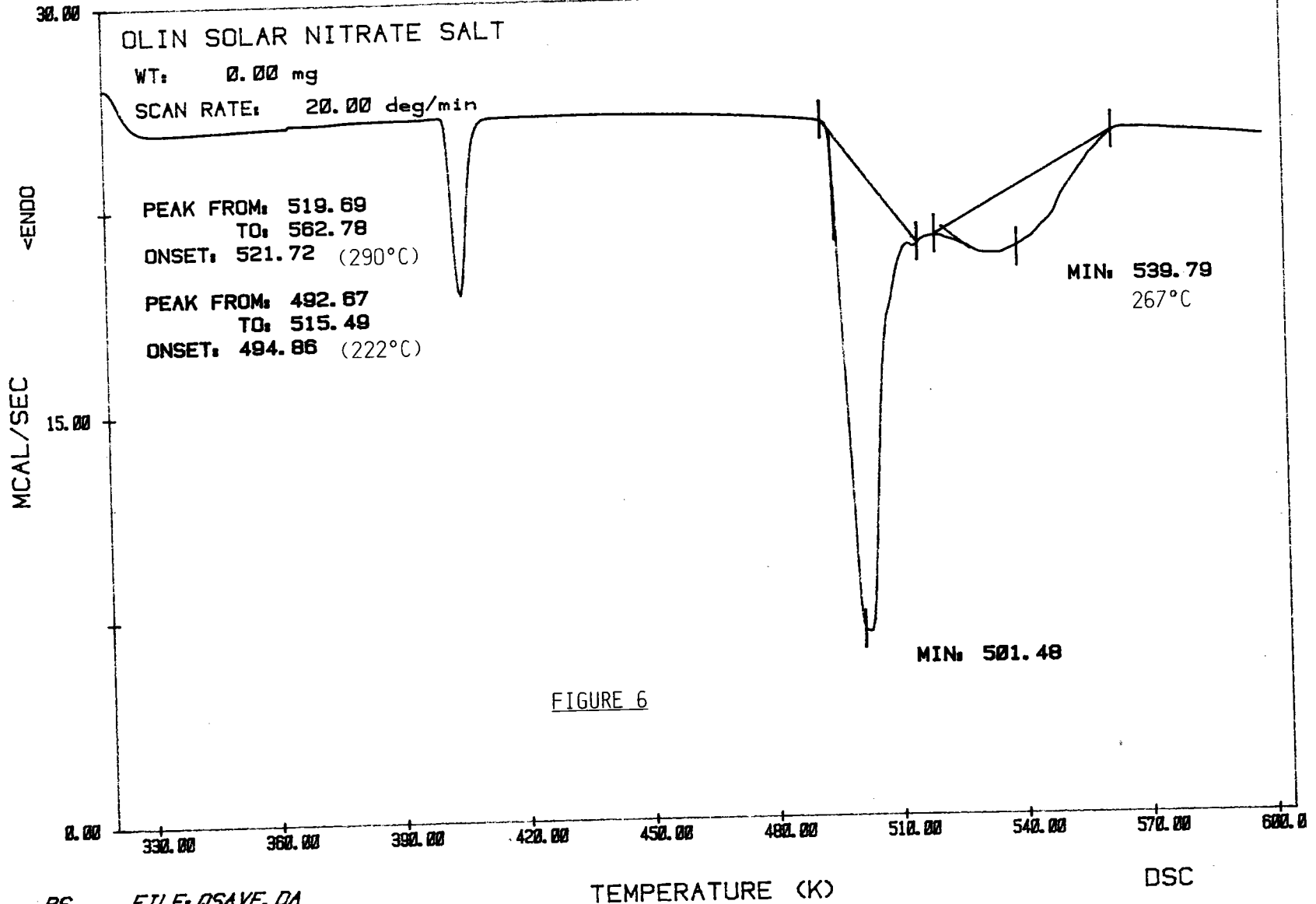
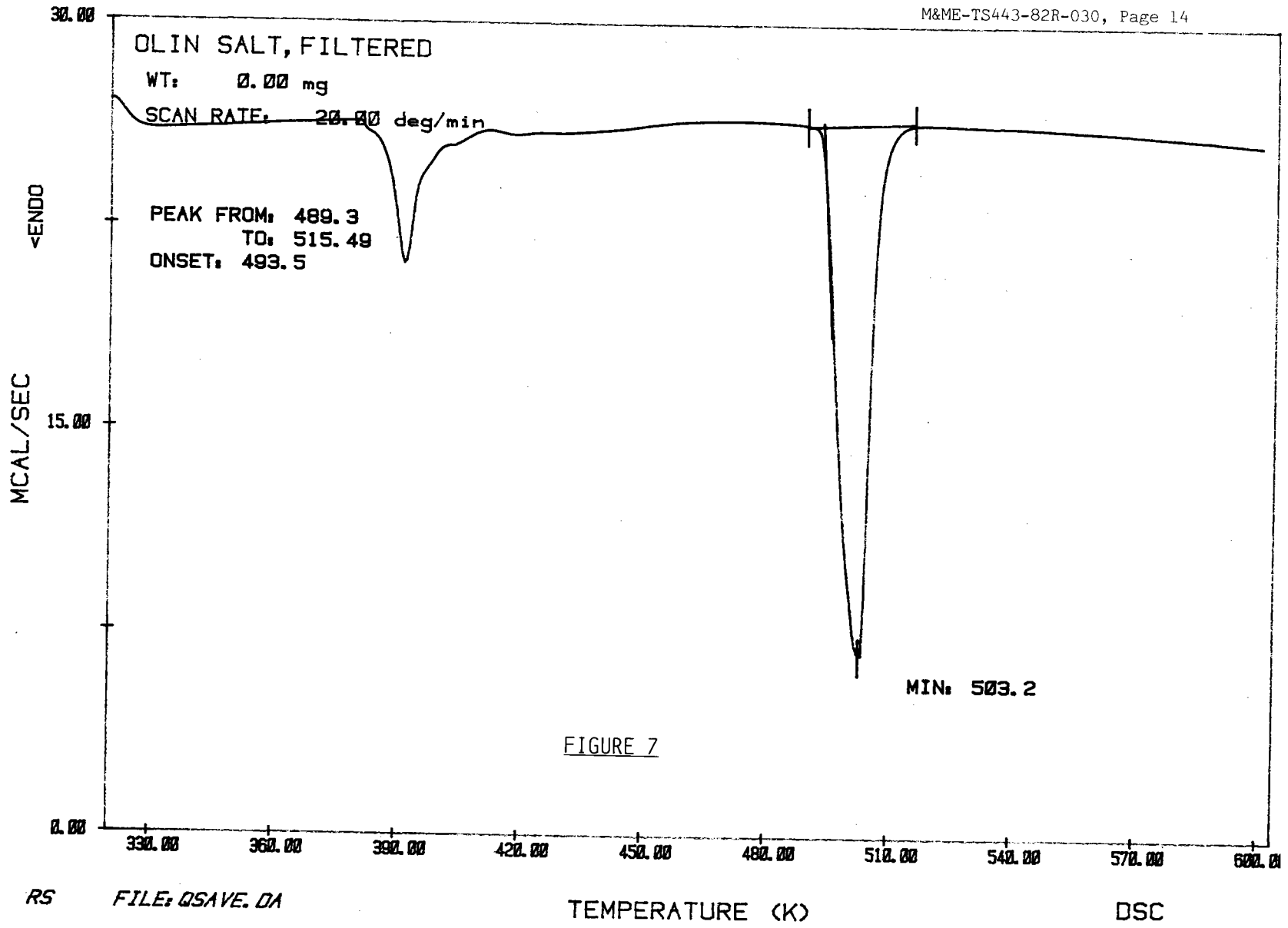


FIGURE 6

B-15

RS FILE: QSAVE.DA  
DATE: 10/05/82 TIME: 01:15

SERI/STR-230-2065



B-16

RS FILE: QSAVE.DA  
DATE: 10/05/82 TIME: 01:40

SERI/STR-230-2065

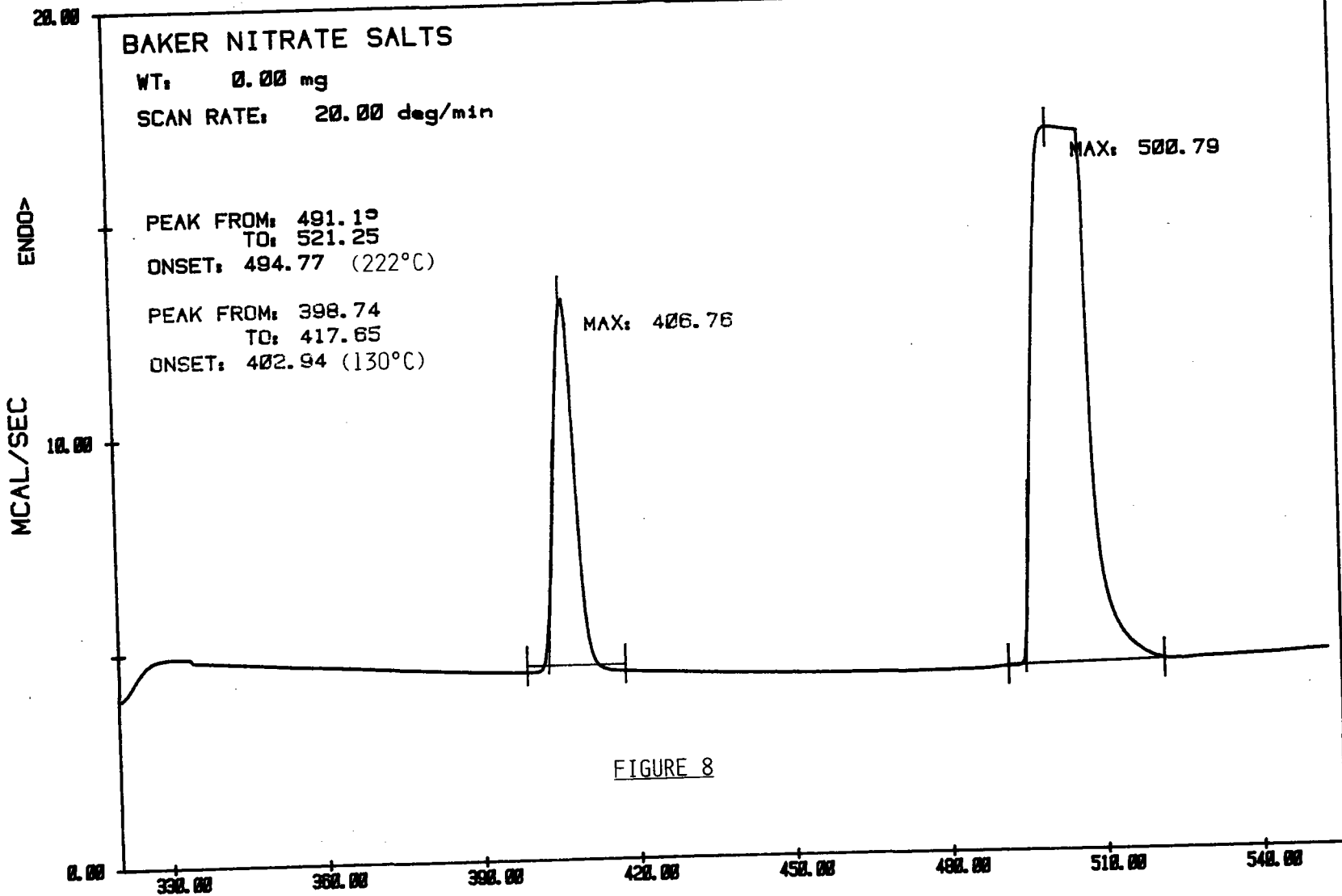


FIGURE 8

(NaNO<sub>3</sub>)  
 FOOD GRADE FILE: QSAVE.DA  
 DATE: 09/11/82 TIME: 08:51

TEMPERATURE (K)

DSC  
 PERKIN-ELMER Thermal Analysis

B-17

SERI/STR-230-2065

REAGENT GRADE

M&ME-TS443-82R-030, Page 16

### K AND NA NITRATE SALTS

WT: 0.00 mg

SCAN RATE: 20.00 deg/min

ENDO

PEAK FROM: 488.15

TO: 522.24

ONSET: 494.49 (222°C)

PEAK FROM: 397.3

TO: 413.92

ONSET: 402.12 (129°C)

MAX: 499.75

MCAL/SEC

10.00

MAX: 404.95

FIGURE 9

0.00

330.00

360.00

390.00

420.00

450.00

480.00

510.00

540.00

570.00

600.00

R SPINDS

FILE: QSAVE.DA

TEMPERATURE (K)

DSC

DATE: 06/15/82

TIME: 03:00

PERKIN-ELMER Thermal Analysis

B-18

SERI/STR-230-2065

APPENDIX C  
 DESIGN SPECIFICATION SUMMARY FOR  
 DIRECT-CONTACT LATENT THERMAL ENERGY STORAGE HEAT EXCHANGER

C.1 MATERIALS

- Salt: 46%  $\text{NaNO}_3$  / 54%  $\text{KNO}_3$ , % = % Wt  
 Melting Point = 227°C  
 Total Weight Required = 263 kg  
 Design Flow Rate = 0.073 kg/s
- Liquid Metal: 44.5%Pb / 55.5% Bi (Indalloy No. 255)  
 Melting Point = 125°C  
 Total Weight Required = 499 kg  
 Design Flow Rate = 3.07 kg/s
- Tank Modules: 1020 mild steel
- Liquid Metal/Air Heat Exchanger: Stainless Steel
- Pump: Cast Iron

C.2 TANK VOLUMES (NET),  $\text{m}^3$

- Molten Salt Module: 0.153 (0.61 m Dia)
- Liquid Metal Module: 0.043 (0.30 m Dia)
- Heat Exchange (HX) Module
  - HX Column: 0.035
  - Solid Salt Section: 0.361

C.3 LIQUID METAL PUMP REQUIREMENTS

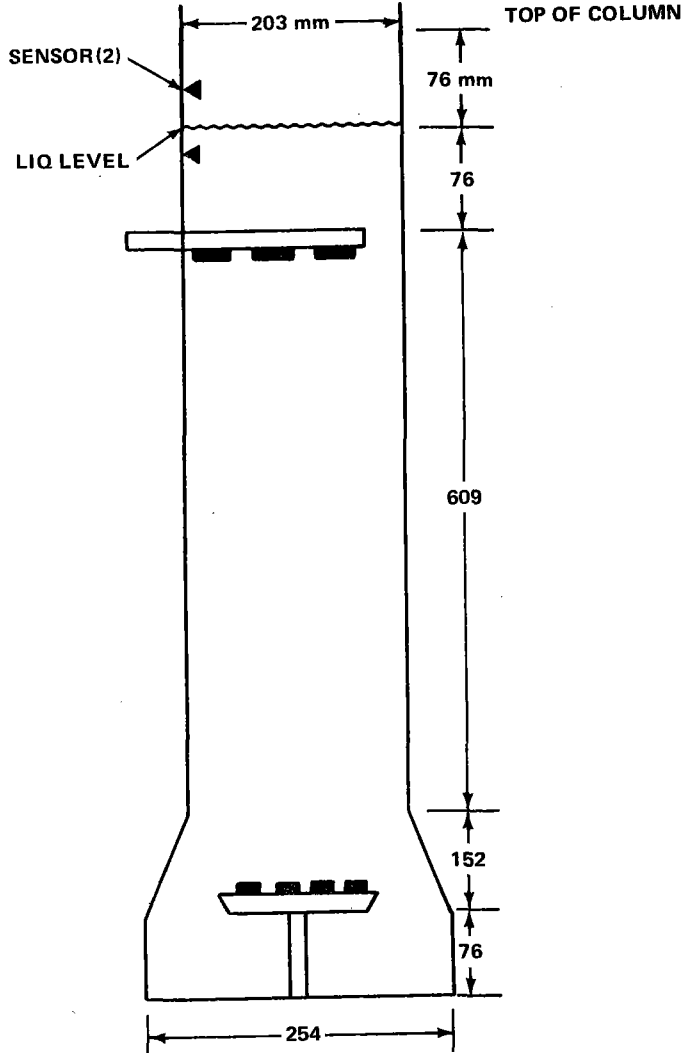
Fluid Density ( $\text{kg}/\text{m}^3$ ) . . . . .	9995.0
Nominal Flow Rate ( $\text{kg}/\text{s}$ ). . . . .	3.07
Max Lift, m . . . . .	2.29
Line Dia, mm. . . . .	25.4
Max System Design Pressure, kPa . . . . .	275.6



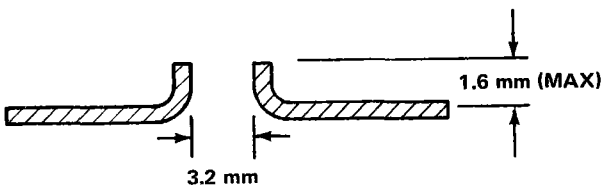
C.4 CRITICAL COMPONENTS

- HX Reservoir (Fig. C-1)
- Salt Injector:
  - Spray Head Dia = 152 mm
  - Orifice Opening = 3.2 mm dia
  - No. of openings: 105 min → 150 max (128 actual)
  - Predicted Salt Bubble Dia: 3.2 mm
- Liquid Metal Injector
- Air/Liquid Metal Heat Exchanger (Fig. C-2)
- Insulation (Fiberglass, SR-26)

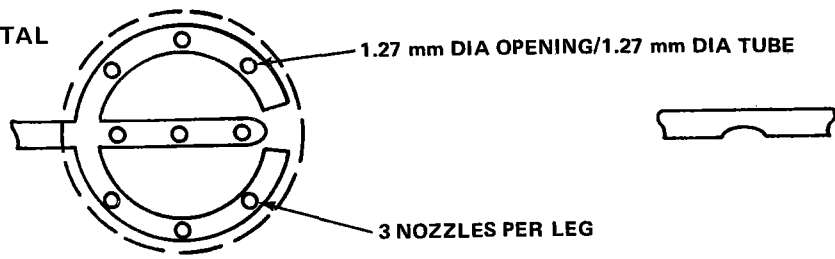
	<u>Thickness, (mm)</u>
Main Modules . . . . .	228
Pipes. . . . .	76



SALT INJECTOR ORIFICE  
(128 REQ)

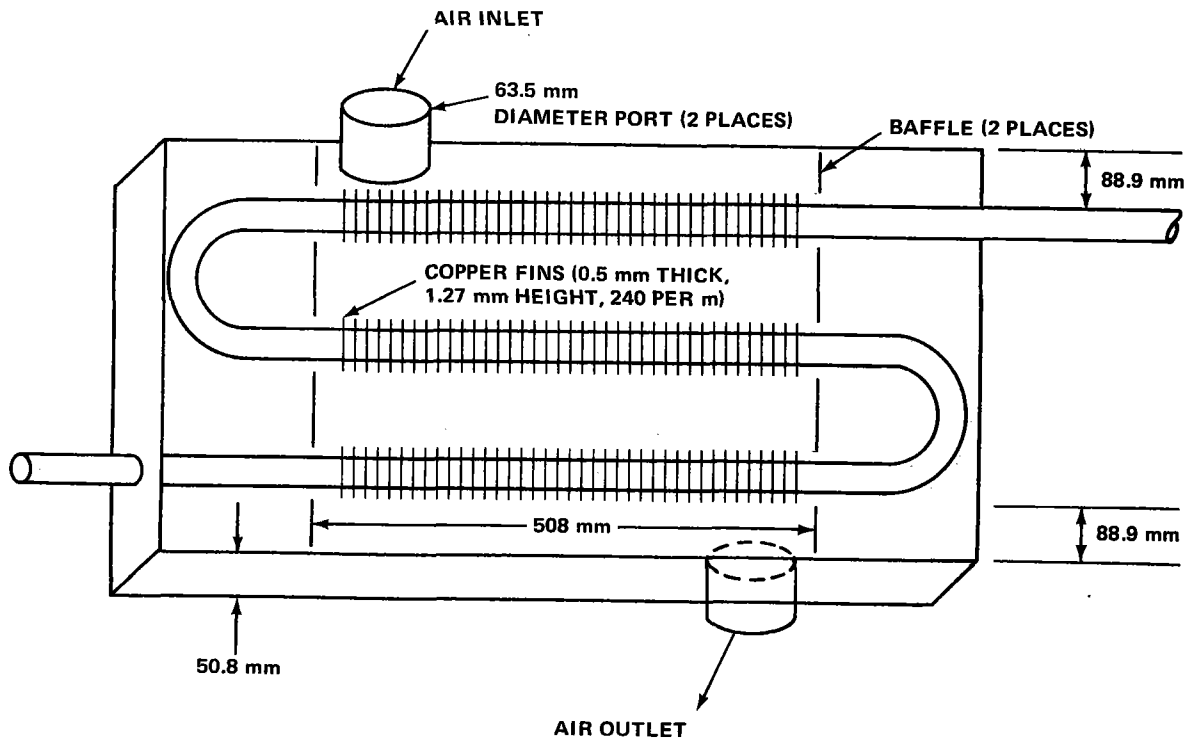


LIQUID METAL  
INJECTOR



R83-0720-041PP

Fig. C-1 Heat Exchange Column



R83-0720-042PP

Fig. C-2 Air/Liquid Metal Heat Exchanger Cooling

<b>Document Control Page</b>	1. SERI Report No. SERI/STR-230-2065	2. NTIS Accession No.	3. Recipient's Accession No.
4. Title and Subtitle Direct-Contact High-Temperature Thermal Energy Storage Heat Exchanger		5. Publication Date September 1983	
7. Author(s) Joseph Alario, Richard Brown		6.	
9. Performing Organization Name and Address Grumman Aerospace Corporation Bethpage, New York 11714		8. Performing Organization Rept. No.	
		10. Project/Task/Work Unit No. 1298.12	
		11. Contract (C) or Grant (G) No. (C) XP-0-9383-1 (G)	
12. Sponsoring Organization Name and Address Solar Energy Research Institute 1617 Cole Boulevard Golden, Colorado 80401		13. Type of Report & Period Covered Technical Report	
		14.	
15. Supplementary Notes  Technical Monitor: Werner Luft			
16. Abstract (Limit: 200 words) A 10-kW-h scale model high-temperature direct-contact latent-heat-exchange thermal energy storage system was designed and fabricated. A research program was structured in three separate phases to permit: Phase I--the inspection and evaluation of the original hardware, which suffered extensive corrosion and damage in a previous experimental program; Phase II--redesign and fabrication of a modified system; and Phase II--detailed test evaluation. On the basis of the findings of Phase I, the design was modified to eliminate previous deficiencies. A test plan was also prepared that contained detailed information concerning instrumentation (type and location), measured parameters, and equipment operating procedures. Phase II entailed component procurement and fabrication, system assembly, and instrumentation. At the end of Phase II, the system was in a ready-for-test condition but the program was terminated before the start of the Phase III test evaluation. Since testing was never implemented, this report presents only the results for the design and fabrication phases of the program.			
17. Document Analysis a. Descriptors Corrosion ; Direct Contact Heat Exchangers ; Heat Exchangers ; Leaks ; Liquid Metals ; Molten Salts b. Identifiers/Open-Ended Terms  c. UC Categories 62e			
18. Availability Statement National Technical Information Service U.S. Department of Commerce 5285 Port Royal Road Springfield, Virginia 22161		19. No. of Pages 99	
		20. Price A05	

UNITED STATES DEPARTMENT OF ENERGY

P.O. BOX 62  
OAK RIDGE, TENNESSEE 37830

OFFICIAL BUSINESS  
PENALTY FOR PRIVATE USE, \$300

POSTAGE AND FEES PAID

UNITED STATES  
DEPARTMENT OF ENERGY



10723 FS- 1  
US DEPARTMENT OF ENERGY  
ATTN S D ELLIOTT, DIR  
SOLAR ONE PROJECT OFFICE  
PO BOX 366  
DAGGETT, CA 92327